PRINCIPLES OF PERCEPTUAL DECISION MAKING: INSIGHTS FROM A SOMATOSENSORY COMPARISON TASK

Dissertation

zur Erlangung des akademischen Grades

Doktor der Naturwissenschaften (Dr. rer. nat. / Ph. D.)

am Fachbereich Erziehungswissenschaften und Psychologie

der Freien Universität Berlin

vorgelegt von

Jan Herding, M. Sc.

Berlin 2017

Erstgutachter: Prof. Dr. Felix Blankenburg

Zweitgutachter: Prof. Dr. Hauke Heekeren

Tag der Disputation: 31.08.2017

Acknowledgements

First of all, I would like to thank Felix Blankenburg for being such an approachable supervisor, readily taking the time to dive into any in-depth Discussion – and, in general, for creating such a nice environment to do science in.

My thanks go also out to all my colleagues from the NNU and CCNB, especially to Simon Ludwig, spending endless hours with me in the airless, stuffy EEG labs over the last four years to collect heaps of, admittedly awesome, data. In this regard, also Bernhard Spitzer deserves a special mention, for being my EEG mentor and sharing his immense knowledge with me. Doing science with all of you guys puts the fun into fundamental research. :)

Obligatory but sincere thanks go out to the Bernstein Center, not only for supporting me financially, but also for introducing me to an inspiring and interactive research community.

Last but not least, a very special thank you goes to Julia for being so very patient with my seemingly endless endeavor of finishing this thesis – and for pushing me every now and then to ensure that you don't have to be patient for too long. Of course, also Ole's part is worth mentioning here, being the best baby boy ever and granting me unexpectedly many hours of sleep during his first year. If you ever read this, I expect nothing less of you than a frigging doctoral degree!!! – just kidding. ;)

Thank you all once more for making this possible.

Table of Contents

Abbreviations

2-AFC	two-alternative forced choice
BA	Brodman area
BOLD	blood oxygenation level dependent
CPP	centro-parietal positivity
EEG	electroencephalogram
FEF	frontal eye fields
fMRI	functional magnetic resonance imaging
IFG	inferior frontal gyrus
IPS	intraparietal sulcus
LIP	lateral intraparietal
MI	primary motor cortex
MIP	medial intraparietal
PFC	prefrontal cortex
dlPFC	dorsolateral prefrontal cortex
PMC	premotor cortex
dPMC	dorsal premotor cortex
mPMC	medial premotor cortex
vPMC	ventral premotor cortex
PPC	posterior parietal cortex
PRR	parietal reach region
RF	receptive field
SI	primary somatosensory cortex
SII	secondary somatosensory cortex
SC	superior colliculus
SDT	signal detection theory
SSEP	steady-state evoked potential
TMS	transcranial magnetic stimulation

Zusammenfassung

Im täglichen Leben müssen wir uns fast ununterbrochen zwischen möglichen Optionen entscheiden: z.B. ‘Soll ich eine Jeans oder eine Chino tragen?’ oder ‘Soll ich einen Kaffee oder einen Tee trinken?’ usw. Die einfachste Form einer solchen Entscheidung betrifft Entscheidungen, die ausschließlich auf Grund von sensorischen Reizen getroffen werden. Wenn wir z.B. entscheiden müssen, ob wir die heiße Tasse Kaffee, die wir gerade in Händen halten, sofort trinken können oder ob wir sie besser noch etwas abkühlen lassen sollten. Solche rein sensorisch getriebenen Entscheidungen werden als perzeptuelle Entscheidungen bezeichnet und liefern ausgezeichnete Rahmenbedingungen, um die neuronalen Prozesse zu untersuchen, die einer Umwandlung von sensorischen Reizen in willentliche Handlungen zu Grunde liegen. Anders ausgedrückt, in den Neurowissenschaften wird die Einfachheit von perzeptuellen Entscheidungen oftmals dazu genutzt, um die Grundlagen von Entscheidungen im Allgemeinen zu verstehen. In den letzten Jahrzenten haben gerade elektrophysiologische Daten aus Tierversuchen unser Verständnis von den zugrundeliegenden neuronalen Prozessen vorangetrieben. Die Resultate aus dieser Forschung implizieren, dass Entscheidungen als Handlungsabsichten implementiert sind; und zwar in den Hirnregionen, die auch für die Ausführung der resultierenden Handlung zuständig sind. Insbesondere beinhaltet dies ein fronto-parietales kortikales Netzwerk.

In den hier vorgestellten Arbeiten versuchen wir, diese aus Tierversuchen gewonnen Einsichten, direkt mit dem vom Menschen abgeleiteten Elektroenzephalogram (EEG) in Verbindung zu bringen. Dazu haben wir das EEG Signal während eines Vergleichs zweier nacheinander präsentierter Vibrationen untersucht. In vier Studien, die insgesamt sechs Experimente mit dieser einfachen Vergleichsaufgabe beinhalten, konnten wir zeigen, dass die Erkenntnisse, die man aus Tierversuchen gewonnen hat, übereinstimmend auch aus menschlichen EEG Signalen abgeleitet werden können und, darüber hinaus, sogar auf bis dato unerforschte Entscheidungen übertragen werden können. Im Einzelnen bedeutet dies, dass je nachdem wie die Teilnehmer unserer Experimente ihre Entscheidung mitteilen mussten, bzw. je nachdem welche Entscheidungsregel sie anwenden mussten, ein EEG Korrelat gefunden wurde, welches nicht nur die Entscheidung der Teilnehmer widergespiegelt hat, sondern jeweils auch den Hirnarealen zugeordnet werden konnte, die für die Umsetzung der entsprechenden Entscheidungskonsequenz zuständig waren. Beachtenswert hierbei ist außer-

dem, dass diese Hirnregionen demselben fronto-parietalen Netzwerk entsprachen, welches auch in Tierversuchen identifiziert wurde. Darüber hinaus konnten wir zum ersten Mal ein detailliertes Evidenzsignal in parietalen Hirnarealen nachweisen, welches zwar aus anderen perzeptuellen Entscheidungsstudien bekannt ist, allerdings noch nie zuvor in einer Vergleichsaufgabe berichtet wurde. Interessanterweise hat uns die Anwendung einer solchen Vergleichsaufgabe zusätzlich ermöglicht, zu zeigen, dass eben jenes parietale Evidenzsignal scheinbar mehr Informationen beinhaltet als bisher angenommen. Diese Einsicht lädt wiederum zu Spekulationen ein, ob gegenwärtige Theorien zu perzeptuellen Entscheidungen womöglich weiter generalisiert werden können und zu einem globalen Konzept zur Schätzung von Größenordnungen im Allgemeinen erweitert werden können.

Abstract

Navigating through everyday life requires deciding between alternatives almost constantly: For instance, 'Should I wear a pair of Jeans or chinos?' or 'Should I have coffee or tea?' etc. The simplest form of decisions we face is based on sensory information only, e.g., when we need to decide whether we can drink the cup of hot coffee in our hands just now, or whether we should wait a couple of more minutes. Such purely sensory-driven decisions, which fall into the domain of perceptual decision making, constitute a prime example for studying the neural processes that are involved in the transformation of sensory information into behavior. In other words, the simplistic nature of perceptual decision making is often exploited in neuroscience to understand the principles of decision making in general. Over the last decades, especially electrophysiological recordings in animals have fostered the understanding of the involved neural processes. The according findings suggested that decisions are formed as intentions to act in those brain structures, which also implement the ensuing behavior. In particular, this implicated a fronto-parietal network of cortical areas.

The work presented here aimed at linking these insights from animal research to electroencephalogram (EEG) recordings in humans. In particular, we investigated the EEG signal during a simple task in which participants compared the frequencies of two vibrations that were sequentially presented to their index finger. In four studies, comprising six experiments employing this simple comparison task, we demonstrated that the findings from invasive animal recordings can be directly related to non-invasive human scalp recordings, and moreover, can even be extended to previously unexplored decision contexts. That is, depending on response modality and decision rule, we found a choice-indicative signal originating from those structures that implemented the consequences of the comparison task, notably, implicating the same fronto-parietal network as suggested by animal research. Moreover, we identified a fine-grained evidence signal in parietal areas that was previously known from other perceptual decision making tasks, however, has never been reported in a sequential comparison task. Interestingly, by using a comparison task, we could reveal that the parietal evidence signal appears to convey more information than assumed before, inviting for speculations about whether current theories of perceptual decision making might actually be extended to a more general framework of magnitude estimation.

List of original research articles

The thesis is based on the following research articles:

Herding, J.*, Spitzer, B.*, and Blankenburg, F. (2016). Upper beta band oscillations in human premotor cortex encode subjective choices in a vibrotactile comparison task. Journal of cognitive neuroscience, 28(5): 668 – 679. doi: 10.1162/jocn_a_00932

Herding, J., Ludwig, S., and Blankenburg, F. (2017). Response-modality-specific encoding of human choices in upper beta band oscillations during vibrotactile comparisons. Frontiers in Human Neuroscience, 11. doi: 10.3389/fnhum.2017.00118

Ludwig, S.*, **Herding, J.***, and Blankenburg, F. (*submitted*). Oscillatory EEG signatures of postponed somatosensory decisions. Human Brain Mapping.

Herding, J., Ludwig, S., Spitzer, B., and Blankenburg, F. (*submitted*). Centro-parietal EEG potentials in perceptual decision making: from subjective evidence to confidence. Journal of Neuroscience.

* Shared authorship

1 Introduction

In everyday life, we are constantly exposed to an overwhelming amount of sensory input. This plethora of information enters our brain via different sensory pathways where it is further processed in specialized brain areas. Only a small fraction of the bulk of sensory input eventually yields conscious percepts of the things that we see, hear, smell, taste or feel. In certain situations, such elementary percepts can directly influence our behavior. For instance, before we leave our homes to go outside, we might be unsure of whether to take a jacket or not. To make a decision regarding this issue, we can open a window and feel the temperature outside. Or imagine you want to buy a woolen pullover. Among those that suit your taste, you might choose the pullover that feels softest on your skin.

These two scenarios describe situations in which we make decisions based on how something feels on our skin. Whether it is the feeling of temperature or touch, these sensations fall into the somatosensory domain. Aside from somatosensation, we can of course also form decisions based on information from our other senses. The study of perceptual decision making is concerned with these decisions that transform the bare percepts – nourished by any of our various senses – into overt or covert actions.

In the following, I will provide an overview of how such decisions are investigated within a neuroscientific context. I will introduce various approaches on how to operationalize perceptual decision making, and present the current understanding of the underlying neural processes, based on research conducted in humans and other species. Then, I will turn to my own contribution to the field and present new insights into human decision making, obtained by examining choice behavior in combination with electroencephalogram (EEG) recordings during a somatosensory comparison task. Finally, I will discuss my findings in the light of current theories of perceptual decision making and provide a new perspective on the prevailing interpretations.

1.1 The study of perceptual decisions

Linking sensations with purposeful behavior – the goal of perceptual decision making – has long been a focus of scholarly interest, even reaching back to the ancient Greeks (see Glimcher, 2003 for comprehensive historical review). Whereas Aristotle assumed in his *de Anima* that a nonmaterial soul must implement the connection between sensation and action (see Aristotle, 1986), already Descartes proposed that, at least for behaviors that are fully determined by sensory input, i.e., reflexes, the link should be found within the material body (see Descartes, 1649, 1664). Interestingly, Descartes – who believed, like Aristotle, that more complex behaviors (i.e., nondeterministic links between sensation and action) must involve a nonmaterial soul – paved hence the way for the first physiological investigations of spinal reflex loops (Sherrington, 1649). These physiological experiments on reflexes, in turn, can be regarded as predecessors of modern neuroscientific studies of perceptual decision making.

Largely avoiding the quest for the physiological roots of the connection between sensations and actions, Gustav Fechner was interested in describing this relationship between "body and soul" using behavioral measures only (see Fechner, 1860). Drawing on exact mathematical formulations used in physics, Fechner aimed at finding quantitative and qualitative regularities in the relation between physical properties of objects in the "outside world" and their subjective perception. In other words, Fechner introduced the study of psychophysics as a means to precisely describe the relationship between physics and psychology – which has remained the gold standard in behavioral neuroscience to the present day. In his classic experiments, Fechner himself lifted two weights and judged which one was heavier, systematically varying temporal and spatial configurations of his experiments (i.e., heavier weight first or last to be picked up / positioned to his left or to his right; Fechner, 1860, pp. 183 – 201). Thus, Fechner studied perceptual decision making using a two-alternative forced choice (2-AFC) task while controlling for possible confounding factors in the experimental setup. The effect of temporal order of stimulus presentation on choice behavior in 2-AFC tasks also played a major role in my own studies and will be discussed in detail later (see 1.2.2 The time-order error). With the advent of signal detection theory (SDT) in psychological research, a powerful theoretical framework became available for investigating the empirical observations from 2-AFC tasks (see Green and Swets, 1966; Macmillan and Creelman, 2004). Originally, SDT was implemented – as its name

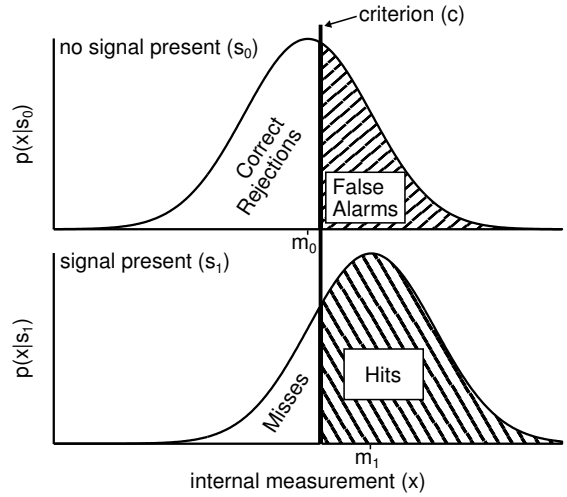

Figure 1.1: Intuition underlying SDT. Upper panel displays a scenario in which no signal was present, and a percept (i.e., internal measurement) can be regarded as a sample from a pure noise distribution with mean m_0. Lower panel shows a distribution centered on an existing stimulus (i.e., m_1) and an according sample of this distribution can be conceived as a percept of a (weak) signal. The placement of the (decision) criterion determines the probability of a hit, miss, correct rejection and false alarm, given that a stimulus was present (s_1) or not (s_0). (Figure adopted from Macmillan and Creelman, 2004)

suggests – to provide a mechanistic account of the process underlying the detection of weak signals, e.g., detecting whether a light is dimly lit or not (Tanner and Swets, 1954). Such "yes-no" detection tasks have four possible outcomes depending on the presence or absence of a stimulus, and the observer's response. In the presence of a stimulus, an observer can correctly detect it (hit) or fail to do so (miss). In the absence of a stimulus, the observer might correctly report the lack of a stimulus (correct rejection) or erroneously detect a stimulus (false alarm). Conventional approaches to investigating performance in these tasks focused on the proportion of correct responses only (i.e., proportion of hits and correct rejections), and treated false alarms as uninformative random guesses independent of any sensory information. SDT, however, assumes that false alarms and hits vary together. In particular, SDT postulates that when faced with a detection task, an observer computes an internal measurement of the stimulus feature that is to be detected, e.g., the intensity of a potentially lit light (Tanner and Swets, 1954). This internal measurement is noisy, but proportional to the actual intensity of the stimulus feature in question. Conceptually, the internal measurement can be regarded as a sample taken from one of two separate but likely overlapping probability distributions. From a distribution of pure noise in the absence of a signal, or from a noisy distribution centered on the true intensity of the stimulus feature in case a signal was indeed present (Figure 1.1).[†] The

[†]From a modern Bayesian perspective, the internal measurement can be regarded as a single percept of the actual stimulus feature (e.g., see Petzschner et al., 2015).

observer has to apply a simple criterion to this internal measurement in order to decide whether a stimulus was present or not. Accordingly, this internal measurement is often referred to as a decision variable (DV) in the context of decision making studies. If the internal measurement (or DV) falls above the criterion, the observer reports the presence of a stimulus and denies it's presence otherwise. In this framework, the four possible outcomes of a "yes-no" detection task (i.e., rates of hits, misses, correct rejections, and false alarms) are precisely defined by the areas under the respective probability distributions on either side of the criterion (i.e., as probabilities; Figure 1.1). Consequently, the four measures are tightly interrelated. That is, they covary depending on the location of the decision criterion with respect to the internal measurement. Thus, if the cost of missing a signal is high (e.g., missing the presence of a tumor in an X-ray image), observers can choose to set their criterion very low, thereby ensuring few (or no) misses, however, producing a considerable amount of false alarms as a trade-off. In other words, the placement of the criterion can be conceived as a bias in favor of one response over the other. At the same time, no matter where observers place their criterion, they cannot change their sensitivity for the task at hand. That is, sensitivity (or accuracy) in SDT (denoted as d') can be regarded as the distance between the means of the two hypothetical distributions that correspond to the two possible stimulus configurations (i.e., signal present or absent). Thus, observers' accuracy is assumed to be constant for a given task and session. Only the criterion, i.e., a response bias, can be willingly changed. Consequently, accuracy and bias in decision making tasks can be investigated independently using SDT, whereas the conventional measure of proportions of correct responses varies with response bias (see Macmillan and Creelman, 2004). Importantly, the theoretical considerations underlying SDT were experimentally confirmed in numerous psychophysical studies (e.g., see Swets, 1986). Moreover, the concepts introduced for "yes-no" detection tasks can be easily extended to 2-AFC tasks. For instance, the two distributions from which the internal measurement is assumed to be sampled can be conceived to represent the two choice alternatives in 2-AFC tasks (see Macmillan and Creelman, 2004). In more general terms, the distributional form of SDT is nowadays routinely used to model the perception of all kinds of sensory stimuli, mostly in a Bayesian context (e.g., see Petzschner et al., 2015).

1.2 Perceptual decision making in neuroscience

The notion of an internal measurement inherent in SDT provides a direct link to neuroscience. In fact, Tanner and Swets (1954) already suggested that the internal measurement on which choices are based, i.e., a DV, is likely implemented by neuronal activity (i.e., the perception of sensory stimuli). Applying a simple criterion to the DV would hence suffice to relate neuronal activity to behavior. Indeed, several decades later William Newsome, Michael Shadlen, and co-workers demonstrated that the firing rates of specific neurons implemented a DV as hypothesized by SDT (Britten et al., 1992, 1996). Indeed, Newsome and colleagues identified a dynamically accumulating DV in neuronal activity, extending beyond the implicit assumption of stationarity in SDT (i.e., decisions are based on a single internal measurement), well in line with classic sequential sampling models as outlined below (e.g., see review in Gold and Shadlen, 2007). Alongside the work of Newsome and colleagues, Vernon Mountcastle spearheaded a parallel stream of research investigating perceptual decisions (e.g., see Mountcastle et al., 1969), which was continued by his student Ranulfo Romo (e.g., see Mountcastle et al., 1990). The corresponding studies provide an impressive body of work on perceptual decision making, which will be reviewed in depth afterwards (e.g., see comprehensive review in Romo and Salinas, 2003).

1.2.1 Visual decisions based on evidence accumulation

To explore the relation of neuronal activity and perceptual decisions, Newsome and colleagues devised a simple 2-AFC task, in which an observer judged the direction of apparent visual motion (see Newsome and Pare, 1988). In particular, observers had to identify the net motion (e.g., leftward vs. rightward) in a visually presented random dot kinematogram (RDK). A RDK is a cloud of dots, with each dot changing position over a brief period of time before being replaced by a new dot at a random location (see Newsome and Pare, 1988). By varying the proportion of dots that move coherently (i.e., with a fixed spatiotemporal relation), the perceived net motion of the RDK, and hence task difficulty, can be controlled by the experimenter (e.g., 0% coherence: all dots move independently in random directions; 100% coherence: all dots move together in the same direction).

Newsome and colleagues trained macaque monkeys to perform such a random dot motion (RDM) task and recorded neuronal activity from the motion selective middle temporal (MT) visual area (e.g.,

Britten et al., 1992, 1996). Neurons in area MT are known to exhibit complex response patterns to visual stimuli. Among other things, firing rates of MT neurons are tuned to stimuli moving in a certain direction through their receptive fields (RFs; Maunsell and Van Essen, 1983). By recording neurons that were specifically tuned to the motion directions of either choice alternative in a RDM task, Britten and colleagues (1992) were able to probe the relationship between firing rates of single neurons and behavior. Indeed, the activity in MT showed the very same pattern as predicted by SDT. That is, single-trial firing rates could be conceived as being drawn from either of two distinct distributions of possible firing rates (i.e. high or low), each representing one of the two possible motion directions (or choices). For instance, neurons that preferred leftward motion exhibited high firing rates when the net motion in the RDK was leftward, and low firing rates for rightward motion. Notably, the distance between the distributions of observed firing rates (i.e., high vs. low) reflected the varying proportions of coherently moving dots (i.e., task difficulty). In line with the notion of accuracy in SDT, high coherence levels yielded almost completely separated distributions of firing rates, accompanied by near perfect performance (Britten et al., 1992). Strikingly, when all dots in the RDK were moving independently in random directions (i.e., 0% coherence), firing rates of MT neurons still predicted the monkeys' choices significantly above chance (Britten et al., 1996). That is, firing rates of MT neurons were linked with choice behavior even in the absence of any physical motion information in favor of either choice. Additionally, Salzman et al. (1990) provided evidence indicating that the link is indeed causal. Microstimulating MT neurons tuned to a specific motion direction increased the probability of monkeys reporting to have perceived motion in that very direction. Taken together, this series of studies impressively established the behavioral relevance of area MT for simple motion discriminations as required in the RDM task. Particularly, firing rates in area MT seem to index the momentarily perceived motion of RDKs which drives decisions in the RDM task.

A fronto-parietal network subserves oculomotor decisions

In the classic RDM experiments, monkeys reported their choices by making a saccade to one of two visual targets. Saccades denote quick eye movements that are executed in order to shift the visual focus. Consequently, Newsome and colleagues reasoned that information about decisions in the RDM task must also be accessible to areas responsible for the preparation of saccades. Specif-

ically, they assumed that cortical areas located hierarchically between area MT and areas directly responsible for the execution of saccades, i.e., superior colliculus (SC) and frontal eye fields (FEF), might readout the information from MT and preserve it until a saccade is performed (see Shadlen and Newsome, 1996). Due to the anatomical projections of MT, the lateral intraparietal (LIP) sulcus was their preferred target. Neurons in area LIP are active when visual stimuli are presented within their RFs, or when a saccade is planned into their RFs (e.g., Andersen et al., 1987). To specifically refer to the latter response property, RFs of LIP neurons are also termed movement fields. Thus, as a result of the sensory- and motor-related RF properties, LIP is typically considered a sensorimotor integration area (see Andersen et al., 1987; Andersen, 1995; Colby and Goldberg, 1999; Andersen and Buneo, 2002), and is likely to play a central role in the sensorimotor transformation at the heart of perceptual decision making. Shadlen and Newsome (1996, 2001) recorded LIP neurons whose movement fields were aligned with one of the two targets in the RDM task. The other target was placed in the opposite direction from this movement field. Not surprisingly, they found that activity in LIP neurons whose movement fields were aligned with the chosen target was elevated before responses were given (Shadlen and Newsome, 1996, 2001). These findings simply reflected the characteristics of the LIP cells according to which they were initially identified, i.e., increased activity before a saccade was made to their movement field. However, the striking observation was that the activity in single LIP neurons ramped up during the presentation of RDKs – faster and steeper for easy than for difficult trials – and hence, was interpreted to reflect evidence for a decision that was accumulating over time (Shadlen and Newsome, 1996, 2001). When allowing monkeys to report their decision as soon as they committed to a choice, LIP firing rates peaked at the time of the saccade and reached a fixed level independent of task difficulty, i.e., independent of presented motion coherence (e.g., Roitman and Shadlen, 2002). Bennur and Gold (2011) finally showed that a decision-informative signal in LIP was also present when no fixed response mapping was provided for the RDM task. That is, monkeys had to map their choices onto a spatially undetermined color-code. Only later, colors were assigned to two visual targets, and monkeys selected a target based on its color. Still, neurons in LIP encoded the evidence for the upcoming decision, even before colors were assigned to targets. That is, LIP encoded evidence for oculomotor choices, even though the target for the ensuing saccade was not yet defined (Bennur and Gold, 2011). Thus, this study was

the first to provide direct evidence for the notion that LIP does not solely index an ensuing decision report, but also tracks decision-relevant evidence independent of the specific motor response.

For decisions that were associated with a fixed motor response, a very similar ramping signal that tracked evolving oculomotor choices was also found in firing rates of neurons in FEF (e.g., Hanes and Schall, 1996; Kim and Shadlen, 1999; Ding and Gold, 2012), and SC (e.g., Horwitz and Newsome, 1999; Ratcliff et al., 2003), i.e., in those areas that are directly involved in the execution of saccades. The apparent redundancy of similar signals in sensorimotor (i.e., LIP) and motor areas (i.e., FEF and SC) remains highly controversial, however, the different sites might play distinct roles in decision making. Recently, Hanks et al. (2015) found that rats' parietal areas reflected graded evidence for a decision, whereas frontal motor areas indicated a categorized choice signal, possibly suggesting a gradual signal change from parietal to motor areas. Gold and Shadlen (2003) had previously shown (in monkeys) that the experimental task per se can influence the extent to which such a sensorimotor transformation of decision-relevant information can proceed. When the response mapping was clear in a RDM task (i.e., fixed mapping of choices onto specific saccade directions), accumulated evidence for a decision was apparently already available to neurons in FEF. Microstimulating FEF, while the RDK was still presented, evoked premature saccades biased towards the later chosen targets. However, when the response mapping was not fixed and monkeys reported choices by a saccade to a colored target, whose position was not predictable, microstimulation-evoked saccades during evidence accumulation were not biased at all (Gold and Shadlen, 2003; similar task as in Bennur and Gold, 2011). These findings are both trivial and remarkable. Of course, an oculomotor choice can only be prepared in relevant brain areas (i.e., FEF) when the specifics regarding the ensuing saccade are known. However, these results also imply a remarkable flexibility within the decision network, modifying the relay of information within a sensorimotor transformation process depending on the given circumstances. Taken together, the reviewed findings of parietal and motor areas imply that both sites might implement distinct functions for perceptual decision making, giving rise to the notion of a fronto-parietal network subserving decision formation. Parietal areas seem to represent a more detailed evidence signal, and appear to play the classic role of a sensorimotor integration area (see Colby and Goldberg, 1999; Andersen and Buneo, 2002). This involves multiplexing sensory evidence and choice signals that can be read out by downstream motor areas as

soon as a motor response is clearly specified (Meister et al., 2013; Park et al., 2014). Nevertheless, lesioning the relevant parietal areas does not seem to hinder perceptual decision making in general. In tasks with a fixed choice-to-motor mapping, reversible lesioning of parietal areas had no influence on decision performance (Erlich et al., 2015; Goard et al., 2016; Katz et al., 2016), whereas motor areas (Erlich et al., 2015; Goard et al., 2016) and sensory areas (Goard et al., 2016; Katz et al., 2016) were indispensable. That is, parietal areas do not seem to be mandatory for decision making. In fact, if the motor mapping is known in advance, and relevant motor areas are intact, these motor areas appear to be sufficient to enable simple perceptual decisions.

Identifying decision-related activity in this fronto-parietal network, which is also involved in the preparation and execution of the decision report (i.e., saccades), culminated in the formulation of an intentional framework of decision making (Shadlen et al., 2008). That is, decisions are thought to be expressed as intentions to act, and hence, are formed in brain areas that are responsible for the execution. At the same time, an analogous theory of "affordance competition" was developed (Cisek, 2007; Cisek and Kalaska, 2010). Cisek and colleagues found that competing actions were simultaneously prepared in premotor structures until the required action was fully disclosed (Cisek and Kalaska, 2005). In line with these views – which I will collectively refer to as the intentional framework of decision making hereafter – de Lafuente et al. (2015) found that, when the decision report was changed from saccades to reaches in the RDM task, a decision-relevant ramping signal was identified in the medial intraparietal (MIP) area, also known as the parietal reach region (PRR).

Computational models of evidence accumulation

SDT provided a powerful framework for the analysis of stationary firing rates of single MT neurons during a RDM task, and relate them to the choice behavior of monkeys (see Britten et al., 1992, 1996). Particularly, considering the firing rate from a single trial (i.e., spike count per second) yielded a DV in the sense of an internal measurement inherent in SDT. The DV could be used to explain the monkeys' performance by comparing it to a decision criterion (Britten et al., 1992, 1996). The ramping firing rates in areas LIP, FEF, and SC, however, suggested a dynamically evolving DV (e.g., see Shadlen and Newsome, 1996, 2001) rather than a stationary DV that is read out at the end of a trial. Hence, Shadlen and Newsome (2001) suggested that the ramping signal in LIP might reflect

the accumulation of the momentarily perceived motion represented in MT. Formally, they proposed sequential sampling models to explain the accumulation process. These models originate from the classic work by Wald on sequential tests of statistical hypotheses (Wald, 1945; Wald and Wolfowitz, 1948), and can be considered a direct extension of SDT. That is, whereas SDT implicitly assumed that decisions are based on a single internal measurement, i.e., a stationary DV, sequential sampling models repeatedly sample these internal measurements while accumulating the outcomes, i.e., an accumulating DV (see Gold and Shadlen, 2007). Recall that according to SDT, the internal measurement in a 2-AFC task, i.e., the DV, is conceived as a sample from either of two (possibly overlapping) distributions that reflect two distinct stimulus configurations (see high vs. low firing rates in MT depending on preferred or null direction of motion; Britten et al., 1992, 1996). The internal measurement is hence more or less likely to be drawn from either of the two distributions. Formally, one probability can be computed given that the sample was drawn from the first distribution, and a second probability can be computed given that the sample belongs to the other distribution (i.e., two likelihoods per sample). Wald (1945) showed that combining the ratio of two such likelihoods for every sample in a sequence provides an optimal sequential test procedure for deciding from which distribution the sequence of samples was drawn (see also Wald and Wolfowitz, 1948). Specifically, this famous sequential probability ratio test can be implemented by summing the logarithm of the likelihood ratios from each sample (see also Gold and Shadlen, 2007 for an accessible description). By defining a minimum amount of evidence that has to be accumulated before committing to a decision, a boundary for the sequential sampling procedure can be set. Furthermore, the boundary can be defined in accordance with classic statistical test procedures (i.e., controlling for alpha and beta errors), notably, requiring fewer samples than the classic tests under identical conditions (Wald, 1945). Aside from the test's optimality, the simplicity is appealing as, in principle, such an additive integration of evidence could be implemented by single neurons (or populations of neurons). However, the explicit computation of likelihoods for each sample would require detailed knowledge of the two alternative distributions, i.e., their probability densities, or at a minimum their mean values (Gold and Shadlen, 2001). To circumvent this problem, Gold and Shadlen (2001) suggested that instead, an approximation of the log-likelihood ratio may be computed, by pairing neurons with opposing response profiles (e.g., one preferring leftward motion, the other rightward). In particular,

they demonstrated that the differences in firing rates of such neuron pairs – which they name the neuron and antineuron (e.g., see also Shadlen and Newsome, 1996) – scales with the combined log-likelihood ratio given the firing rates of both neurons (Gold and Shadlen, 2001). Hence, summing the differences in firing rates of pairs of opposing MT neurons until a decision boundary is reached, yields an optimal strategy for solving the RDM task – and neurons in LIP appear to do exactly that (e.g., Shadlen and Newsome, 2001; Roitman and Shadlen, 2002; Mazurek et al., 2003).

In addition to the work of Shadlen and colleagues, behavioral research on human decision making has nourished the development of several sequential sampling models (e.g., see recent review in Ratcliff et al., 2016). These models account for observed choice behavior in great detail by explaining response time variability for correct and incorrect decisions, as well as the accuracy of choices itself. One aspect that all models have in common is that they describe the accumulation of evidence as a noisy integration process (e.g., noisy accumulators, a diffusion process or a random walk). Incorporating randomness enables these models to account for erroneous decisions and variations in response times. Moreover, all models implement decision boundaries for the accumulation process that mark the minimum amount of evidence that is necessary to commit to a choice – just like the test procedure of Wald (see Wald, 1945). In particular, this can be implemented as absolute bounds for two (or more) totals of evidence, or as relative bounds for a single total of evidence (see Ratcliff et al., 2016; Gold and Shadlen, 2007). Ratcliff et al. (2003) were the first to directly link recorded neural activity from monkey SC to one of these models. Specifically, they fitted a drift diffusion model (DDM; e.g., see Ratcliff and Rouder, 1998) to the observed choice behavior. The virtual traces of the diffusion process in this model drift towards either choice alternative (specified by a certain drift rate depending on observed response times), and hence, serve as a single-trial proxy for evidence accumulation. When averaged across trials, these traces accurately reflected the according mean firing rates of single cells in SC (Ratcliff et al., 2003). Ever since this first successful application of the DDM to electrophysiological data, numerous studies have utilized the DDM, or similar models, to explain neuronal firing as accumulating evidence in perceptual decision making (e.g., Huk and Shadlen, 2005; Ding and Gold, 2012).

Accumulation-based decisions in humans

Inspired by the findings from animal research, work in human neuroscience has investigated the process of evidence accumulation for perceptual decisions along similar lines. Heekeren and colleagues (2004) wanted to identify a "neuron/antineuron mechanism" that could be resolved at the brain-region-specific level using functional magnetic resonance imaging (fMRI). Thus, using similar principles as in the RDM task, human participants were presented with noisy pictures of either a face or a house for a fixed period of time. After a delay, they reported via button presses, which of the two items they had perceived. Importantly, the level of noise that degraded the pictures varied across trials, to introduce different levels of available evidence, and hence, task difficulty. Perceived images of faces are known to elicit increases in the blood oxygenation level dependent (BOLD) signal in the fusiform face area (FFA; e.g., Kanwisher et al., 1997), whereas images of houses are associated with BOLD signal increases in the parahippocampal place area (PPA; e.g., Epstein and Kanwisher, 1998). Heekeren et al. (2004) thus reasoned that the perceived evidence for a decision in this face-vs-house task should scale with the difference in activity between PPA and FFA. Moreover, they hypothesized that a brain area which accumulates this relative evidence should exhibit a higher BOLD signal for easy trials than for hard trials. That is, assuming a similar accumulation process as observed in the monkey research, easy trials should lead to a faster increase in neural activity to a certain threshold value which is maintained until a response is given (see Shadlen and Newsome, 1996, 2001). Given that fMRI lacks the temporal resolution to identify the dynamics of this accumulation process, the BOLD signal can only pick up the overall activity during any given trial (i.e., one accumulation process). Consequently, easy trials (i.e., high activity reached early during the stimulus presentation) should be associated with a higher BOLD signal than hard trials.[†] The only brain area that fulfilled these two postulated requirements (i.e., scaling with differential activity from PPA and FFA and higher BOLD signal for easy trials) was the left dorsolateral prefrontal cortex (dlPFC; Heekeren et al., 2004). Notably, when replicating the RDM task in humans, the left dlPFC also showed higher activity during easy trials as compared to hard trials, independent of the response modality, i.e., button presses or saccades (Heekeren et al., 2006). Furthermore, Philiastides

[†] Note that this reasoning only applies for tasks with a forced delay before responses (see Hanks and Summerfield, 2017). In response time tasks, the argument actually goes in the opposite direction, i.e., a higher BOLD signal for low evidence as compared with high evidence, as in this scenario with self-paced responses the accumulation process presumably ends earlier in easy trials (e.g., see Ho et al., 2009; Kayser et al., 2010; Liu and Pleskac, 2011).

et al. (2011) showed that an inactivation of the left dlPFC via transcranial magnetic stimulation (TMS) indeed reduced the performance of participants in the face-vs-house task, most likely by deteriorating the participants' ability to integrate evidence (i.e., a decrease in the drift rate of the DDM). Based on these studies, the left dlPFC was suggested as a generic decision making area that integrates sensory evidence independent of the ensuing motor actions (see Heekeren et al., 2008). Similarly, the right anterior insular (aINS) has also been associated with this role (e.g., Ho et al., 2009; Liu and Pleskac, 2011). Moreover, many fMRI studies have also identified the human homologue of monkey LIP, i.e., the intraparietal sulcus (IPS), as well as the FEF as being involved in the formation of a decision (e.g., Heekeren et al., 2006; Ho et al., 2009; Kayser et al., 2010; Liu and Pleskac, 2011).

Taken together, the fMRI literature consistently reports overlapping brain areas as being involved in perceptual decision making. Besides those areas that are known from animal research, and which are associated with the preparation of a decision report (i.e., IPS and FEF), additional general-purpose decision areas have been identified by fMRI (i.e., DLPFC and aINS). Whether these latter areas are indeed involved in the decision formation per se or whether they are active during decision making tasks, because they exert some form of cognitive control, remains elusive nevertheless (e.g., see Cardoso-Leite et al., 2014). Moreover, the indirect relationship between the sluggish BOLD signal and the fast neuronal dynamics underlying evidence accumulation leaves some uncertainty regarding how to interpret fMRI results in this context (see also Hanks and Summerfield, 2017).

On the other hand, EEG and magnetoencephalography (MEG) can capture the dynamics underlying the formation of perceptual decisions, however, at the expense of spatial resolution. Although the relationship between M/EEG signals and fMRI BOLD signals is not completely understood (but see Logothetis et al., 2001; Scheeringa et al., 2011), the dlPFC was also implicated by MEG findings to be involved in perceptual decision making (Donner et al., 2007). In the RDM task, beta band power ($\sim 12 - 30$ Hz) in the dorsal visual pathway (MT, IPS, and dlPFC) was higher for correct than for incorrect decisions (Donner et al., 2007). This finding supports the notion that the dlPFC is rather involved in global control processes instead of general-purpose evidence accumulation (see also Cardoso-Leite et al., 2014). At the same time, in line with the intentional framework of decision making, Donner et al. (2009) found that a large-scale motor preparation signal in human MEG recordings tracked the accumulating evidence for perceptual decisions (e.g., see also O'Connell et

al., 2012). Particularly, the well-known lateralized decrease in beta band activity in preparation of button press responses (e.g., see Jasper and Penfield, 1949; Pfurtscheller, 1981) scaled with the proportion of coherent motion in the RDM task (Donner et al., 2009). Furthermore, in analogy to the micro-stimulation of FEF in monkeys that evoked saccades biased in the direction of subsequent choices (Gold and Shadlen, 2003), perturbating hand position prior to reporting choices with a reach, evoked reflexes in human participants that were biased toward the final decision reports (Selen et al., 2012). In particular, the evolving DV (based on a RDM task) seemed to have proceeded even as far as the peripheral motor system, as was revealed by electromyographic recordings (Selen et al., 2012).

Preceding these clearly motor-related signals, a centro-parietal positivity in the human EEG (abbreviated CPP) was recently shown to track evidence accumulation in various perceptual decision making tasks (reviewed in Kelly and O'Connell, 2015). This event related potential (ERP), which is arguably identical to the classic P300 wave (see Twomey et al., 2015), has been suggested to be the human homologue of the signal recorded in monkey LIP (see Kelly and O'Connell, 2015). Specifically, the CPP increased faster and steeper for trials with high evidence as compared to low-evidence trials (e.g., in the RDM task Kelly and O'Connell, 2013; Twomey et al., 2016), and always attained a common threshold at the time of the decision report (e.g., O'Connell et al., 2012; Kelly and O'Connell, 2013; but see Philiastides et al., 2014). Of note, these tasks eliminated any stimulus evoked signals by employing an elegant continuous task design, ruling out possible task-onset confounds which might have contaminated previous fMRI findings (see Cardoso-Leite et al., 2014). Given the variety of tasks with different sensory modalities that were employed (e.g., see O'Connell et al., 2012), the CPP was suggested to reflect a modality-independent (i.e., general-purpose) evidence accumulation signal (see Kelly and O'Connell, 2015). Moreover, the CPP was also found to index the evidence for a deviant detection in a classic oddball paradigm, further generalizing the role of the CPP beyond the limits of classic accumulation-based decision making (Twomey et al., 2015).

In sum, this selected review of human M/EEG research is well in line with results from the animal literature. That is, a parietal signal appears to track evidence accumulation for decisions that are based on the integration of noisy sensory input, and motor structures that are responsible for the decision report also have access to this information – at least when a clear response mapping is

provided. The overall agreement between human and animal research also includes the previously discussed findings from the fMRI literature that also implicated a fronto-parietal network subserving perceptual decision making.

1.2.2 Vibrotactile frequency comparisons

All studies described up to now were based on judgments of single noisy percepts, mostly in the visual domain. In these studies, the presence of noise allowed the experimenters to control the difficulty of according decisions, and forced observers to accumulate sensory information until they reached a specific percept, or no further evidence was presented. Aside from this accumulation-based approach, there is another popular way to investigate perceptual decision making by examining how a stimulus is evaluated in comparison to a percept held in working memory. In this scenario, two stimuli are presented sequentially and the observer is asked to compare both stimuli based on a specific stimulus feature. These tasks come in many flavors, ranging across all stimulus modalities, here, however, I focus on a variant that uses vibrotactile stimuli. This somatosensory version has been extensively studied in monkeys, yielding one of the most complete pictures of the processes involved in a sensorimotor transformation from perception via decision to action (see Romo and de Lafuente, 2013 for a review). Vernon Mountcastle pioneered this work, and introduced the vibrotactile comparison task to the study of electrophysiology in monkeys, training them to decide whether the second stimulus had a higher or lower frequency than the first one (e.g., Mountcastle et al., 1969, 1990). The frequencies of the stimuli in this task typically lie in the range of 5 – 50 Hz, as in this range, the involved mechanoreceptors in the skin (Meissner's corpuscles) are most sensitive (e.g., Talbot et al., 1968). On a more descriptive level, these stimuli are known to create a so-called 'flutter' sensation. In order to compare two such flutter stimuli, a cascade of cognitive operations associated with different neural processes must be completed: (1) the frequencies of both stimuli (f1 and f2) have to be reliably encoded; (2) f1 has to be kept in working memory during the retention interval; and (3) a comparison between f2 and the memory trace of f1 has to be computed and transformed into a motor response (comprehensive review in Romo and de Lafuente, 2013). A summary of the most important findings from Romo and colleagues is provided in the following paragraph.

In a typical setup of the frequency comparison task, both flutter stimuli (with frequencies f1 and

f2) were sequentially presented to the glabrous skin at the monkeys' fingertip, interleaved by a brief retention interval (typically a couple of seconds; see Romo and de Lafuente, 2013). The animals decided whether f2 < f1 or f2 > f1 and reported their decisions via a button press after the second stimulus, either immediately or after a short delay period (again, typically a couple of seconds). Electrophysiological recordings from contralateral primary somatosensory cortex (SI) revealed that quickly adapting (QA) neurons in Brodman areas (BAs) 3b and 1 encoded the frequencies of the flutter stimuli during presentation (Mountcastle et al., 1990; Hernández et al., 2000). The QA neurons in BA 3b receive afferent inputs (via the Thalamus) from rapidly adapting mechanoreceptors (Meissner's corpuscles) in the skin, and BA 1 in turn is innervated by neurons from BA 3b (e.g., Talbot et al., 1968; Mountcastle et al., 1969). Most of the recorded neurons in SI encoded the stimulus frequency by discharging periodically and phase-locked to the stimuli (e.g., Mountcastle et al., 1990). However, a fraction of neurons did not convey the exact temporal structure of the stimuli, rather they encoded stimulus frequencies by a monotonically increasing rate code, i.e., the higher the stimulus frequency, the higher the average firing rate during stimulus presentation (e.g., Hernández et al., 2000). Notably, the monkeys' behavioral performance was better explained by the activity of neurons that employed a rate code (Hernández et al., 2000; Salinas et al., 2000; Luna et al., 2005). That is, evaluating mean firing rates of neurons (i.e., rate code) in the framework of SDT (i.e., comparing them against a decision criterion just like the firing rates from MT in the RDM task; see Britten et al., 1992, 1996) revealed that the resulting neurometric response functions were very similar to the psychometric response function computed from behavioral performance (Hernández et al., 2000). Neurometric functions computed from the periodicity in neuronal firing (i.e., temporal code), on the other hand, predicted a much higher performance than observed, suggesting that monkeys did not use this detailed information for their decisions. Moreover, neurons in secondary somatosensory cortex (SII), the subsequent region along the somatosensory processing hierarchy, almost exclusively encoded stimulus frequencies using a rate code (Salinas et al., 2000). These observations led to the conclusion that the behaviorally relevant information in this tactile comparison task is likely conveyed via a rate code, and not by a temporal code (e.g., Hernández et al., 2000; Salinas et al., 2000; Luna et al., 2005). Interestingly, the rate code in SII could be either positively or negatively correlated with the stimulus frequency (i.e., either increasing or decreasing firing rates with higher

stimulus frequencies; Salinas et al., 2000). This dual coding scheme was also observed in all other downstream brain areas that were involved in the frequency comparison task at later stages, i.e., in prefrontal cortex (PFC), ventral, medial, and dorsal premotor cortex (vPMC, mPMC, dPMC; see Hernández et al., 2010). Particularly, during the retention interval – in the absence of any sensory input – the firing rates of neurons in all of the listed frontal regions (most prominently in PFC) were found to scale with the frequency that had to be kept in working memory, i.e., f1 (e.g., Romo et al., 1999; Brody et al., 2003; Barak et al., 2010; Jun et al., 2010; Hernández et al., 2010). In the decision phase of the task, when both stimuli had to be compared, firing rates, especially in premotor cortices, scaled with the differences between f2 and f1 (e.g., Hernández et al., 2002; Romo et al., 2002, 2004; Jun et al., 2010; Hernández et al., 2010). Notably, the correlation of firing rates and differences between f2 and f1 was reversed for incorrect decisions, associating the recorded neural activity with the monkeys' actual choices (e.g., Hernández et al., 2002; Romo et al., 2002, 2004). The central role of the PMC in decision formation was further supported by a study investigating monkeys' local field potentials (LFPs). Haegens et al. (2011) found that the beta band power ($\sim$15 – 30 Hz) in LFPs recorded from mPMC and dPMC was also modulated by the difference between f2 and f1, suggesting that choice-related information can also be read-out at a larger scale than single-cell firing. Specifically, beta band power was always higher for "f2 > f1" choices as compared to "f2 < f1" choices, irrespective of whether decisions were correct or incorrect (Haegens et al., 2011). Importantly, the choice-related PMC signals in LFPs, as well as in the neuronal firing rates, were specific to the comparison task, and did not merely represent the motor preparation of the decision report. That is, when monkeys were instructed in advance how to respond, regardless of the stimuli, both the beta band modulation and the firing rate modulation were no longer observed (Hernández et al., 2002; Romo et al., 2002, 2004; Haegens et al., 2011). Finally, that such a choice-related signal was primarily observed in premotor structures is – analogously to the choice signals in FEF and LIP during oculomotor choices – in line with an intentional framework of decision making, as monkeys always reported their choices by button presses in the vibrotactile comparison task.

Computational models of the frequency comparison task

Recall that Romo and colleagues observed a dual coding scheme in the firing rates of neurons throughout the comparison task in all brain areas except for SI (i.e., either positive or negative correlation with encoded quantity; see Romo and de Lafuente, 2013). They argued that this coding scheme with two oppositely tuned neuronal populations may be exploited to improve discrimination performance in the task (Romo and Salinas, 2003). Specifically, an appropriate subtraction of activity from both pools can result in an increase in discrimination capacity (when assuming that an ideal observer forms decisions based on the difference in firing rates; Romo and Salinas, 2003). Such a subtraction of oppositely tuned neuronal activity could in general provide more robust representations at any stage of the task (i.e., during encoding, working memory and comparison; Romo and Salinas, 2003). Interestingly, note that a similar mechanism has also been suggested by Gold and Shadlen (2001) in the context of the RDM paradigm (i.e., the neuron/antineuron hypothesis), possibly hinting at a general principle of robust neural coding. For the vibrotactile comparison task, Machens et al. (2005) implemented this idea in a neural network model based on mutual inhibition between two oppositely tuned neuronal pools. In brief, the model accounts for the firing rate modulations observed in frontal cortex during encoding and working memory (i.e., representing f1), and decision making (i.e., representing f2 - f1) by reaching different attractor states at the different stages of the task. An important property of this model is the recurrent connectivity within the two pools of neurons to create a line attractor. In plain words, this line attractor allows for stable/sustained activity with varying firing rates depending on f1 during the working memory phase of the task (see Wang, 2001; Miller et al., 2003). To generate such a line attractor, however, the model requires some manual fine tuning, and consequently, does not reflect the heterogeneity of firing rates typically observed in neuronal recordings, i.e., the model is “too good” (Jun et al., 2010). Barak et al. (2013) solved these problems (i.e., manual tuning and lack of heterogeneity) by demonstrating that also more realistic model configurations (i.e., recurrent random neural networks) can be trained to exhibit the desired activity patterns. Finally, these attractor models can also be used to mimic the conceptual models associated with accumulation-based decision making (i.e., evidence accumulation in RDM task; Wang, 2002), providing a possible link between both streams of research via biologically-inspired modeling (comprehensive review in Deco et al., 2013).

The time-order error

Remarkably, none of the available models of the frequency comparison task considers that the temporal order of stimulus presentation has a strong influence on choices in sequential comparisons (see Fechner, 1860). That is, in the vibrotactile comparison task, comparing 20 Hz with 24 Hz is not the same as comparing 24 Hz with 20 Hz – one of the presentation orders results in a higher proportion of correct responses than the other. Yet, a symmetry in performance between presentation orders is usually assumed for modeling or analysing behavioral data in this context (e.g., see Hellström, 2003 for an extensive critique). Early psychophysical work investigated and quantified the effect of temporal order in comparison tasks on the level of stimulus pairs, and referred to the mismatch in performance between presentation orders as the time-order error (TOE; or time-order effect; e.g., Fechner, 1860; Köhler, 1923; Lauenstein, 1933; Woodrow, 1935; Jamieson and Petrusic, 1975; comprehensive review in Hellström, 1985). Notably, the TOE varies across observers, and hence, needs to be quantified individually. Conceptually, the TOE was early on suggested to be caused by a shift/assimilation of the remembered first percept toward a reference value (e.g., Köhler, 1923; Lauenstein, 1933; Woodrow, 1935). Formally, this idea led to a model of "sensation weighting", which suggests that the two stimuli are weighted differently relative to a reference value (Hellström, 1985; see also Michels and Helson, 1954). This reference value was found to be closely related to the physical mean of the applied stimulus set (e.g., see Hellström, 1985), which has been consistently replicated in more recent work, including the vibrotactile frequency comparison task (e.g., Preuschhof et al., 2010; Karim et al., 2012; Sanchez, 2014). Consequently, the TOE, which is traditionally defined for a single stimulus pair, can also be embedded within a more global perspective. That is, in a sequential comparison task, observers appear to compare the second stimulus not only with the first stimulus, but also with the mean of all previously presented stimuli (i.e., the mean of the stimulus set over the course of an experiment). This idea can be readily incorporated within the framework of Bayesian inference (e.g., Ashourian and Loewenstein, 2011; Sanchez, 2014), however, the TOE is still largely neglected in the context of perceptual decision making (but see Preuschhof et al., 2010).

Vibrotactile frequency comparisons in humans

The literature on human perceptual decision making in the vibrotactile frequency comparison task is rather scarce (reviewed in Pleger and Villringer, 2013). Only a few fMRI studies are available that identified brain areas which were active during the different stages of the task (Preuschhof et al., 2006; Pleger et al., 2006; Li Hegner et al., 2007; Kostopoulos et al., 2007). The studies found that the BOLD signal increased during stimulus encoding in somatosensory cortices (SI and SII), prefrontal, and premotor areas (Preuschhof et al., 2006; Li Hegner et al., 2007), during the retention interval in prefrontal as well as in parietal areas (Preuschhof et al., 2006; Kostopoulos et al., 2007), and in SI, prefrontal, premotor and motor areas during the decision phase (Preuschhof et al., 2006; Pleger et al., 2006), in general agreement with the results from monkey electrophysiology. Moreover, Pleger et al. (2006) demonstrated that the absolute difference between the two stimulus frequencies scaled positively with the BOLD signal in left dlPFC for correct but not for incorrect trials. Together, the results from fMRI research are consistent with the findings from animal research, again, suggesting an additional role of dlPFC in perceptual decision making (see Heekeren et al., 2008).

In a series of EEG studies, Spitzer and Blankenburg showed that, in analogy to the work in monkeys, the encoding and working memory aspects of the vibrotactile comparison task can be recorded at the human scalp level in the form of large-scale oscillatory signatures (Spitzer et al., 2010; Spitzer and Blankenburg, 2011, 2012; Spitzer et al., 2014). Specifically, during the presentation of the flutter stimuli, somatosensory steady-state evoked potentials (SSEPs) were recorded from contralateral SI (e.g., Tobimatsu et al., 1999; Spitzer et al., 2010). That is, the EEG signal showed a power increase in the frequency band that corresponded to the stimulus frequency, temporally confined to the stimulus presentation. Possibly, these SSEPs directly reflect the phase-locked firing of neurons identified in monkey SI (e.g., see Hernández et al., 2000). During the retention interval of the task, Spitzer et al. (2010) found that upper beta band power ($\sim$20 – 30 Hz) in the PFC, specifically the right inferior frontal gyrus (IFG), increased with the frequency of the stimulus that was kept in working memory (i.e., f1; Spitzer and Blankenburg, 2011, 2012). Notably, these findings imply that the PFC represented the content kept in working memory, in analogy to the firing rate code known from monkey electrophysiology (see Romo et al., 1999). The role of prefrontal upper beta band in working memory processing was further generalized to other stimulus features, as well as to other

stimulus modalities in the context of the sequential comparison paradigm (Spitzer and Blankenburg, 2012; Spitzer et al., 2014). Moreover, impairing IFG function with TMS, deteriorated performance in a vibrotactile working memory task, providing causal evidence for the crucial involvement of IFG in working memory processing (Auksztulewicz et al., 2011).

Taken together, the results obtained from human studies, using both fMRI and EEG, are well in line with the seminal electrophysiology work in monkeys using the vibrotactile frequency comparison task. Here, the EEG results are of particular interest. EEG recordings provided the temporal resolution to investigate different stages of the task, and revealed oscillatory signatures that were directly related to according observations in the monkey data. Strikingly, however, no study has yet investigated the decision phase of the vibrotactile frequency comparison task using human M/EEG recordings, which was thus the first goal of the present thesis.

1.3 Aims of the thesis

The primary goal of this thesis is to bridge the gap between the work in monkeys and humans on perceptual decision making in the vibrotactile frequency comparison task (Studies 1 - 3). Furthermore, it aims at advancing the current understanding about how the two introduced major streams of research in the field can be brought closer together within an intentional framework of decision making (Studies 2 and 3). Finally, the thesis investigates whether the role of the CPP in perceptual decision making also generalizes to the vibrotactile frequency comparison task, and whether the CPP may hence indeed index a generic proxy of evidence for perceptual choices (Study 4).

2 Summary and Discussion of Results

In order to achieve the stated aims, 64-channel EEG data (BioSemi, ActiveTwo) was recorded in six experiments utilizing the vibrotactile frequency comparison task (see Figure 2.1). The six experiments varied in response modality, response timing, and response mapping, however, the comparison task per se remained the same in all variants. Participants were briefly presented with two vibrotactile stimuli to their left index finger (250 ms each, separated by 1000ms), and had to decide whether the frequency of the second stimulus (f2) was higher or lower than the frequency of the first stimulus (f1). All stimuli exhibited frequencies in the flutter range (i.e., 12 - 32 Hz), with f1 randomly taking 16, 20, 24 or 28 Hz, and f2 varying by $\pm$ 2 or $\pm$ 4 Hz. In Studies 3 and 4, also trials with identical stimulus frequencies were included in the experiments (i.e., f1 = f2). Participants were not aware of this possibility, and always indicated whether f2 > f1 or f2 < f1. Notably, in all experiments, participants completed over 1000 trials, yielding rich data sets for EEG analysis. In the following, I briefly summarize the main findings of each study, before giving a more detailed description and discussion of the individual study results. In Study 1 (Herding et al., 2016), participants were asked

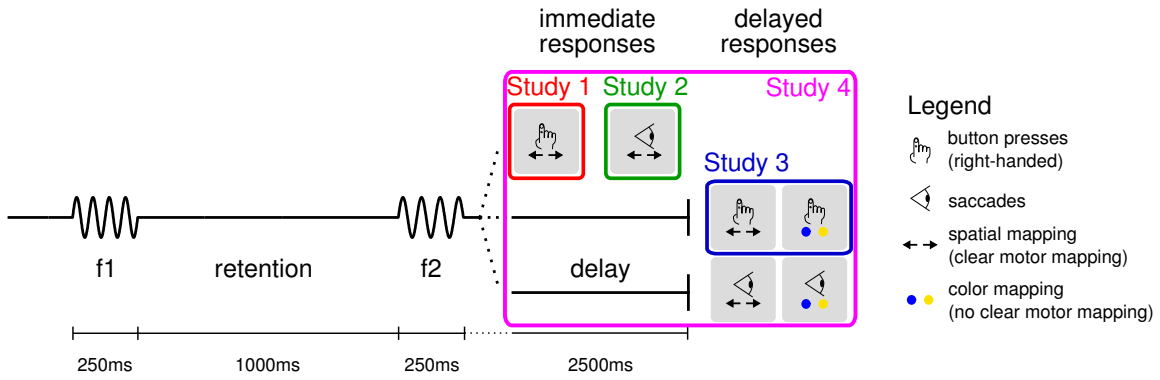

Figure 2.1: Overview of the studies presented in this thesis, and the according experimental designs. All experiments employed the same stimulus protocol, but varied in how participants were instructed to report their decisions. Each gray box refers to a single experiment. The colored frames indicate which experiment(s) were investigated in which of the four studies.

to report their decisions immediately after the presentation of the second stimulus by a button press. Upper beta band power[†], most likely originating from mPMC, was modulated by the choices of participants well before the decision report, irrespective of whether decisions were correct or incorrect. In particular, "f2 > f1" choices were accompanied by higher beta band power than "f2 < f1" choices, just as in monkey LFPs recorded from PMC (Haegens et al., 2011).

In the second study (Herding et al., 2017), the same setup was used, except that participants had to report choices by horizontal saccades. In line with the findings from Study 1, we found again that premotor upper beta band power was higher for "f2 > f1" choices than for "f2 < f1" choices for both correct and incorrect decisions. This time, however, a more lateral part of PMC was implicated as the most likely source of the modulation, importantly, including FEF. That is, in line with an intentional framework of decision making (see Shadlen et al., 2008), the same choice-informative signal as before was found (i.e., choice-modulated upper beta band power), again originating from the premotor structure that is involved in the ensuing decision report (i.e., in line with Study 1).

For Study 3 (Ludwig et al., *submitted*), a response delay was introduced to the experimental setup, forcing participants to postpone their decisions for 2500 ms. In particular, this study comprised two experiments. In the first experiment, decisions were associated with a fixed motor mapping as before (i.e., left vs. right button press), whereas in the second experiment, choices were associated with a spatially undetermined color-mapping. That is, participants selected targets via button presses based on the color of targets (i.e., yellow vs. blue), with each color indicating one of the choice alternatives (i.e., "f2 > f1" vs. "f2 < f1"). The colored targets only appeared at the end of the response delay – with equal probability on either side of a computer screen in front of the participants – eliminating the possibility of preparing a specific motor response beforehand. When a fixed motor mapping was given (i.e., no color-mapping required), effectively identical results as in Study 1 were found during the response delay. That is, upper beta band power over premotor areas was higher for "f2 > f1" than for "f2 < f1" choices. When choices were not associated with a well-defined motor response, i.e., a color-mapping was required, the same modulation of upper beta band power was observed, however, now over occipital/parietal regions. Also these findings can be interpreted in an intentional framework of decision making. In the absence of a clear motor mapping, choices

[†]Technically, we investigated spectral amplitude, i.e., the square-root transform of spectral power, in Studies 1 and 2 (see Herding et al., 2016, 2017 for details). For clarity, however, we will collectively refer to the observed effects as modulations of beta band power in this thesis.

needed to be mapped onto a more abstract intention, i.e., selecting a target on the left or on the right based on its color (see Shadlen et al., 2008). Such an abstract intention is most likely represented in parietal cortex (see de Lafuente et al., 2015; see also Andersen and Buneo, 2002), and cannot be passed along to premotor structures, as a specific motor response is not yet known (see microstimulation of FEF in Gold and Shadlen, 2003).

In Study 4 (Herding et al., *submitted*), EEG data from all experiments were pooled to investigate whether the idea of the CPP as a domain-general proxy of decision evidence also extends to the vibrotactile comparison task (see Kelly and O'Connell, 2015). That is, data from studies 1 - 3, as well as data from two more experiments, were analyzed together, yielding a total of 116 data sets from six experiments. The two additional data sets were recorded in a setup identical to the one of Study 3, however, requiring participants to respond with saccades instead of button presses (separate manuscript on oscillatory choice signatures in preparation). The CPP was indeed found to index evidence for decisions in the frequency comparison task, i.e., a modulation by the signed (perceived) difference between f2 and f1, immediately after the second stimulus. Later, however, the CPP switched to representing the absolute (perceived) difference between f2 and f1. This finding refines the current understanding of the CPP, and suggests that the CPP first represents the signed quantity on which a decision is based, and later the confidence in that decision.

2.1 Behavioral model of choices and confidence for all studies

In all of the experiments, we observed a strong influence of the TOE on choice behavior. That is, participants showed the tendency of comparing f2 not only with f1, but also with the mean of the stimulus set (f_{mean}; see 1.2.2 The time-order error). In other words, the quantity that determined choices in the given task could be best described by a difference between f2 and a representation of f1 that deviates from its physical value towards f_{mean}. Since we were interested in identifying EEG signatures that represented this very quantity on which decisions are based, we needed a formal description of these subjectively perceived frequency differences (SPFDs) for each stimulus pair and each participant. Therefore, we introduced a measure corresponding to a mean-biased version of f1 – which we will call $f1'$ – as a weighted average of the mean of all stimulus frequencies and the physical value of f1 (see also sensation weighting; e.g., Hellström, 1985; Michels and Helson, 1954):

$$f1' = w_s \cdot f1 + w_m \cdot f_{mean} \tag{2.1}$$

where w_s and w_m denote the respective weights for both quantities, with $w_s + w_m = 1$. We assumed that the difference between f2 and $f1'$ (i.e., $f2 - f1'$) is evaluated at the time of stimulus comparison, and can be conceived as an approximation of the SPFD driving choices for any given stimulus pair. In this intuitive formulation, the influence of the TOE is simply explained by the weight that is given to f_{mean} – the larger w_m, the larger the TOE.

Following the principles of SDT (i.e., a percept can be seen as a sample from a distribution centered on the true stimulus), this intuition can be readily implemented in the framework of Bayesian inference (see Figure 2A in manuscript of Study 4; Herding et al., *submitted*). That is, $f1'$ can be realized as the expected value of a Gaussian posterior distribution of f1, when assuming a Gaussian prior centered on the stimulus set (i.e., with mean f_{mean}). Note that in contrast to previous Bayesian models of the TOE (e.g., see Ashourian and Loewenstein, 2011; Sanchez, 2014; Petzschner et al., 2015), we assumed that only the remembered percept of f1 is shifted towards f_{mean} (i.e., $f1'$), whereas f2 is assumed to be perceived as it is. In other words, we propose that the perception of f1 (retrieval from working memory) is qualitatively different from the perception of f2 (newly arriving stimulus).[†]

Now, let σ^2_{stim} denote the variance of the likelihood function for a given stimulus (i.e., $1/\sigma^2_{stim}$ is the precision with which a stimulus can be encoded; identical for f1 and f2), and σ^2_{prior} the variance of the prior distribution (i.e., $1/\sigma^2_{prior}$ is the precision with which the mean of the stimulus set can be estimated), then

$$f1' = \frac{1}{\frac{\sigma^2_{stim}}{\sigma^2_{prior}} + 1} \cdot f1 + \frac{1}{\frac{\sigma^2_{prior}}{\sigma^2_{stim}} + 1} \cdot f_{mean}. \tag{2.2}$$

That is, in this Bayesian formulation, the ratio of σ^2_{stim} and σ^2_{prior} determines the weights that are assigned to f1 and f_{mean} for describing the perception of $f1'$, as introduced in eq. (2.1) (see also Ashourian and Loewenstein, 2011; Herding et al., 2016). We used variational Bayes, as imple-

[†]Also the first ideas of the mechanisms behind the TOE proposed this view (e.g, Boas, 1882; Köhler, 1923).

mented in the VBA toolbox (Daunizeau et al., 2014), to estimate σ^2_{stim}, σ^2_{prior} and an overall bias term (i.e., a decision criterion as known from SDT) for each participant based on individual choices. More precisely, we fitted the difference distribution between the likelihood function of f2 and the posterior of f1 to the observed proportions of "f2 < f1" choices for any given stimulus pair (for intuition see Figure 2A in manuscript of Study 4; Herding et al., *submitted*). Importantly, this model clearly outperformed a "null" model that was based on the physical frequency differences for nearly all recorded data sets (i.e., f2 − f1; Bayes Factors > 3 for 106/116 data sets; for details see manuscript of Study4; Herding et al., *submitted*).

One advantage of formulating the model in the framework of Bayesian inference, and drawing on concepts of SDT, is that the model parameters can be interpreted in a meaningful way. Although we did not exploit this possibility extensively in the presented studies, we could at least show that the estimated parameters were highly correlated with individual behavioral measures across participants in a sensible way. That is, we found that the precision with which participants were able to encode stimulus frequencies (i.e., $1/\sigma^2_{stim}$) correlated with their d' values. At the same time, the precision with which participants were assumed to represent the mean of the stimulus set (i.e., $1/\sigma^2_{prior}$) matched the size of the TOE, and predicted how much the suggested model would exceed the "null" model in explaining the observed choices (all correlation coefficients > 0.8; see Study 1; Herding et al., 2016). In other words, the introduced mechanism accounted for the influence of the TOE just as intended. To further explore the underlying mechanisms of the TOE, we suggest for future studies, to systematically vary the duration of the retention interval in the task, and to investigate how the TOE is affected by this. Many studies suggest that the TOE increases with longer retention intervals, however, the overall picture in the literature is rather diffuse (see Hellström, 1985 for review of early work; Preuschhof et al., 2010; Ashourian and Loewenstein, 2011). The presented model can be easily extended to incorporate an independent mechanism that explicitly accounts for the influence of varying retention intervals. That is, the precision of f1-representation (i.e., $1/\sigma^2_{stim}$) can be modeled to change over time until a comparison with f2 is computed, simply by introducing a multiplicative factor to σ^2_{stim} in eq. (2.2) (see Sanchez, 2014). A factor larger than one would correspond to an increase of the TOE, and might be associated with long retention intervals, whereas a factor below one would indicate a decrease of the TOE, possibly observed for short retention intervals. Hence,

this time-dependent mechanism would introduce an additional means to explain the varying impact of the TOE on choice behavior.

Another advantage of the Bayesian model formulation is its distributional form. That is, based on the difference distribution between the likelihood of f2 and the posterior of f1, we could compute a measure of confidence derived from SDT (e.g., Sanders et al., 2016; Hangya et al., 2016). In brief, the difference distribution allowed us to compute the average perceived evidence for correct and incorrect decisions, given any stimulus pair (i.e., the center of mass of the distribution on either side of the decision criterion; see Figure 2B in manuscript of Study4; Herding et al., *submitted*). The average perceived evidence, in turn, is proportional to the average confidence for a given (correct or incorrect) choice (see Sanders et al., 2016). Hence, we could also infer confidence levels based on our behavioral model without having recorded explicit confidence ratings (see manuscript of Study 4).

Finally, it should be noted that the suggested model is formulated in very generic terms. That is, there is no apparent reason to assume that it is specific to the vibrotactile frequency comparison task. In fact, a similar Bayesian account was used to explain the influence of the TOE (or contraction bias, as it is called by the authors) on choices in sequential comparisons of two visually presented lines (i.e., a comparison of their lengths; Ashourian and Loewenstein, 2011). Furthermore, we suggest that the proposed model might also extend beyond the scope of mere perceptual comparison tasks. In particular, we argue that, as soon as two quantities have to be compared in a sequential fashion, the here described mechanisms of Bayesian inference should apply. In other words, we predict that the TOE should also be observed in sequential comparisons of two (continuously quantifiable) values that are not solely driven by sensory input. Indeed, we found preliminary evidence that choosing one of two sequentially presented snacks is affected by the TOE in the same way (however, weaker) as choices are affected in the vibrotactile frequency comparison task (see also Hogarth and Einhorn, 1992; Trueblood and Busemeyer, 2011 for further examples of the TOE beyond perceptual comparisons). These promising results are planned to be pursued in future research, investigating whether also the here identified correlates in the EEG signal extend beyond perceptual decisions.

2.2 Study 1 - Upper Beta Band Oscillations in Human Premotor Cortex Encode Subjective Choices in a Vibrotactile Comparison Task

As reviewed in the Introduction, the vibrotactile comparison task has been studied extensively in non-human primates using electrophysiological recordings, leading to one of the most complete understandings of the processes involved in perceptual decision making (see Romo and de Lafuente, 2013 for review). Human EEG recordings, on the other hand, have only investigated correlates of working memory processes in this task until now (e.g., Spitzer et al., 2010). In the initial study (Herding et al., 2016), we hence aimed at filling this void, and tried to link the previous human EEG findings (i.e., on working memory) with the work in monkeys (on decision making). In particular, upper beta band power in human EEG recordings was found to represent the working memory content during the retention interval of the vibrotactile frequency comparison task (i.e., f1; e.g., see Spitzer et al., 2010). At the same time, beta band power in LFPs recorded from PMC encoded choices of monkeys during the decision phase of the task (Haegens et al., 2011). Here, we investigated whether these findings can be brought together, i.e., whether the results from monkey research are directly transferable to human EEG recordings.

We recorded 64-channel EEG data while participants completed the vibrotactile frequency comparison task introduced above. Participants were asked to indicate whether f2 > f1 or f2 < f1 via button presses, always with their right hand, i.e., index vs. middle finger button presses. Importantly, the response mapping was counterbalanced across participants to avoid a direct mapping of choices onto button presses, which might have been associated with specific motor preparatory signals. In order to investigate oscillatory signatures of decision making, we analyzed time-frequency transformed, response-locked EEG data. That is, we examined at which frequencies spectral power correlated with the differences between f2 and f1 before responses were given. In particular, we used subjectively perceived frequency differences (SPFDs) between f2 and f1 (i.e., $f2 - f1'$) as estimated from our Bayesian model (see 2.1 Behavioral model above).

We found that upper beta band power ($\sim$20 - 30 Hz) in medial-frontal electrodes (FCz, FC2, C2) was modulated by SPFDs well before decisions were reported ($\sim$750 - 350 ms before responses were given). Importantly, the modulation changed its sign between correct and incorrect trials. That is, for correct decisions, beta band power was positively correlated with SPFDs, whereas for incorrect

decisions, a negative correlation was observed. Investigating these relations more closely, revealed that the modulation was in fact driven by participants' choices and not by the graded values of SPFDs. More precisely, upper beta band power could be divided into two classes. Higher power was associated with "f2 > f1" choices, whereas "f2 < f1" choices were accompanied by relatively lower power – irrespective of whether choices were correct or incorrect. Moreover, when analyzing the data separately for both response mappings, we found the same modulation with very similar scalp topographies for both mappings, suggesting that the choice signal in the beta band was likely independent of the specific motor response. A source reconstruction implicated mPMC (also known as supplementary motor area, SMA) as the most likely origin for the effect observed at the scalp level.

Remarkably, our results were qualitatively the same as reported for monkey LFPs. That is, frequency band, location, and the modulation per se (i.e., "f2 > f1" choices associated with higher beta band power than "f2 < f1" choices) were in fact identical (see Haegens et al., 2011). Beyond this notable agreement, our data even imply that the choice-selective beta band modulation is specific to premotor structures, as we found it by analyzing a globally recorded signal. Moreover, our findings align well with previous human EEG work on oscillatory signatures of working memory processes: upper beta band power was found to scale with f1 during the retention interval of the task (e.g., see Spitzer et al., 2010). These findings, together with our results, suggest that upper beta band oscillations might index the quantity that is relevant at different stages of the vibrotactile comparison task. Notably, this interpretation of upper beta band oscillations is markedly different from the classic sensorimotor beta band, which is also used to study decision making. That is, power decreases over contralateral primary motor cortex are reliably found to reflect the accumulating evidence for a decision when choices are reported by lateralized button presses (e.g., see Donner et al., 2009; O'Connell et al., 2012). Nevertheless, sensorimotor beta band activity and the identified upper beta band activity in premotor structures are not mutually exclusive. The here reported premotor signal might indicate the categorical decision outcome, i.e., the content on which a decision is based, which is ultimately transformed into a specific motor response, possibly detectable in classic sensorimotor beta signals, such as the lateralized power decrease.

In sum, Study 1 successfully linked human and monkey research, and additionally, extended the

previously identified role of upper beta band oscillations from working memory processes to decision making.

2.3 Study 2 - Response-Modality-Specific Encoding of Human Choices in Upper Beta Band Oscillations during Vibrotactile Comparisons

In the context of the vibrotactile comparison task, the work in non-human primates, as well as our previous study (Study 1), was restricted to investigating decisions that were reported by button presses. In the visual domain on the other hand, a large body of work focused on perceptual decisions that were reported by saccades, finding that oculomotor brain regions play a central role in decision formation (e.g., see Gold and Shadlen, 2007 for review). These studies gave rise to the formulation of an intentional framework of decision making, which proposes that decisions are represented as intentions to act in brain structures that are associated with the execution of the decision report (see Shadlen et al., 2008). The previous findings from both monkey and human research in the context of the vibrotactile comparison task, are also in general agreement with an intentional framework of decision making, as choice-related signals were consistently found in mPMC/SMA (e.g., see Hernández et al., 2002; Haegens et al., 2011; Herding et al., 2016). Here, we aimed at directly relating the findings from oculomotor decision making to the work in the somatosensory domain. In particular, we probed whether the previously reported choice-selective upper beta band modulation is only observed for button press responses (see Haegens et al., 2011; Study 1; Herding et al., 2016), or whether it is preserved when saccades are used for responding. If it is preserved, will it be transferred to the oculomotor system in accordance to an intentional framework of decision making?

We applied the same experimental setup as in Study 1, however, asked participants to indicate decisions by horizontal saccades instead of button presses. Again, choices were dissociated from specific motor responses by counterbalancing the choice-to-saccade mapping across participants. Based on the findings from Study 1, i.e., beta band power was modulated by participants' choices and not by the graded SPFDs, we contrasted time-frequency transformed EEG data directly between

choices, including both correct and incorrect trials in the analysis.

We found that upper beta band power (∼24 - 32 Hz) in frontal electrodes (FC2, FC4) was modulated by choices clearly before decisions were reported (∼ 750 - 450 ms prior to decision report) – just as observed in Study 1. That is, "f2 > f1" choices were accompanied by higher power than "f2 < f1" for correct as well as for incorrect decisions. By inspecting the time courses of upper beta band power, extracted for different levels of SPFDs, we could furthermore confirm that the modulation was indeed categorical (i.e., by choice), and not driven by the graded SPFDs. Moreover, a separate analysis of the data for either fixed saccade-to-choice mapping, yielded again very similar scalp topographies of the choice-modulated beta band signal, corroborating the notion that the modulation is independent of a specific motor response. Finally, the most likely cortical sources of the effect were located again in premotor areas, however, in more lateral parts as in Study 1, now, including FEF.

These results confirmed our previous findings (Study 1) by showing that the choice-selective modulation of upper beta band power was also present for a different response modality. Additionally, our findings suggest that the beta band signal might indeed be effector specific in accordance to an intentional framework of decision making (see Shadlen et al., 2008). That is, the most likely sources of the effect were now located in FEF, which is known to be involved in saccade planning (e.g., Schall et al., 1995). Moreover, FEF is also long known to be involved in decision formation, however, typically in accumulation-based decision making in the visual domain (e.g., see Glimcher, 2003; Gold and Shadlen, 2007). Here, we could show for the first time that when the vibrotactile comparison task is combined with oculomotor responses, a choice-indicative signal known from a different response modality (i.e., upper beta band power), is simply transferred to the new response modality (i.e., saccades).

In sum, Study 2 confirmed the findings from Study 1 in all aspects, and extended them to a new response modality that has never been probed in the context of vibrotactile comparisons before. Hence, the results from this study established a direct link between the two major lines of research in perceptual decision making (i.e., Romo's work on vibrotactile comparisons and Shadlen's work typically based on oculomotor responses), and provided further evidence in favor of an intentional interpretation of perceptual decisions.

2.4 Study 3 - Oscillatory EEG Signatures of Postponed Somatosensory Decisions

In Studies 1 and 2, decisions were followed by an immediate and well-defined motor response. However, in a more realistic setting, decisions are usually neither associated with a direct motor response, nor is the ensuing action fully defined at the time of a decision. Such rather abstract decisions, which are decoupled from a specific motor response, were targeted in the current study. Research with monkeys utilizing the RDM task showed that LIP is also involved in the formation of these abstract decisions (Bennur and Gold, 2011). That is, monkeys were trained to map decisions onto a color code, and report choices by making a saccade to one of two targets, selecting a target according to its color (e.g., if leftward motion, chose green target). Importantly, the color of targets was dissociated from the target locations, and was only revealed either before, during or after stimulus presentation. Firing rates of LIP neurons encoded the evidence for a decision even before the targets' colors were disclosed, i.e., before the monkeys knew to which target a saccade had to be prepared. On the other hand, FEF does not seem to have access to decision-relevant information in such a scenario (see Gold and Shadlen, 2003). Microstimulating FEF during stimulus presentation evoked saccades that were biased towards the later selected target, i.e., saccades that incorporated decisional evidence, however, only when a fully defined motor mapping was provided beforehand, but not when a mapping onto a spatially undetermined color code was required. In the current study, we adapted a similar color mapping scheme to the vibrotactile comparison task, and compared it with a direct motor mapping in the same task. In other words, we investigated how choice-selective signals in the EEG signal might be influenced by varying the consequences of the decision outcome, i.e., a mapping onto a well-defined motor response or onto a color code.

This study comprised two experiments, both deploying the same vibrotactile comparison task as in Studies 1 and 2, this time, however, with a response delay. We recorded EEG data while participants completed one of these two variants, which differed from each other in that choices were either reported according to a fixed spatial mapping (i.e., select left vs. right target via button press) that was consequently also associated with a fixed motor mapping (i.e., press left-arrow vs. press right-arrow), or according to a color mapping (i.e., select blue vs. yellow target via button press). That is, 2000 ms after the presentation of f2, two target dots appeared on the left and on the right

side of a screen in front of the participants. On each trial, one of the targets was blue, whereas the other target was yellow (counterbalanced across trials). After another 500 ms, a response cue was provided, and participants reported their decisions. For the experiments with a fixed spatial mapping, the colors of the targets were irrelevant and choices were reported by selecting a target according to its location (e.g., if "f2 > f1", chose left target). Analogously, for the experiment with a color mapping, choices were indicated by selecting a target based on its color (e.g., if "f2 > f1", chose yellow target). Importantly, the response rules were counterbalanced across participants in both experiments to fully dissociate decisions from the decision report. Another novelty in the current study (as compared to Studies 1 and 2) comprised the presentation of trials with two identical stimulus frequencies (i.e., f1 $=$ f2) in 25% of all comparisons. Participants were not aware of this possibility, and were instructed to always respond whether f2 > f1 or f2 < f1. For the analysis of EEG data, we contrasted the time-frequency transformed EEG signal between both choice alternatives (including correct and incorrect trials) to identify time-frequency windows in which spectral power was modulated by participants' choices. Additionally, we were interested in whether also f1 or f2 alone might be represented by oscillatory signals during the response delay, in analogy to the identified working memory processes during the retention interval of the task (e.g., Spitzer et al., 2010).

For the experiment with a fixed spatial/motor mapping, we found essentially the same modulation of upper beta band power as reported in Study 1. That is, after the presentation of f2, but before the response cue, upper beta band power in medial prefrontal electrodes (11 electrodes; strongest in F1, F2, AF4) was higher for "f2 > f1" choices as compared to "f2 < f1" choices, for both correct and incorrect decisions (including trials with f1 $=$ f2). The most likely sources of this modulation were again located in premotor areas. When no well-defined motor mapping was provided, and a color mapping was required, we still found the same choice-selective modulation of upper beta band power, however, in parietal electrodes (CP3, CP1, CPz, CP2, CP4, and Pz). A source reconstruction of this effect suggested PPC as the most likely origin. In addition to these choice effects, we also found that f1 and f2 alone were indexed by upper beta band power in right prefrontal electrodes (AF4, F2, F4, F6, FC6, FC4, FC2) after the presentation of f2, but before the choice-selective modulation was observed.

Our findings again confirm the notion of upper beta band power indexing choices in the vibrotactile

comparison task, notably, also when responses are postponed, and even when no well-defined motor response is associated with a choice. Depending on whether a motor response could be prepared or not (fixed spatial mapping vs. color mapping), this modulation was either observed in PMC or in PPC. Arguably, the color-mapping condition also provided some spatial information about the ensuing choice (i.e., target dots were always at same locations). A choice-informative signal in PPC can hence be related to the idea of parietal areas implementing intentional or saliency maps of the visual field (e.g., see Andersen and Buneo, 2002). Moreover, these findings align well with results from monkey electrophysiology that also found decision signals in premotor structures only when a specific motor mapping was provided (Gold and Shadlen, 2003). Otherwise, parietal areas showed decision-related neural activity (Bennur and Gold, 2011). The modulation of upper beta band power by f1 and f2 during the response delay, nicely extends the previous findings on working memory processes associated with beta band power (e.g., Spitzer et al., 2010). That is, the response delay arguably constitutes an additional working memory phase in the given task, and during this delay, apparently not only the decision outcome, but also the quantities that were used to compute this outcome were still maintained. The availability of this information might allow for a flexible re-evaluation of the decision at later times.

In sum, Study 3 showed that the choice-selective modulation of beta band power is also present when decisions are not associated with an immediate and fully defined motor response. Moreover, the obtained results support the notion of distinct roles for premotor and parietal areas during decision formation, dissociating both sites based on the decision consequences (i.e., a motor response vs. a more abstract mapping).

2.5 Study 4 - Centro-parietal EEG Potentials in Perceptual Decision Making: From Subjective Evidence to Confidence

In Studies 1 - 3, we successfully identified oscillatory signals in the human EEG that indexed participants' choices in the vibrotactile frequency comparison task. In a number of different response contexts, we consistently found that upper beta band power was modulated by the categorical decision outcome of the comparison between f1 and f2. That is, we identified a binary modulation

of beta band power: "f2 > f1" choices were always associated with higher beta band power than "f2 < f1" choices. However, we did not observe any signal that corresponded to the graded SPFDs between f1 and f2 (i.e., $f2 - f1'$), although this signed quantity needs to be evaluated in order to make an informed choice. In fact, it can be seen as the evidence for a decision in the vibrotactile comparison task. Recently, a series of studies suggested that the CPP in the human EEG signal (most likely identical to the classic P300) serves as a domain-general proxy of accumulating evidence in perceptual decision making (see review in Kelly and O'Connell, 2015). In particular, these findings suggest that the CPP might correspond to a similar accumulation-to-bound signal as known from monkey LIP recordings (but see Philiastides et al., 2014). Notably, these previous studies were constrained to experimental setups in which unsigned evidence had to be evaluated, and hence, also the CPP could only be related to this form of undirected evidence. For instance, in a RDM task, the CPP indexed the proportion of coherently moving dots, however, ignoring the direction of motion (i.e., same modulation by coherence for leftward and rightward motion; Kelly and O'Connell, 2013). In the current study, we examined whether the CPP might also index directed or signed evidence. In particular, we probed whether the CPP might represent the signed quantity that underlies decision making in the vibrotactile comparison task, i.e., SPFDs. Since decisional evidence in the given task is represented by a signed quantity, we additionally investigated how the absolute strength of evidence, i.e., the absolute values of SPFDs, might influence the EEG signal. In fact, these absolute values correspond to a measure of confidence based on SDT that was shown to be a valid proxy of explicit confidence ratings (i.e., statistical decision confidence; Sanders et al., 2016; also see 2.1 Behavioral model and Figure 2 in manuscript; Herding et al., *submitted*).

We pooled the data from Studies 1 - 3, plus two additional data sets obtained from two experiments identical to those described in Study 3, however, requiring saccade responses. This gave us in total 116 EEG data sets of participants completing the vibrotactile frequency task. The varying response contexts across tasks were only interesting as to investigate whether the CPP indexes evidence independent of different response requirements. We used SPFDs as well as their absolute values as covariates in a multiple regression analysis of broadband single-trial EEG data, to separately assess the influence of both measures on the CPP.

For all response contexts, we consistently found that, immediately after f2, the CPP was modu-

lated by the signed SPFDs, and later by the absolute values of SPFDs. Strikingly, the early modulation was also observed when only trials with two identical stimuli were considered (i.e., f2 $=$ f1). That is, in these trials, no objective frequency differences were present (i.e., f2 $-$ f1 $= 0$). However, our behavioral model predicted non-zero SPFDs (i.e., f2 $-$ f1$'$ $\neq 0$), which modulated the CPP even in the absence of any objective evidence. Notably, all modulations by SPFDs were only observed for correct trials, associating a successful discrimination of f1 and f2 with an accurate representation of the perceived frequency difference in the CPP. Moreover, we found that the early CPP (i.e., during the modulation by signed SPFDs) was correlated with the choice-indicative level of upper beta band power known from the previous studies – at least for those studies that required an immediate transformation of evidence into a motor response (Studies 1 and 2). Based on the framework of statistical decision confidence, we furthermore found that the late CPP corresponded to a valid measure of confidence. That is, the amplitude of the late CPP (1) correlated with performance; (2) increased with increasing evidence (i.e., higher absolute values of SPFDs) for correct trials, but decreased for incorrect trials; (3) was at the same intermediate level for correct and incorrect trials if evidence was at its lowest (i.e., absolute values of SPFDs ≈ 0); and (4) predicted performance even when the same amount of evidence was provided. Lastly, the most likely cortical sources of the observed effects were located in overlapping parts of IPS for both the early and the late modulation, and additionally in IFG, only for the late modulation.

Our findings corroborate the notion that the CPP is involved in perceptual decision making, however, the simplistic interpretation as an accumulation-to-bound signal might need to be refined based on our results. That is, we suggest that the CPP first indexes the (signed) quantity on which a decision is based, and then switches to indicate the confidence that the decision was correct. In support of the interpretation of the late part of the CPP, EEG decoding studies also showed that a similar parietal potential scales with certainty in decision making around the time of a decision report (Philiastides et al., 2014; Gherman and Philiastides, 2015). Notably, the refined interpretation of the CPP is not at odds with previous results (e.g., see Kelly and O'Connell, 2015). We argue that a distinct modulation of the CPP by evidence and confidence was simply overlooked up to now (or rather, could not be detected), due to the experimental settings that were used to study the CPP. In particular, previous studies used tasks in which unsigned/undirected evidence had to be evaluated,

confounding evidence with confidence. In contrast, we used a comparison task, in which decisions were informed by a signed quantity, allowing for a natural distinction between the signed and the absolute value of this quantity – which in turn index different measures (i.e., evidence and confidence, respectively). Besides refining the notion of the CPP, our data possibly provide the missing graded evidence signal in the vibrotactile frequency comparison task. That is, in line with the distinct roles of the nodes in a fronto-parietal network subserving perceptual decision making (see Hanks et al., 2015), we found that a parietal signal indicated a graded evidence signal, which was additionally correlated with a categorical choice signal in premotor areas (Studies 1 and 2).

In sum, Study 4 suggests a refined interpretation of the CPP during perceptual decision making, first indexing evidence, and later confidence. Additionally, the results provide, for the first time, a graded evidence signal in PPC during decision formation in the vibrotactile comparison task.

3 General Discussion

By scrutinizing the vibrotactile frequency comparison task, this thesis aimed at (i) closing the gap between monkey and human data, (ii) providing first evidence for a direct link between the two major streams of research in perceptual decision making via an intentional framework (i.e., a link between Romo's and Shadlen's work), and (iii) examining the role of the CPP in sequential comparisons.

(i) In remarkable agreement with the monkey literature, we found that upper beta band power indexed participants' choices for correct and incorrect decisions in the vibrotactile comparison task. That is, frequency band (upper beta band), location (premotor structures, if choices were associated with a fixed motor mapping), and the overall pattern (i.e., increased upper beta band power for "f2 > f1" choices as compared with "f2 < f1" choices) of this large-scale oscillatory signature were in fact identical to a previously identified choice signal in monkey LFPs (Haegens et al., 2011). Moreover, we were able to show for the first time that this particular choice signal also generalizes to novel response modalities (i.e., saccades), as well as to more abstract decision consequences (i.e., a color mapping). Specifically, the choice-selective modulation of upper beta band power was relocated to according effector-specific (or consequence-implementing) brain structures in these scenarios (i.e., to FEF and PPC, respectively). Hence, the choice-informative signaling in upper beta band power might indicate a common theme for providing the relevant input to those brain areas that are responsible for the realization of a decision.

(ii) By combining the vibrotactile comparison task with saccade responses, which are usually used in visual, accumulation-based decision making, we were able to directly compare the findings from both of these major paradigms in perceptual decision making (i.e., oculomotor decision making vs. vibrotactile comparisons; e.g., see Glimcher, 2003; Gold and Shadlen, 2007; Romo and de Lafuente, 2013). As noted before, when saccades were used for indicating decisions in the vibrotactile comparison task, the choice-indicative beta band signal was observed in an according effector-specific

premotor area (i.e., FEF), which has also been strongly implicated in forming decisions based on visual evidence-accumulation (e.g., see Glimcher, 2003; Gold and Shadlen, 2007). Hence, we could effectively link both major streams of research within an intentional framework of decision making. Moreover, we were able to show that the notion of an intentional framework of decision making also covers more abstract intentions, such as the intention to chose a target of a certain color (based on the outcome of a comparison between two vibrotactile stimuli).

(iii) Finally, the link between the two major lines of research could be further intensified by revealing that the CPP also indexes decisional evidence in the vibrotactile frequency comparison task. While the CPP is well-known to track an evolving evidence signal in accumulation-based decision paradigms (e.g., see review in Kelly and O'Connell, 2015), it has never before been reported in a 2-AFC comparison task. In particular, we were able to demonstrate that the CPP not only indexes evidence for a decision in these tasks, but likely also the confidence in the corresponding choice afterwards. That is, our data corroborate the notion that the CPP indexes evidence for perceptual decisions. At the same time, however, the novel insight that the CPP might convey more information than previously thought, demands for a refined interpretation of the CPP in decision making.

Since the individual study results were already discussed in the previous section, in the following, the broader implications of the overall findings are discussed in the context of prevailing theories of perceptual decision making.

3.1 The role of (upper) beta band activity in perceptual decision making

The most prominent motif of our findings is the involvement of (upper) beta band activity during decision formation. However, the functional role of beta band activity in general is still unclear and highly debated. When beta band oscillations are associated with perceptual decision making, mostly the classic sensorimotor beta rhythm is concerned ($\sim$ 15 - 25 Hz). That is, prior to a voluntary limb movement, power in this lower beta range is known to decrease over contralateral motor areas – specifically over the primary motor cortex (MI) – in preparation of a motor act, and to rebound afterwards (e.g., see Jasper and Penfield, 1949; Pfurtscheller, 1981). The preparatory part is often

exploited to investigate an evolving decision variable. In particular, experiments are designed in such a way that participants are required to report decisions with their right or with their left hand in order to distinguish between choice alternatives. Remarkably, the lateralized decrease in beta band power over contralateral MI was found to scale with the accumulating evidence for a decision in this setting (e.g., Donner et al., 2009; O'Connell et al., 2012). In our studies, however, participants were required to always respond with their right hand (Studies 1 and 3), or by making a saccade to a visual target (Study 2), effectively ruling out that we might have simply observed a variant of the classic sensorimotor beta band desynchronization.

Notably, beta band power was also reported to scale with accuracy of perceptual judgments (Donner et al., 2007). In particular, it was higher for correct than for incorrect decisions during a RDM task in brain areas along the the dorsal visual pathway (i.e., MT, IPS and dlPFC). The authors explicitly emphasized that the observed beta band signature did not reflect a representation of the content on which a decision was based, but rather that this form of modulation by accuracy "*indexes the computations transforming such representations into actions*" (Donner et al., 2007). Hence, although this interpretation at least suggests an active role in cognitive processing for beta band activity, the given interpretation contradicts the representational modulation of upper beta band power as observed in our data. Possibly, the relation between beta band power and accuracy, with a likely source also in dlPFC, suggests a link to the fMRI findings that identified the same region to exhibit a higher BOLD signal for easy trials as compared to hard trials (Heekeren et al., 2004, 2006). Accordingly, we also found a modulation of prefrontal beta band power by performance (i.e., increased beta power for correct as compared with incorrect decisions), however, only after a decision was reported and according performance feedback was provided (unpublished observation in Studies 1 and 2). In sum, this form of beta band signature can possibly be associated with a feedback (i.e., top-down) signal exerting some form of cognitive control. Notably, such a role is typically also ascribed to beta (or alpha) band oscillations in (micro)circuit models (e.g., see Wang, 2010 for comprehensive review).

Engel and Fries (2010) tried to unify the sensorimotor and cognitive aspects of beta band activity, by suggesting that the beta band might signal the status quo in both domains. In particular, in both sensorimotor and cognitive contexts, beta band activity should remain the same if no changes occur, should decrease if a novel, unpredicted event occurs, and should increase if the current state has to

be actively maintained. This generalized formulation can account for both signatures of beta band activity as described above, however, it cannot account for the content representation in upper beta band power as observed in the vibrotactile frequency comparison task. Recall that beta band power was always higher for “f2 > f1” choices than for “f2 < f1” choices, irrespective of whether decisions were correct or incorrect. In other words, upper beta band power indicated the perceived outcome of the comparison between f1 and f2 – already categorized according to the two choice alternatives – as we argue, to inform the ensuing decision consequence (i.e., either a motor response or a color mapping). Additionally, we found that also f1 and f2 alone were indexed by prefrontal upper beta band power after the presentation of f2, during a response delay (Study 3). This signature of upper beta band activity is well in line with previous human EEG studies that found prefrontal upper beta band power to scale with f1 during the retention interval between both stimuli (e.g., Spitzer et al., 2010). Together, these findings imply that upper beta band power might index task-relevant content during different stages of the task (see also Herding et al., 2016). In particular, given the respective brain structures, in which the modulations were observed, upper beta band activity might reflect the input to the brain systems that are responsible for further processing of the relevant content. That is, PFC for an update of working memory, mPMC for informing button press responses, FEF for informing saccade responses, and PPC for informing a mapping onto a (spatially constrained) color code.

Based on the close correspondence to the large body of work on electrophysiological data in monkeys, we suggest a pragmatic approach to interpreting the observed beta band modulations. That is, we propose that beta band oscillations (in LFPs and EEG) directly reflect the known firing rate code, only recorded on a larger scale. Hence, finding a link between the firing rate code and an according modulation of power in the beta band can provide a mechanistic explanation of the observed large-scale effects. Recall that a network model, utilizing varying attractor states, is readily available to account for the firing rates observed at different stages of the vibrotactile comparison task (Machens et al., 2005; Barak et al., 2013). Therefore, a straightforward idea would be to extend the underlying mechanisms of the model to account for oscillatory signals. Although technically demanding, conceptually, this would simply mean to model the attractor states at different stages of the tasks as stable limit cycles instead of stable fixed points (e.g., see Breakspear, 2017 for review

on dynamical systems for large scale activity). Even if such a model could be constructed, it would be based on the assumption that ongoing beta oscillations are modulated at different stages of the task. However, whether beta band oscillations are indeed ongoing during active cognitive processing is currently questioned (Sherman et al., 2016). In particular, the authors found that in human and animal data (monkeys and rats), beta bursts, whose exact timing is variable across trials, can lead to the impression of ongoing oscillations when analyzing trial-averaged data. Moreover, they provided a biologically-inspired network model that was able to reproduce the observed beta bursts in both human and animal data with remarkable detail. Most interestingly, the suggested model links the firing rates of certain neurons in the proposed network with the amplitude (i.e., oscillatory power) of the beta bursts. That is, this model provides a possible mechanism to directly link firing rate modulations, as known from the seminal work of Romo and colleagues (see Romo and de Lafuente, 2013), to the oscillatory signals observed in LFP and EEG recordings (see Haegens et al., 2011; Herding et al., 2016, 2017). Future work, however, will need to clarify in a first step whether the observed modulations in beta band activity are indeed driven by underlying bursting activity or rather by ongoing oscillations.

In sum, the modulation of upper beta band power that we observed in the vibrotactile comparison task is not captured by any of the popular theories of beta band activity. Therefore, we propose to take the signal as it is: neural activity that indexes task-relevant content at different stages of the task. Such a signal is well-known from single-neuron firing rates in monkeys, notably, in corresponding brain areas. Hence, instead of relating the observed beta band modulation to existing theories, the goal should be to find a mechanistic explanation of how firing rate modulations translate into modulations of beta band power. To this end, pursuing the idea of beta band bursting seems currently very promising.

3.2 The fronto-parietal network in perceptual decision making

Animal research – mostly focusing on oculomotor decisions – implicated a fronto-parietal network underlying decision formation (e.g., Glimcher, 2003; Gold and Shadlen, 2007). Importantly, the involved areas were also associated with the preparation and planning of the decision report, leading to the formulation of an intentional framework of decision making (Shadlen et al., 2008; see also

Cisek, 2007). Moreover, recent studies suggested a gradual change in the decision signal from parietal to frontal areas (Hanks et al., 2015). In particular, parietal areas appeared to signal a more detailed, graded evidence signal, whereas frontal (motor) areas were found to index a categorical choice signal. In full accordance with these results from animal research, we found a graded evidence signal in parietal areas (i.e., the early CPP; Study 4), and a categorical choice signal in frontal premotor structures – or more generally speaking – in brain areas that implemented the consequences of a decision (i.e., choice-selective modulation of beta band power; Studies 1 - 3). In other words, our data suggest that the term "fronto-parietal" network might need to be refined in order to account for a more functional distinction of involved brain areas.

3.2.1 Do parietal areas serve as a quantity processing module?

Whereas the here reported categorical choice signal was effectively identical to known signatures from monkey research (i.e., the choice-selective upper beta band modulation), the parietal signal indicating fine-grained evidence (i.e., the CPP) revealed some interesting novel aspects when compared to the literature. That is, previous studies investigated the CPP in experimental paradigms that required the accumulation of undirected evidence, and found that the CPP scaled with this unsigned quantity (see Kelly and O'Connell, 2015). For instance, in a RDM task, the CPP indicated the perceived proportion of coherently moving dots, but concealed the according motion direction (Kelly and O'Connell, 2013). Based on these findings, the CPP was interpreted as an accumulation-to-bound signal in line with the seminal work in monkeys by Shadlen and colleagues (but see Philiastides et al., 2014). Here, in the vibrotactile comparison task, however, the CPP first scaled with a signed quantity that corresponded to the evidence for a decision, and later with the absolute value of the quantity, likely indexing confidence. Notably, these findings are at odds with an interpretation of the CPP as an accumulation-to-bound signal. Presumably, this exciting revelation was only possible, because we applied a paradigm, in which decisions were based on the comparison of two (abstract) quantities (f2 vs. f1), rather than on judging noisy sensory input presented over time. Specifically, we propose that a decision in a 2-AFC comparison task is based on evidence that can be expressed on the same continuous axis for both choice options, with the alternative options being distinguished by opposing signs. Hence, the evidence for a choice can be computed as a single signed quantity.

In an accumulation-based 2-AFC task, on the other hand, we suppose that evidence is represented on two distinct, strictly positive axes, one for each alternative (e.g., proportion of rightward motion and proportion of leftward motion). As a result, two strictly positive quantities (i.e., absolute values) that index the evidence for either choice alternative would need to be computed separately.[†] Assuming that the (absolute) strength of evidence is a valid proxy for confidence, evidence and confidence are indistinguishable in this scenario. Consequently, distinct neural processes underlying these two measures can hardly be resolved using tasks with indistinguishable measures of evidence and confidence. Taken together, the novel modulations of the CPP in our data (i.e., first signed, then absolute evidence in a comparison task), as compared to previous work (i.e., only absolute evidence for accumulation-based decisions), can possibly be explained by the suggested differences in evidence representations in the respective tasks. In particular, in accumulation-based decision making, the CPP might reflect the sum of the independently computed positive quantities indicating the evidence for either choice option (possibly implemented by two competing neuronal populations; see Mazurek et al., 2003; Shadlen and Kiani, 2013), whereas in comparison tasks, the CPP might indicate a single signed quantity. As a simple, testable prediction of our interpretation, we expect the same modulations of the CPP as reported here in an oddball paradigm with 'deviant' stimuli varying in both directions (on a quantitative scale) from the 'standard', potentially only if the sign of the deviation has to be reported (i.e., a direct extension to Twomey et al., 2015).

Assuming that our hypothesis of different evidence representations in accumulation-based decisions and explicit comparisons is true, this would further imply that, depending on which experimental paradigm is deployed, *every* neuronal decision signal should differ accordingly. In particular, one might wonder whether a change in experimental paradigm (i.e., using a comparison task instead of a RDM task) would reveal different neuronal activity in monkey PPC as well? That is, would those neurons that usually track the accumulating evidence for a decision index the signed quantity reflecting a comparison instead? Unfortunately, Romo and colleagues never recorded from those PPC areas in question (i.e., intraparietal areas) during the vibrotactile comparison task, however, research on the "sense of number" has probed these areas in a very similar context, i.e., in a delayed-match-to-sample paradigm (e.g., see Nieder and Dehaene, 2009 for a recent review; see Nieder, 2017

[†]This distinction is conceptually comparable to the differentiation between diffusion models (e.g., drift diffusion model) and accumulation models (e.g., race model; see Smith and Ratcliff, 2004).

for the relation between vibrotactile frequency comparison and his delayed-match-to-sample task). Interestingly, neurons in PPC (notably not exactly in those areas that were recorded by Shadlen and colleagues) were found to encode numerosity (or quantity) during the retention interval of the delayed-match-to-sample task, importantly, not only displaying a 'labeled-line' code (i.e., preference of one particular numerosity; e.g., see Nieder and Miller, 2004), but also using a 'summation' code (i.e., monotonic scaling with numerosity; Roitman et al., 2007). Hence, neurons in PPC are in fact known to encode quantities. However, whether those neurons, which are usually associated with the accumulation of evidence, are also capable of encoding quantities, remains to be shown. If this was the case, the accumulation-to-bound signal usually observed in PPC firing rates during RDM tasks, could be interpreted as an estimation of a quantity instead. That is, in order to solve the RDM task, monkeys might try to estimate the number of dots that move coherently. As soon as they have perceived the minimum amount of coherently moving dots that convinced them to have seen motion in a certain direction, they report it. In the end, our results invite for speculations about whether the framework of perceptual decision making, based on the seminal work by Shadlen and colleagues, might possibly be extended to a general framework of quantity estimation.

3.2.2 Functional connectivity within the fronto-parietal network

Remarkably, the graded parietal evidence signal (i.e., CPP) and the categorical choice signal (i.e., beta band power) were correlated on a single-trial level, at least when a direct mapping of decisions onto motor responses was provided (Study 4). Several recent studies, however, questioned whether such a relation can be causal (Erlich et al., 2015; Goard et al., 2016; Katz et al., 2016). In particular, reversible lesioning of parietal areas had no impact on choice behavior, whereas sensory and motor areas were indispensable. Importantly, these studies probed decisions in which a fully-defined motor response was associated with the decision report. When such a response mapping is provided, studies in animals and humans have shown that premotor areas (or even muscle activity) represent the evidence for an ensuing decision (Gold and Shadlen, 2003; Selen et al., 2012). That is, in such a context, with a clear choice-to-motor mapping, decision information in parietal areas might be redundant, and a direct pathway to respective motor areas might be sufficient to drive decisions. With this in mind, further studies, which do not provide a fixed motor mapping for the

decision report, are required to definitely rule out a causal involvement of parietal areas in decision formation. Alternatively, parietal and frontal areas might not be causally related, but rather share the same (sensory) input that is independently integrated at both sites. We propose that, if such independent processing pathways exist, they might possibly also serve different purposes. Whereas a pathway to premotor structures likely serves the realization of an ensuing decision report, a parietal signal might nourish further cognitive processes, such as confidence assessments of the decision (see Kiani and Shadlen, 2009). In line with such an interpretation, we found that the CPP (i.e., most likely originating from PPC) first indexes evidence, i.e., the signed quantity on which a decision is based, and later, confidence in the corresponding choice. That is, the fine-grained evidence signal in parietal areas might allow for an explicit access to this detailed information for further evaluations of the decision.

In sum, we also found activity in a "fronto-parietal" network to underlie the formation of decisions in the vibrotactile frequency comparison task. In accordance with animal research, decision signals exhibited a gradual change from more detailed evidence representations in parietal areas to categorical choice signals in "frontal" areas, or rather, in areas that implemented the consequences of a decision. Given the questionable causal relation within this "fronto-parietal" network, we propose that both sites might process information independently, and possibly serve different functions. Specifically, parietal structures can be interpreted to compute a more detailed representation of decisional evidence in order to allow for further processing of such information, for instance, to evaluate confidence. As a consequence, we hypothesize that lesioning parietal cortices might not effect decision performance per se (see Erlich et al., 2015; Goard et al., 2016; Katz et al., 2016), however, it might prevent explicit access to the information on which a decision was based, i.e., a dysfunctional PPC might impair confidence judgments.

3.3 Conclusion

This thesis investigated human EEG correlates of perceptual decisions in the vibrotactile frequency comparison paradigm. In remarkable alignment with the animal literature, we found a fronto-parietal network subserving the formation of decisions in this task. In particular, decision signals within

this network exhibited a gradual change from fine-grained sensory evidence representations in parietal areas to categorical choice signals in consequence-implementing areas (i.e., either premotor or posterior parietal areas). The sensorimotor gradient and the temporal relation of both signals (i.e., stimulus-locked sensory evidence and a response-locked choice signal), furthermore invites for speculations about their functional nexus. In particular, both signals were positively correlated on a single-trial level. However, to probe the tempting suspicion that this relation might be causal (with parietal areas driving those areas that implement the consequences of a decision; see also Meister et al., 2013; Park et al., 2014), further dedicated investigations of this connection are necessary (but see Erlich et al., 2015; Goard et al., 2016; Katz et al., 2016 for some evidence speaking against this notion).

Whereas the choice-indicative modulation of upper beta band power in this task was indeed already known from the monkey literature (Haegens et al., 2011), it has never been demonstrated in large-scale human EEG recordings before. Moreover, we were able to show for the first time that this particular choice signal indeed seems to be effector-specific, corroborating an intentional interpretation of the beta band effect. On the other hand, the graded, parietal evidence signal (i.e., the CPP) has been previously shown to track the evolving evidence in accumulation-based decisions (e.g., see Kelly and O'Connell, 2015). Yet, the CPP has never been associated with indexing evidence in a 2-AFC comparison task. Here, we demonstrated for the first time that the CPP not only indexes the signed quantities on which decisions are based in this task, but also revealed that the CPP appears to indicate the confidence in according choices afterwards. Strikingly, the CPP even reflected the subjectively perceived evidence for decisions that were formed in the absence of any objective sensory evidence (i.e., when f2 $=$ f1). That is, our behavioral model predicted that, due to the TOE, participants perceived small differences between f1 and f2, even if both stimuli were identical, and these perceived differences apparently modulated the CPP. Notably, we used this subjective measure of perceived differences for all stimulus pairs (i.e., also when f2 $\neq$ f1), and in all of our analysis, implying that all of the reported effects index subjective decision signals.

On a final note, the Bayesian model that was used to estimate the subjectively perceived differences is formulated in very general terms. At the same time, also the TOE is known to be a generic effect influencing all kinds of sequential comparisons (e.g., visual comparisons: Ashourian

and Loewenstein, 2011; belief updates: Hogarth and Einhorn, 1992). We believe that the here presented model can account for the influence of the TOE on choice behavior in any given context. In other words, we hypothesize that the principles of Bayesian inference might provide a universal explanation for the mechanisms of the TOE. Consequently, when assuming that the same conceptual principles govern the TOE in different circumstances, one might wonder whether also the underlying neural signatures are the same in different scenarios. In particular, we speculate that the here reported decision signals, i.e., the CPP and the choice-selective upper beta band modulation, also extend to other (decision) contexts, and might possibly even relate to more general processes, such as the estimation of magnitudes in general (e.g., see Nieder and Dehaene, 2009 for review).

In sum, the unpretentious vibrotactile comparison paradigm that was scrutinized in this thesis, provides a wide range of possibilities to study both the neural and theoretical priniples that govern the formation of perceptual decisions. The insights that can be gained in this perceptual context might eventually also elucidate our understanding of decision making in a broader sense, and might possibly extend to even more general cognitive processes that determine more complex behaviors.

Bibliography

Andersen RA, Essick GK, Siegel RM (1987) Neurons of area 7 activated by both visual stimuli and oculomotor behavior. *Experimental Brain Research* 67:316–322.

Andersen RA (1995) Encoding of intention and spatial location in the posterior parietal cortex. *Cerebral Cortex* 5:457–469.

Andersen RA, Buneo CA (2002) Intentional maps in posterior parietal cortex. *Annual Review of Neuroscience* 25:189–220.

Aristotle A (1986) *De Anima: On the Soul* Penguin, New York.

Ashourian P, Loewenstein Y (2011) Bayesian inference underlies the contraction bias in delayed comparison tasks. *PLoS ONE* 6.

Auksztulewicz R, Spitzer B, Goltz D, Blankenburg F (2011) Impairing somatosensory working memory using rtms. *European Journal of Neuroscience* 34:839–844.

Barak O, Sussillo D, Romo R, Tsodyks M, Abbott LF (2013) From fixed points to chaos: Three models of delayed discrimination. *Progress in Neurobiology* 103:214–222.

Barak O, Tsodyks M, Romo R (2010) Neuronal population coding of parametric working memory. *Journal of Neuroscience* 30:9424–9430.

Bennur S, Gold JI (2011) Distinct representations of a perceptual decision and the associated oculomotor plan in the monkey lateral intraparietal area. *Journal of Neuroscience* 31:913–921.

Boas F (1882) Ueber die verschiedenen formen des unterschiedsschwellenwerthes. *Pflügers Archiv European Journal of Physiology* 27:214–222.

Britten KH, Shadlen MN, Newsome WT, Movshon JA (1992) The analysis of visual motion: a comparison of neuronal and psychophysical performance. *Journal of Neuroscience* 12:4745–4765.

Britten K, Newsome W, Shadlen M, Celebrini S, Movshon J (1996) A relationship between behavioral choice and the visual responses of neurons in macaque MT. *Visual Neuroscience* 13:87–100.

Brody CD, Hernández A, Zainos A, Romo R (2003) Timing and neural encoding of somatosensory parametric working memory in macaque prefrontal cortex. *Cerebral Cortex* 13:1196–1207.

Cardoso-Leite P, Waszak F, Lepsien J (2014) Human perceptual decision making: Disentangling task onset and stimulus onset. *Human Brain Mapping* 35:3170–3187.

Cisek P (2007) Cortical mechanisms of action selection: the affordance competition hypothesis. *Philosophical Transactions of the Royal Society of London. Series B, Biological Sciences* 362:1585–1599.

Cisek P, Kalaska JF (2005) Neural correlates of reaching decisions in dorsal premotor cortex: specification of multiple direction choices and final selection of action. *Neuron* 45:801–814.

Cisek P, Kalaska JF (2010) Neural mechanisms for interacting with a world full of action choices. *Annual Review of Neuroscience* 33:269–298.

Colby CL, Goldberg ME (1999) Space and attention in parietal cortex. *Annual Review of Neuroscience* 22:319–349.

Daunizeau J, Adam V, Rigoux L (2014) VBA: A probabilistic treatment of nonlinear models for neurobiological and behavioural data. *PLoS Computational Biology* 10.

de Lafuente V, Jazayeri M, Shadlen MN (2015) Representation of Accumulating Evidence for a Decision in Two Parietal Areas. *Journal of Neuroscience* 35:4306–4318.

Deco G, Rolls ET, Albantakis L, Romo R (2013) Brain mechanisms for perceptual and reward-related decision-making. *Progress in Neurobiology* 103:194–213.

Descartes R (1649) *Passions De L'Ame: the Passions of the Soul* Hacket (From French), Indianapolis, IN.

Descartes R (1664) *L'Homme: Treatise on Man* Cambridge, MA.

Ding L, Gold JI (2012) Neural correlates of perceptual decision making before, during, and after decision commitment in monkey frontal eye field. *Cerebral Cortex* 22:1052–1067.

Donner TH, Siegel M, Fries P, Engel AK (2009) Buildup of choice-predictive activity in human motor cortex during perceptual decision making. *Current Biology* 19:1581–1585.

Donner TH, Siegel M, Oostenveld R, Fries P, Bauer M, Engel AK (2007) Population activity in the human dorsal pathway predicts the accuracy of visual motion detection. *Journal of Neurophysiology* 98:345–359.

Engel AK, Fries P (2010) Beta-band oscillations–signalling the status quo? *Current Opinion in Neurobiology* 20:156–165.

Epstein R, Kanwisher N (1998) A cortical representation of the local visual environment. *Nature* 392:598–601.

Erlich JC, Brunton BW, Duan Ca, Hanks TD, Brody CD (2015) Distinct effects of prefrontal and parietal cortex inactivations on an accumulation of evidence task in the rat. *eLife* 4:1–28.

Fechner GT (1860) *Elemente der Psychophysik* Breitkopf & Härtel, Leipzig.

Gherman S, Philiastides MG (2015) Neural representations of confidence emerge from the process of decision formation during perceptual choices. *NeuroImage* 106:134–143.

Glimcher PW (2003) The neurobiology of visual-saccadic decision making. *Annual Review of Neuroscience* 26:133–179.

Goard MJ, Pho GN, Woodson J, Sur M (2016) Distinct roles of visual, parietal, and frontal motor cortices in memory-guided sensorimotor decisions. *eLife* 5:1–30.

Gold JI, Shadlen MN (2001) Neural computations that underlie decisions about sensory stimuli. *Trends in Cognitive Sciences* 5:10–16.

Gold JI, Shadlen MN (2003) The influence of behavioral context on the representation of a perceptual decision in developing oculomotor commands. *Journal of Neuroscience* 23:632–651.

Gold JI, Shadlen MN (2007) The neural basis of decision making. *Annual Review of Neuroscience* 30:535–574.

Green D, Swets J (1966) *Signal detectability and psychophysics* Wiley, New York.

Haegens S, Nácher V, Hernández A, Luna R, Jensen O, Romo R (2011) Beta oscillations in the monkey sensorimotor network reflect somatosensory decision making. *PNAS* 108:10708–10713.

Hanes DP, Schall JD (1996) Neural Control of Voluntary Movement Initiation. *Science* 274:427–430.

Hangya B, Sanders JI, Kepecs A (2016) A mathematical framework for statistical decision confidence. *Neural Computation* .

Hanks TD, Kopec CD, Brunton BW, Duan Ca, Erlich JC, Brody CD (2015) Distinct relationships of parietal and prefrontal cortices to evidence accumulation. *Nature* 520:220–3.

Hanks TD, Summerfield C (2017) Perceptual Decision Making in Rodents , Monkeys , and Humans. *Neuron* 93:15–31.

Heekeren HR, Marrett S, Bandettini Pa, Ungerleider LG (2004) A general mechanism for perceptual decision-making in the human brain. *Nature* 431:859–862.

Heekeren HR, Marrett S, Ungerleider LG, Ruff DA, Bandettini PA (2006) Involvement of human left dorsolateral prefrontal cortex in perceptual decision making is independent of response modality. *PNAS* 103:10023–10028.

Heekeren HR, Marrett S, Ungerleider LG (2008) The neural systems that mediate human perceptual decision making. *Nature Reviews Neuroscience* 9:467–479.

Hellström Å (1985) The time-order error and its relatives: Mirrors of cognitive processes in comparing. *Psychological Bulletin* 97:35–61.

Hellström Å (2003) Comparison is not just subtraction: effects of time- and space-order on subjective stimulus difference. *Perception & Psychophysics* 65:1161–1177.

Herding J, Ludwig S, Blankenburg F (2017) Response-modality-specific encoding of human choices in upper beta band oscillations during vibrotactile comparisons. *Frontiers in Human Neuroscience* 11:1–11.

Herding J, Spitzer B, Blankenburg F (2016) Upper beta band oscillations in human premotor cortex encode subjective choices in a vibrotactile comparison task. *Journal of Cognitive Neuroscience* 28:668–679.

Hernández A, Nácher V, Luna R, Zainos A, Lemus L, Alvarez M, Vázquez Y, Camarillo L, Romo R (2010) Decoding a perceptual decision process across cortex. *Neuron* 66:300–314.

Hernández A, Zainos A, Romo R (2000) Neuronal correlates of sensory discrimination in the somatosensory cortex. *PNAS* 97:6191–6196.

Hernández A, Zainos A, Romo R (2002) Temporal evolution of a decision-making process in medial premotor cortex. *Neuron* 33:959–972.

Ho TC, Brown S, Serences JT (2009) Domain general mechanisms of perceptual decision making in human cortex. *Journal of Neuroscience* 29:8675–8687.

Hogarth RM, Einhorn HJ (1992) Order effects in belief updating: The belief-adjustment model. *Cognitive Psychology* 24:1–55.

Horwitz GD, Newsome WT (1999) Separate signals for target selection and movement specification in the superior colliculus. *Science (New York, N.Y.)* 284:1158–1161.

Huk AC, Shadlen MN (2005) Neural activity in macaque parietal cortex reflects temporal integration of visual motion signals during perceptual decision making. *J. Neurosci.* 25:10420–10436.

Jamieson DG, Petrusic WM (1975) Presentation order effects in duration discrimination. *Perception & Psychophysics* 17:197–202.

Jasper H, Penfield W (1949) Electrocorticograms in man: effect of voluntary movement upon the electrical activity of the precentral gyrus. *Arch. Psychiatr. Z. Neurol.* 183:163–174.

Jun JK, Miller P, Hernández A, Zainos A, Lemus L, Brody CD, Romo R (2010) Heterogenous population coding of a short-term memory and decision task. *Journal of Neuroscience* 30:916–929.

Kanwisher N, McDermott J, Chun MM (1997) The fusiform face area: a module in human extrastriate cortex specialized for face perception. *Journal of neuroscience* 17:4302–4311.

Karim M, Harris Ja, Morley JW, Breakspear M (2012) Prior and present evidence: How prior experience interacts with present information in a perceptual decision making task. *PLoS ONE* 7.

Katz L, Yates J, Pillow JW, Huk A (2016) Dissociated functional significance of choice-related activity across the primate dorsal stream. *Nature* 535:Salt Lake City USA.

Kayser AS, Buchsbaum BR, Erickson DT, D'Esposito M (2010) The functional anatomy of a perceptual decision in the human brain. *Journal of Neurophysiology* 103:1179–1194.

Kelly SP, O'Connell RG (2013) Internal and external influences on the rate of sensory evidence accumulation in the human brain. *Journal of Neuroscience* 33:19434–19441.

Kelly SP, O'Connell RG (2015) The neural processes underlying perceptual decision making in humans: recent progress and future directions. *Journal of Physiology-Paris* 109:27 – 37.

Kiani R, Shadlen MN (2009) Representation of confidence associated with a decision by neurons in the parietal cortex. *Science (New York, N.Y.)* 324:759–764.

Kim JN, Shadlen MN (1999) Neural correlates of a decision in the dorsolateral prefrontal cortex of the macaque. *Nature Neuroscience* 2:176–185.

Köhler W (1923) Zur theorie des sukzessivvergleichs und der zeitfehler. *Psychological Research* 4:115–175.

Kostopoulos P, Albanese MC, Petrides M (2007) Ventrolateral prefrontal cortex and tactile memory disambiguation in the human brain. *Proceedings of the National Academy of Sciences* 104:10223–10228.

Lauenstein O (1933) Ansatz zu einer physiologischen theorie des vergleichs und der zeitfehler. *Psychological Research* 17:130–177.

Li Hegner Y, Saur R, Veit R, Butts R, Leiberg S, Grodd W, Braun C (2007) Bold adaptation in vibrotactile stimulation: neuronal networks involved in frequency discrimination. *Journal of neurophysiology* 97:264–271.

Liu T, Pleskac TJ (2011) Neural correlates of evidence accumulation in a perceptual decision task 48824:2383–2398.

Logothetis NK, Pauls J, Augath M, Trinath T, Oeltermann A (2001) Neurophysiological investigation of the basis of the fmri signal. *Nature* 412:150–157.

Luna R, Hernández A, Brody CD, Romo R (2005) Neural codes for perceptual discrimination in primary somatosensory cortex. *Nature Neuroscience* 8:1210–1219.

Machens CK, Romo R, Brody CD (2005) Flexible control of mutual inhibition: a neural model of two-interval discrimination. *Science* 307:1121–1124.

Macmillan NA, Creelman CD (2004) *Detection theory: A user's guide* Psychology press.

Maunsell JH, Van Essen DC (1983) Functional properties of neurons in middle temporal visual area of the macaque monkey. i. selectivity for stimulus direction, speed, and orientation. *Journal of neurophysiology* 49:1127–1147.

Mazurek ME, Roitman JD, Ditterich J, Shadlen MN (2003) A Role for Neural Integrators in Perceptual Decision Making. *Cerebral Cortex* 13:1257–1269.

Meister MLR, Hennig Ja, Huk aC (2013) Signal Multiplexing and Single-Neuron Computations in Lateral Intraparietal Area During Decision-Making. *Journal of Neuroscience* 33:2254–2267.

Michels WC, Helson H (1954) A quantitative theory of time-order effects. *The American Journal of Psychology* 67:327–334.

Miller P, Brody CD, Romo R, Wang XJ (2003) A recurrent network model of somatosensory parametric working memory in the prefrontal cortex. *Cerebral Cortex* 13:1208–1218.

Mountcastle VB, Steinmetz Ma, Romo R (1990) Frequency discrimination in the sense of flutter: psychophysical measurements correlated with postcentral events in behaving monkeys. *Journal of Neuroscience* 10:3032–3044.

Mountcastle V, Talbot W, Sakata H, Hyvärinen J (1969) Cortical neuronal mechanisms in flutter-vibration studied in unanesthetized monkeys: neuronal periodicity and frequency discrimination. *Journal of Neurophysiology* 32:452–484.

Newsome WT, Pare EB (1988) A selective impairment of motion perception following lesions of the middle temporal visual area (MT). *Journal of Neuroscience* 8:2201–2211.

Nieder A (2017) Magnitude codes for cross-modal working memory in the primate frontal association cortex. *Frontiers in Neuroscience* 11:202.

Nieder A, Dehaene S (2009) Representation of number in the brain. *Annual Review of Neuroscience* 32:185–208.

Nieder A, Miller EK (2004) A parieto-frontal network for visual numerical information in the monkey. *Proceedings of the National Academy of Sciences of the United States of America* 101:7457–7462.

O'Connell RG, Dockree PM, Kelly SP (2012) A supramodal accumulation-to-bound signal that determines perceptual decisions in humans. *Nature Neuroscience* 15:1729–1735.

Park IM, Meister MLR, Huk AC, Pillow JW (2014) Encoding and decoding in parietal cortex during sensorimotor decision-making. *Nature Neuroscience* .

Petzschner FH, Glasauer S, Stephan KE (2015) A Bayesian perspective on magnitude estimation. *Trends in Cognitive Sciences* pp. 1–9.

Pfurtscheller G (1981) Central beta rhythm during sensorimotor activities in man. *Electroencephalography and Clinical Neurophysiology* 51:253–264.

Philiastides MG, Heekeren HR, Sajda P (2014) Human scalp potentials reflect a mixture of decision-related signals during perceptual choices. *Journal of Neuroscience* 34:16877–16889.

Philiastides MG, Auksztulewicz R, Heekeren HR, Blankenburg F (2011) Causal role of dorsolateral prefrontal cortex in human perceptual decision making. *Current Biology* 21:980–983.

Pleger B, Ruff CC, Blankenburg F, Bestmann S, Wiech K, Stephan KE, Capilla A, Friston KJ, Dolan RJ (2006) Neural coding of tactile decisions in the human prefrontal cortex. *Journal of Neuroscience* 26:12596–601.

Pleger B, Villringer A (2013) The human somatosensory system: from perception to decision making. *Progress in Neurobiology* 103:76–97.

Preuschhof C, Heekeren HR, Taskin B, Schubert T, Villringer A (2006) Neural correlates of vibrotactile working memory in the human brain. *Journal of Neuroscience* 26:13231–13239.

Preuschhof C, Schubert T, Villringer A, Heekeren HR (2010) Prior Information biases stimulus representations during vibrotactile decision making. *Journal of Cognitive Neuroscience* 22:875–887.

Ratcliff R, Cherian A, Segraves M (2003) A comparison of macaque behavior and superior colliculus neuronal activity to predictions from models of two-choice decisions. *Journal of Neurophysiology* 90:1392–1407.

Ratcliff R, Rouder JN (1998) Modeling response times for two-choice decisions. *Psychological Science* 9:347–356.

Ratcliff R, Smith PL, Brown SD, McKoon G (2016) Diffusion Decision Model: Current Issues and History. *Trends in Cognitive Sciences* 20:260–281.

Roitman JD, Brannon EM, Platt ML (2007) Monotonic coding of numerosity in macaque lateral intraparietal area. *PLoS Biology* 5:1672–1682.

Roitman JD, Shadlen MN (2002) Response of neurons in the lateral intraparietal area during a combined visual discrimination reaction time task. *Journal of Neuroscience* 22:9475–9489.

Romo R, Brody CD, Hernández A, Lemus L (1999) Neuronal correlates of parametric working memory in the prefrontal cortex. *Nature* 399:470–473.

Romo R, de Lafuente V (2013) Conversion of sensory signals into perceptual decisions. *Progress in Neurobiology* 103:41–75.

Romo R, Hernández A, Zainos A (2004) Neuronal correlates of a perceptual decision in ventral premotor cortex. *Neuron* 41:165–173.

Romo R, Hernández A, Zainos A, Lemus L, Brody CD (2002) Neuronal correlates of decision-making in secondary somatosensory cortex. *Nature Neuroscience* 5:1217–1225.

Romo R, Salinas E (2003) Flutter discrimination: neural codes, perception, memory and decision making. *Nature Reviews Neuroscience* 4:203–218.

Salinas E, Hernandez A, Zainos A, Romo R (2000) Periodicity and firing rate as candidate neural codes for the frequency of vibrotactile stimuli. *Journal of Neuroscience* 20:5503–5515.

Salzman CD, Britten KH, Newsome WT (1990) Cortical microstimulation influences perceptual judgements of motion direction. *Nature* 346:174–177.

Sanchez G (2014) Real-time electrophysiology in cognitive neuroscience: towards adaptive paradigms to study perceptual learning and decision making in humans Ph.D. diss.

Sanders JI, Hangya B, Kepecs A (2016) Signatures of a statistical computation in the human sense of confidence. *Neuron* 90:499–506.

Schall JD, Hanes DP, Thompson KG, King DJ (1995) Saccade target selection in frontal eye field of macaque. I. Visual and premovement activation. *Journal of Neuroscience* 15:6905–18.

Scheeringa R, Fries P, Petersson KM, Oostenveld R, Grothe I, Norris DG, Hagoort P, Bastiaansen MC (2011) Neuronal dynamics underlying high-and low-frequency eeg oscillations contribute independently to the human bold signal. *Neuron* 69:572–583.

Selen LPJ, Shadlen MN, Wolpert DM (2012) Deliberation in the motor system: reflex gains track evolving evidence leading to a decision. *Journal of Neuroscience* 32:2276–86.

Shadlen MN, Kiani R (2013) Decision making as a window on cognition. *Neuron* 80:791–806.

Shadlen MN, Kiani R, Hanks TD, Churchland AK (2008) Neurobiology of decision making: an intentional framework In Engel C, Singer W, editors, *Better Than Conscious? Decision Making, the Human Mind, and Implications For Institutions*, pp. 71–101. MIT Press, Cambridge.

Shadlen M, Newsome W (1996) Motion perception: seeing and deciding. *PNAS* 93:628–633.

Shadlen MN, Newsome WT (2001) Neural basis of a perceptual decision in the parietal cortex (area LIP) of the rhesus monkey. *Journal of Neurophysiology* 86:1916–1936.

Sherman MT, Seth AK, Kanai R (2016) Predictions shape confidence in right inferior frontal gyrus. *Journal of Neuroscience* 36:10323–10336.

Sherrington CS (1649) *The Integrative Action of the Nervous System* Yale, New Haven, CT.

Smith PL, Ratcliff R (2004) Psychology and neurobiology of simple decisions. *Trends in Neurosciences* 27:161–168.

Spitzer B, Blankenburg F (2011) Stimulus-dependent EEG activity reflects internal updating of tactile working memory in humans. *PNAS* 108:8444–8449.

Spitzer B, Blankenburg F (2012) Supramodal parametric working memory processing in humans. *Journal of Neuroscience* 32:3287–3295.

Spitzer B, Gloel M, Schmidt TT, Blankenburg F (2014) Working memory coding of analog stimulus properties in the human prefrontal cortex. *Cerebral Cortex* 24:2229–2236.

Spitzer B, Wacker E, Blankenburg F (2010) Oscillatory correlates of vibrotactile frequency processing in human working memory. *Journal of Neuroscience* 30:4496–4502.

Swets JA (1986) Form of empirical ROCs in discrimination and diagnostic tasks: implications for theory and measurement of performance. *Psychological Bulletin* 99:181–198.

Talbot WH, Darian-Smith I, Kornhuber HH, Mountcastle VB (1968) The sense of flutter-vibration: comparison of the human capacity with response patterns of mechanoreceptive afferents from the monkey hand. *Neurophysiology* 31:301–334.

Tanner WPJ, Swets Ja (1954) A decision-making theory of visual detection. *Psychological Review* 61:401–409.

Tobimatsu S, Zhang YM, Kato M (1999) Steady-state vibration somatosensory evoked potentials: physiological characteristics and tuning function. *Clinical Neurophysiology* 110:1953–1958.

Trueblood JS, Busemeyer JR (2011) A quantum probability account of order effects in inference. *Cognitive Science* 35:1518–1552.

Twomey DM, Kelly SP, O'Connell RG (2016) Abstract and effector-selective decision signals exhibit qualitatively distinct dynamics before delayed perceptual reports. *Journal of Neuroscience* 36:7346–52.

Twomey DM, Murphy PR, Kelly SP, O'Connell RG (2015) The classic P300 encodes a build-to-threshold decision variable. *The European Journal of Neuroscience* 42:1636–1643.

Wald A (1945) Sequential tests of statistical hypotheses. *The Annals of Mathematical Statistics* 16:117–186.

Wald A, Wolfowitz J (1948) Optimum character of the sequential probability ratio test 19:326–339.

Wang XJ (2001) Synaptic reverberation underlying mnemonic persistent activity. *Trends in Neurosciences* 24:455–463.

Wang XJ (2002) Probabilistic decision making by slow reverberation in cortical circuits. *Neuron* 36:955–968.

Wang XJ (2010) Neurophysiological and computational principles of cortical rhythms in cognition. *Physiological reviews* 90:1195–1268.

Woodrow H (1935) The effect of practice upon time-order errors in the comparison of temporal intervals. *Psychological Review* 42:127–152.

A Original research articles

Study 1 - Upper Beta Band Oscillations in Human Premotor Cortex Encode Subjective Choices in a Vibrotactile Comparison Task

Herding, J.*, Spitzer, B.*, and Blankenburg, F. (2016). Upper beta band oscillations in human premotor cortex encode subjective choices in a vibrotactile comparison task. Journal of cognitive neuroscience, 28(5): 668 – 679. doi: 10.1162/jocn_a_00932

Upper Beta Band Oscillations in Human Premotor Cortex Encode Subjective Choices in a Vibrotactile Comparison Task

Jan Herding[1,2*], Bernhard Spitzer[1*], and Felix Blankenburg[1,2]

Abstract

■ Comparisons of sequentially presented vibrotactile frequencies have been extensively studied using electrophysiological recordings in nonhuman primates. Although neural signatures for working memory aspects of such tasks were recently also identified in human oscillatory EEG activity, homologue correlates of the comparison process are yet unknown. Here, we recorded EEG activity while participants decided which of two sequentially presented vibrotactile stimuli had a higher frequency. Because choices in this type of task are known to be systematically biased by the time-order effect, we applied Bayesian modeling to account for individual choice behavior. Using model-based EEG analysis, we found that upper beta band amplitude (~20–30 Hz) was modulated by participants' choices. The modulation emerged ~750 msec before a behavioral response was given and was source-localized to premotor areas. Importantly, the choice-dependent modulation of beta band amplitude was invariant to different motor response mappings and reflected the categorical outcome of the subjective comparison between the two frequencies. Consistently, this pattern was evident for both correct and incorrect trials, indicating that the beta band amplitude mirrors the internal representation of the comparison outcome. Our data complement previous findings in nonhuman primates and corroborate that the beta band activity in premotor areas reflects the categorical outcome of a sensory comparison prior to translation into an effector-specific motor command. ■

INTRODUCTION

Over the last decades, studies in nonhuman primates have identified neuronal mechanisms that underlie memory-based perceptual decisions in the somatosensory domain (reviewed in Romo & de Lafuente, 2013). In their seminal work, Romo and colleagues used a vibrotactile two-alternative forced-choice (2AFC) task. Monkeys were trained to decide whether the second of two sequentially presented vibrotactile stimuli (with frequency f2) had a lower or higher frequency than the first one (with frequency f1). Thus, f1 served as the (variable) reference value against which f2 had to be compared. Electrophysiological recordings in several parietal and frontal brain areas revealed a cascade of neuronal processes involved in this task (see Romo & de Lafuente, 2013, for details): (i) during presentation of the tactile stimuli, firing rates in primary and secondary somatosensory cortices (SI and SII) scaled monotonically with the frequency of the stimuli (Hernández, Zainos, & Romo, 2000); (ii) firing rates of neurons in the PFC were parametrically modulated by the values of f1 during the entire retention interval of the task (Romo, Brody, Hernández, & Lemus, 1999; see also Barak, Tsodyks, & Romo, 2010); (iii) crucially, correlates of the comparison process underlying the perceptual decision were evident in firing rates of medial and ventral premotor cortex (mPMC and vPMC, respectively; Romo, Hernández, & Zainos, 2004; Hernández, Zainos, & Romo, 2002). More specifically, neuronal activity in these areas reflected the (to-be-evaluated) signed frequency difference between f1 and f2. Consequently, the premotor cortex could be regarded as a candidate area in which the comparison between the sample stimulus (i.e., f2) and the memory trace of f1 is computed.

More recently, recordings of monkey local field potentials (LFPs) showed that the central role of the premotor cortex in sequential frequency comparisons is also expressed in terms of oscillatory activity. The spectral power of beta band LFP oscillations (~18–26 Hz) recorded from the mPMC mirrored the categorical decisions of the monkeys (Haegens et al., 2011). Specifically, the beta band power was significantly increased when monkeys indicated that f2 was higher than f1, both for correct and incorrect choices. Hence, a decision-related signal in the vibrotactile 2AFC task is not only encoded in the firing rates of single neurons (cf. Romo et al., 2004; Hernández et al., 2002) but also in synchronized ensemble activity on the neural population level, corroborating a central role of neural oscillations in information processing (e.g., see Siegel, Donner, & Engel, 2012).

Along these lines, recent studies in humans found oscillations in a similar frequency band (~20–30 Hz) to reflect working memory (WM)-related processes during

[1]Freie Universität Berlin, [2]Bernstein Center for Computational Neuroscience Berlin

*These authors contributed equally to the work.

© 2016 Massachusetts Institute of Technology

Journal of Cognitive Neuroscience 28:5, pp. 668–679
doi:10.1162/jocn_a_00932

the retention interval of vibrotactile 2AFC tasks (Spitzer & Blankenburg, 2011; Spitzer, Wacker, & Blankenburg, 2010). In particular, EEG recordings showed that upper beta power recorded over PFC scaled parametrically with the frequency that had to be kept in WM (Spitzer & Blankenburg, 2011; Spitzer et al., 2010). However, the decision-related aspects of the vibrotactile 2AFC task have not been investigated in human EEG recordings yet.

In this study, we aimed to close the gap between the results from invasive electrophysiological studies of decision processes in monkeys, on the one hand, and the available findings of WM correlates in oscillatory human EEG data, on the other. In particular, we asked whether human oscillatory EEG signals may encode the decision-relevant quantity (i.e., the difference between f2 and f1) that reflects the comparison of both stimuli (cf. Haegens et al., 2011). To answer this question, we optimized the sequential frequency comparison paradigm to allow for an artifact-free analysis of EEG data during the decision period of the task. Moreover, we applied Bayesian modeling to account for a well-known systematic order effect in choice behavior that is commonly observed in sequential 2AFC comparisons: the so-called time-order error/effect (TOE; cf. Sanchez, 2014; Karim, Harris, Morley, & Breakspear, 2012; Ashourian & Loewenstein, 2011; Preuschhof, Schubert, Villringer, & Heekeren, 2010; Woodrow, 1935; Fechner, 1860). The TOE refers to the finding that, in 2AFC tasks, participants tend to compare the second stimulus against a weighted average of the mean of the whole stimulus set and the first stimulus, instead of the first stimulus alone (cf. Karim et al., 2012). Our Bayesian model yielded individual estimates of these subjectively perceived frequency differences for each stimulus pair as a proxy for the internal representation of the trial-specific f1-versus-f2 comparison. Using time–frequency (TF) analysis, we studied decision-related oscillatory EEG signals by examining in which frequency bands spectral amplitude was correlated with the estimated subjective frequency differences. We found such decision-related signals in the form of categorical EEG amplitude modulations in the upper beta band over premotor areas, in notable agreement with recent invasive recordings in monkeys.

METHODS

Participants

Twenty-four healthy, right-handed volunteers (21–35 years; 14 women) participated in the experiment after giving written informed consent. The study was approved by the local ethics committee at the Freie Universität Berlin. Six participants (three men, three women) were excluded from the analysis because of chance-level behavioral performance (<60% correct answers, five participants) or excessive EEG artifacts (one participant).

Stimuli and Behavioral Task

Suprathreshold vibrotactile stimuli were applied to the left index finger using a piezoelectric Braille stimulator (QuaeroSys Medical Devices, Schotten, Germany). The 16 pins (4 × 4 matrix, consistent peak amplitude ~0.46 mm) of the stimulator's display were driven by a sinusoidal carrier signal (fixed at 133 Hz) that was amplitude-modulated by a lower-frequency sinusoid (varied between 12 and 32 Hz). The resulting stimulation created the sensation of a tactile "flutter" stimulus (Romo & Salinas, 2003; Talbot, Darian-Smith, Kornhuber, & Mountcastle, 1968) at the modulation frequency (i.e., 12–32 Hz), whereas the spectrum of the physical driving signal was confined to frequencies above 100 Hz (e.g., Tobimatsu, Zhang, & Kato, 1999). Thus, the risk of physical artifacts in the EEG analysis range (<100 Hz) was minimized. To mask the sound of the stimulator, white noise of ~80 dB was played during the whole experiment via loudspeakers that were placed below a TFT monitor in front of the participant (e.g., Spitzer & Blankenburg, 2011; Spitzer et al., 2010). Throughout the task, a fixation cross was displayed at the center of the TFT monitor. On each trial, two brief vibrotactile stimuli (with frequencies f1 and f2) were presented for 250 msec each, separated by a retention interval of 1000 msec (Figure 1A). Such short-lived stimulations evoke only transient signals in EEG data and hence facilitate a clean analysis of the decision period immediately after the second stimulus. The values of f1 were randomly chosen from 16, 20, 24, or 28 Hz; f2 could differ from f1 by ±2 or 4 Hz (Figure 1B). Thus, participants could not predict the difference f2 − f1 based on f1. After presentation of the second stimulus, participants indicated whether f2 or f1 was higher by pressing one of two buttons with their right index or middle finger, respectively. Importantly, the response assignment of the buttons was reversed for half of the participants, such that the mapping of choices onto specific button presses (which might have been associated with specific motor preparatory signals) was fully counterbalanced across participants. Twenty milliseconds after each response, performance feedback was provided in form of two "plus" or "minus" signs indicating correct or incorrect responses, respectively, presented to the left and to the right of the fixation cross for 190 msec. The next trial started after a variable intertrial interval (1500–2000 msec). Participants completed seven blocks of 160 f1-versus-f2 comparisons (each block lasted ~12 min), for a total of 1120 trials. Before the experiment started, participants performed ~50 practice trials.

Bayesian Model

To estimate the individually perceived subjective frequency differences that can account for TOE-like biases in sequential comparison tasks, we fitted a Bayesian inference model to the behavioral data. The model we used

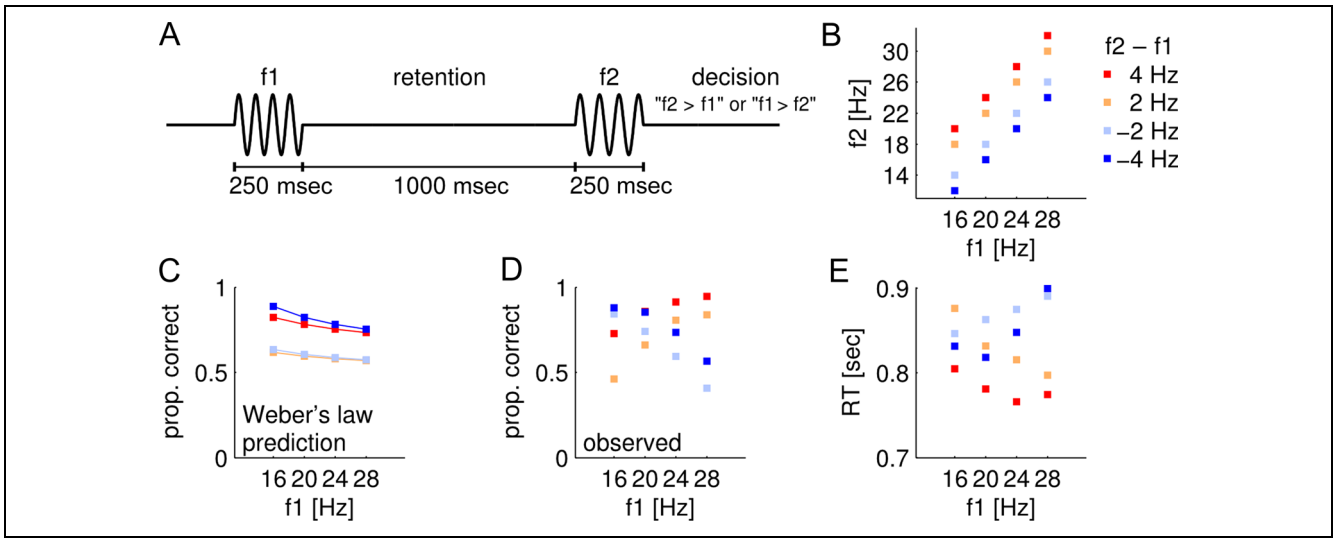

Figure 1. Experimental paradigm and behavioral data. (A) Illustration of the experimental paradigm. Two vibrotactile stimuli with different frequencies (f1 and f2) were sequentially presented to the left index finger, delayed by 1000 msec. After the offset of f2, participants indicated which of the two stimuli had a higher frequency. (B) Each colored square represents a stimulus pair (f1, f2) used in the experiment. Warm and cold colors indicate trials with f2 > f1 and f1 > f2, respectively. (C) PCRs as expected according to Weber's law and under the assumption that the physical difference f2 − f1 describes the comparison of f1 and f2. (D) Grand mean of PCRs as observed in the data. With higher f1, the performance for trials with f2 > f1 increased, whereas the performance for f1 > f2 trials decreased. These two trends intersect at the f1 value that approximates the mean of the stimulus set (cf. regression to the mean). (E) Same as in C with RTs in seconds.

was adopted from earlier work (cf. Sanchez, 2014; Ashourian & Loewenstein, 2011).

In the model, stimulus frequencies are represented on a logarithmic scale according to Weber's law. Each stimulus frequency F_i is assumed to have a neural representation R_{F_i} that is a noisy realization of the true (hidden) stimulus frequency: $R_{F_i} = F_i + z$ with $z \sim \mathcal{N}(0, \sigma^2_{\text{stim}})$. In other words, the probability of the neural representation R_{F_i} for a given stimulus with frequency f* is defined by a normal distribution with mean μ_{stim}, and variance σ^2_{stim}:

$$p(R_{F_i}|F_i = f\ *\ ) \sim \mathcal{N}(\mu_{\text{stim}}, \sigma^2_{\text{stim}})$$

This distribution is also known as the likelihood of the stimulus frequency f*. It was assumed that each participant encodes all stimulus frequencies with fixed, individual precision described by a likelihood function with (individual) variance σ^2_{stim}. The a priori knowledge about the stimulus set (range of stimulus frequencies) was taken into account by a normal distribution with mean $\mu_{\text{prior}} = f_{\text{mean}}$ (mean frequency of the stimulus set) and variance σ^2_{prior} (estimated for each participant):

$$p(F_i) \sim \mathcal{N}\left(\mu_{\text{prior}}, \sigma^2_{\text{prior}}\right)$$

Thus, the posterior distribution $(F_i|R_{F_i})$, which denotes the percept of the respective stimulus (cf. Petzschner, Glasauer, & Stephan, 2015), is given by

$$p(F_i|R_{F_i}) \sim p(R_{F_i}|F_i) \cdot p(F_i)$$

To account for the TOE, we assume that only the percept (i.e., posterior) of f1 incorporates a priori knowledge about the stimulus set as outlined above. Because both likelihood and prior are normally distributed, also the posterior distribution of f1 can be obtained by a normal distribution:

$$p_{f1}\left(F_i|R_{F_i}\right) \sim \mathcal{N}\left(\mu_{\text{post,f1}}, \sigma^2_{\text{post,f1}}\right)$$

with mean $\mu_{\text{post,f1}} = \sigma^2_{\text{post,f1}} \cdot \left(\frac{\mu_{\text{prior}}}{\sigma^2_{\text{prior}}} + \frac{\mu_{\text{stim}}}{\sigma^2_{\text{stim}}}\right)$ and variance $\sigma^2_{\text{post,f1}} = \dfrac{1}{1/\sigma^2_{\text{prior}} + 1/\sigma^2_{\text{stim}}}$

The posterior of f2 was defined to be equal to the likelihood of the given stimulus frequency f2*:

$$p_{f2}(F_i|R_{F_i}) = p(R_{F_i}|F_i = \text{f2}\ *\ )$$

Consequently, the mean and variance of $p_{f2}(F_i|R_{F_i})$ are given by $\mu_{\text{post,f2}} = \mu_{\text{stim}} = \text{f2}*$ and $\sigma^2_{\text{post,f2}} = \sigma^2_{\text{stim}}$, respectively. The probability of "f1 > f2"[1] for two given stimulus representations can then be formulated as

$$p(\text{"f1} > \text{f2"}|R_{\text{f1}}, R_{\text{f2}}) = b + \int_{-\infty}^{+\infty} p_{\text{f1}}(\text{f1}|R_{\text{f1}}) \times \int_{-\infty}^{\text{f1}} p_{\text{f2}}(\text{f2}|R_{\text{f2}})\ d\text{f2}\ d\text{f1}$$

including a term b to account for a potential overall response bias. The model was fitted to the choices of individual participants by optimizing the free parameters σ^2_{stim}, σ^2_{prior}, and b using variational Bayes as implemented in the VBA toolbox (Daunizeau, Adam, & Rigoux, 2014). On the basis of the estimated parameters, we

quantified the subjectively perceived stimulus differences for each stimulus pair and each participant. Subjectively perceived stimulus differences are defined as the differences between the posterior means of the stimuli, that is, $\mu_{post,f2} - \mu_{post,f1}$ with $\mu_{post,f1} = f1'$ and $\mu_{post,f2} = f2$. Figure 3A shows a graphical illustration of the model.

To assess the model's goodness-of-fit, we compared the individual model fits with a "null" model in which decisions were only based on the physical stimulus differences (f2 − f1). That is, the posteriors of f1 and f2 are both directly represented by their respective likelihood function, and only σ^2_{stim} and b was to be estimated. Bayes factors (BFs) were computed for each participant to quantify the goodness-of-fit of the subjective decision model relative to the "null" model while accounting for differences in model complexity (e.g., see Kass & Raftery, 1995).

In addition, we evaluated the predictions of the subjective decision model on an independent test set to control empirically for overfitting. In particular, we randomly divided the trials of each participant condition-wise into a training set and into a test set. Parameters of the model were estimated on the training set and then applied for fitting the test data (cf. Figure 4B–D).

EEG Recording and Analysis

EEG was recorded from 64 electrodes (ActiveTwo, BioSemi, Amsterdam, The Netherlands) positioned in an elastic cap according to the extended 10–20 system. Four additional electrodes were used to register horizontal and vertical eye movements. Individual electrode locations for each participant were obtained prior to the experiment using a stereotactic electrode-positioning system (Zebris Medical GmbH, Isny, Germany). The EEG data were digitized at 2048 Hz, offline down-sampled to 512 Hz, high- and low-pass filtered (with cutoff frequencies of 0.5 and 48 Hz, respectively), and re-referenced to a common average montage. Eye blinks were corrected using adaptive spatial filtering based on individual calibration data (for details, see Ille, Berg, & Scherg, 2002). In addition, trials with signal amplitudes exceeding a threshold of 80 mV (before low-pass filtering) were excluded from further investigations (12.2% of trials on average). The analyses were done in

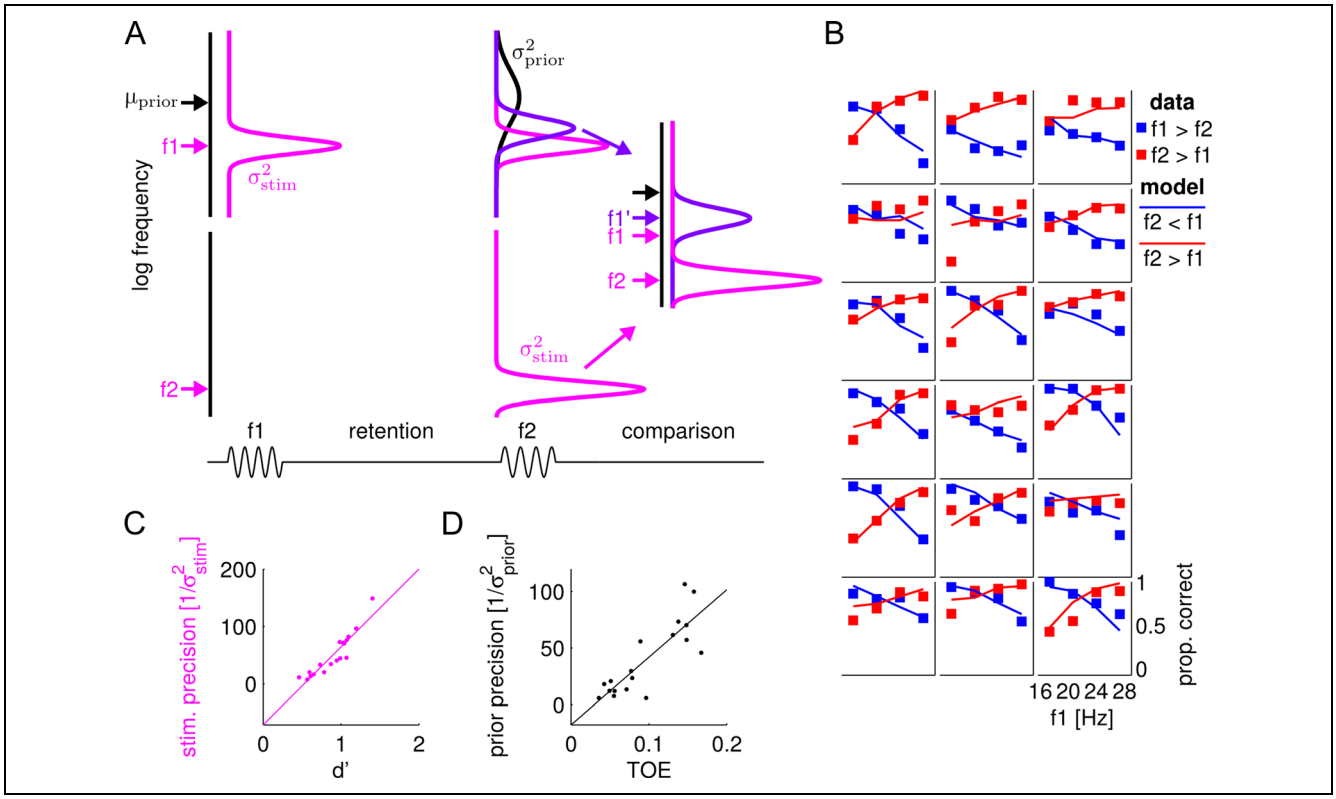

Figure 2. A Bayesian inference model explains choice behavior of each participant well. (A) Graphical illustration of the model described in the Methods section. The *y*-axes show frequency values on a logarithmic scale. Top: Displays how f1 is represented at different stages of the task. The pink distribution corresponds to the likelihood function of f1, the black distribution reflects the prior, and the purple distribution is the posterior of f1 with new mean f1′. The likelihood of f2 (pink distribution, bottom) is used as the posterior of f2 and is compared with the posterior of f1. The task illustration at the bottom serves as a temporal guideline. See text for details. (B) Comparison of each participants' PCRs (squares; obtained from test data set) with simulations from individually optimized models (lines; based on training data set). (C) Scatter plot of d′ versus the precision of stimulus encoding estimated for each participant. (D) The magnitude of the TOE (increase of bias to choose "f2 > f1" with increasing f1) scattered against precision of the prior distribution across all participants. (B–D) Compare models estimated on training data with behavioral measures obtained from independent test data. The color code in C and D refers to distributions and parameters in A.

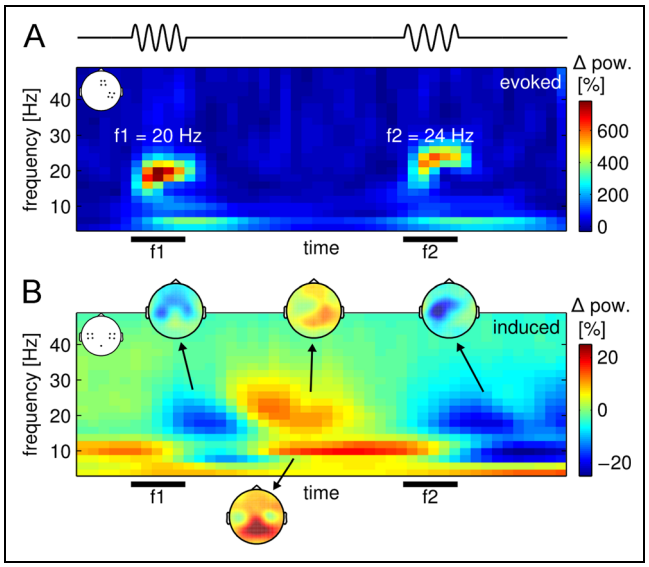

Figure 3. Stimulus-evoked and task-induced TF activity. (A) Grand mean of stimulus-evoked power for an exemplary stimulus pair. The evoked power is displayed as percentage change with respect to a baseline before presentation of f1 (−1000 to 0 msec from first stimulus). Data are shown for representative electrodes as indicated in inset. (B) Grand mean of induced power, collapsed across all correct trials. The TF map shows relative change in percent (same baseline as in A) and is averaged across electrodes indicated in inset. See text for details.

MATLAB (The MathWorks, Natick, MA) using the SPM8 toolbox (Wellcome Department of Cognitive Neurology, London, UK; www.fil.ion.ucl.ac.uk/spm), including the FieldTrip toolbox for EEG/MEG data (Radboud University Nijmegen, Donders Institute; fieldtrip.fcdonders.nl). Unless stated otherwise, only trials with correct choices were used for analysis.

Time–Frequency Analysis

The artifact-free EEG data were segmented into epochs from −2500 to 1000 msec relative to the time of the button press to examine the decision period of the task (i.e., response-locked analysis). TF representations of spectral power between 4 and 48 Hz (in steps of 2 Hz) were computed every 50 msec by applying a Morlet wavelet transformation with a sliding window of 7 cycles length (i.e., TF bin = 50 msec × 2 Hz). Exploratory analysis of higher-frequency bands (up to 100 Hz), using a multitapered Fourier transformation with three Slepian tapers and a sliding window length of 400 msec, yielded no significant effects.

For the main analysis of decision-relevant signals (Figure 4), the TF transformation was applied to single-trial response-locked data, yielding a measure of ongoing "whole" power. Power changes in overall "evoked" (i.e., phase-locked) and "induced" (i.e., non-phase-locked) activity were analyzed on stimulus locked data (−2250 to 2250 msec relative to f2 onset). Evoked power associated with each stimulus pair (f1, f2) was assessed by applying the TF transform to the average (time domain) waveform of the corresponding trials. Induced power was computed by applying the TF transform to single

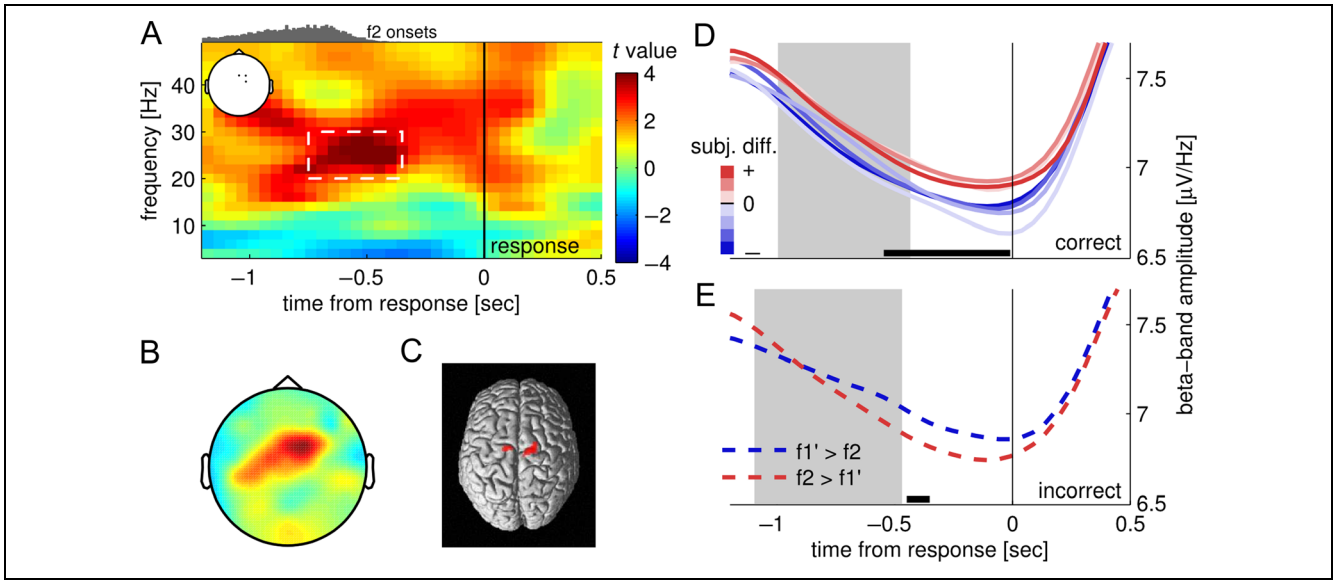

Figure 4. TF analysis revealing choice modulated signal in upper beta band. (A) *t* map of group statistics pooled over electrodes FCz, FC2, and C2 (inset) that showed a significant relationship between beta band amplitude and subjective stimulus differences (f2 − f1′). Histogram on top of the TF map indicates the distribution of onset times of the second stimulus. (B) Scalp topography of the significant TF cluster (dashed rectangle in A). (C) Estimated cortical source of TF cluster from A and B. (D) Grand mean of time courses of response locked narrow band amplitude (20–30 Hz) in electrodes from A. Data were grouped into seven classes of estimated subjective frequency difference before computing the grand mean. The gray area marks the time interval in which the second stimulus was typically presented (central 50%). The black bar indicates time window in which time courses were significantly split according to choices (see text for details). (E) Same as in D for incorrect trials. Note that correct and incorrect trials in D and E were defined based on the modeled subjective frequency differences.

trials from which the ERP, associated with the respective stimulus pair (f1, f2), was subtracted beforehand.

Statistical Analysis

The response-locked single-trial TF data were square root transformed (yielding spectral amplitudes) to approximate normally distributed data (see Kiebel, Tallon-Baudry, & Friston, 2005). To decrease intersubject variability, TF data were smoothed with a 3 Hz × 300 msec FWHM Gaussian kernel (e.g., Litvak et al., 2011; Kilner, Kiebel, & Friston, 2005). For individual participants, we regressed the spectral amplitude in each TF bin of each channel on the zero-centered estimates of subjective frequency differences across trials: We created a vector (across single trials) of subjective frequency differences (i.e., $f2 - f1'$) for each participant, subtracted the mean value, and used the vector as a predictor for between-trial variations of spectral amplitude in each TF bin. Hence, we estimated TF maps that quantified the linear relation between the individual subjective frequency differences (i.e., the results from our Bayesian model) and the spectral amplitude in each TF bin. To identify times, frequencies, and channels for which this linear relationship was significantly different from zero, we used cluster-based permutation testing (Maris & Oostenveld, 2007). We compared the summary statistics of the observed data (one-sample t test across participants in each TF bin) with a distribution of summary statistics obtained from 500 randomly sign-flipped permutations. A cluster was defined as a group of adjacent TF bins that all exceeded a cluster-defining threshold of $p_{\text{threshold}} < .001$ (uncorrected). Clusters that exceeded a family-wise error (FWE)-corrected threshold of $p_{\text{cluster}} < .05$ (corrected for time, frequency, and channels) were considered to be statistically significant.

Time Courses

On the basis of the distribution of subjective frequency difference values across participants, we binned the values into seven levels, such that for every level at least one stimulus pair (i.e., subjective frequency difference value) from each participant was available (i.e., [−0.66 to −0.33]; [−0.33 to −0.18]; [−0.18 to −0.09]; [−0.09 to 0]; [0 to 0.09]; [0.09 to 0.17]; [0.17 to 0.4]). Individual EEG data were grouped according to these levels to assess grand mean time courses and to localize the cortical source of the choice-modulated beta band signal as follows.

Source Reconstruction

The cortical sources of amplitude modulations observed on the scalp level were localized using the 3-D source reconstruction routines provided by SPM8 (Friston, Henson, Phillips, & Mattout, 2006). On the basis of the individually recorded electrode positions for each participant (substituted by default 10–20 locations for two participants because of technical difficulties), a forward model was constructed using a 8196-point cortical mesh of distributed dipoles perpendicular to the cortical surface of a template brain (cf. Friston et al., 2008). The lead field of the forward model was computed using the three-shell boundary elements method EEG head model available in SPM8. Multiple sparse priors (Friston et al., 2008) under group constraints (Litvak & Friston, 2008) were used to invert the forward model. For each condition, the results of model inversion were summarized in a 3-D image that reflected spectral source amplitude in the TF window of interest. Relevant contrasts of these 3-D images served as an estimate for subject-specific source locations and were used for group level statistical analysis (see Litvak et al., 2011). Anatomical reference for source estimates was established on the basis of the SPM anatomy toolbox (Eickhoff et al., 2005) where possible.

Choice-modulated beta band activity was localized using the preprocessed response-locked EEG data (i.e., in the time domain). Additionally, the data were band-pass filtered in the frequency range of the TF cluster identified on the scalp level (±1 Hz to ensure that no information is lost at the cluster borders; see Figure 4A). Before inverting the forward model, single trials of each participant were grouped according to the seven levels of subjective frequency differences (see Time Courses). The 3-D images summarizing each condition were computed over a representative TF window (20–30 Hz; −750 to −350 msec from button press). To identify cortical sources in which beta band amplitude was modulated by subjective frequency differences, the 3-D images were weighted by a contrast vector analogously to the sensor space analysis. Source estimates were statistically analyzed on the group level using conventional t tests and displayed at a threshold of $p < .01$ (uncorrected).

RESULTS

Behavioral Results

On average, participants made correct choices on 74.0% of all stimulus pairs. For detailed analysis, we performed a within-subject ANOVA with the factors Difficulty (±4 Hz vs. ±2 Hz stimulus difference) and Sign (positive vs. negative stimulus difference) on proportions of correct responses (PCRs), using a logit-transform to account for nonnormality of the residuals. The analysis revealed significant main effects of the factors Difficulty ($p < .001$) and Sign ($p = .014$) and a significant interaction of the two factors ($p = .001$). As expected, a larger proportion of trials were judged correctly when the (physical) $f2 - f1$ frequency difference was ±4 Hz (81.0% correct) compared with trials where the difference was only ±2 Hz (67.0%; $p < .001$; paired t test; see difficulty effect, Table 1). We also observed more correct responses for positive (77.8% correct) compared with negative frequency differences (70.3%; $p = .014$ paired t test; see sign effect, Table 1),

Table 1. Behavioral Data

	Frequency Difference of Stimuli (f2 − f1) in Hz					
	−4	*−2*	*2*	*4*	*Difficulty Effect*	*Sign Effect*
PCR (%)	75.9 ± 5.8	64.8 ± 4.9	69.3 ± 3.5	86.2 ± 4.1	− ($p < .001$)*	− ($p = .014$)*
RT correct (msec)	842.2 ± 58.1	867.7 ± 54.7	818.0 ± 65.0	777.9 ± 57.7	32.9 ± 14.1 ($p < .001$)*	57.0 ± 28.8 ($p < .001$)*
RT incorrect (msec)	917.6 ± 78.4	889.2 ± 75.8	933.1 ± 69.6	971.6 ± 81.0	−33.4 ± 30.7 ($p = .034$)*	−49.0 ± 37.7 ($p = .014$)*

PCRs and RTs as a function of the physical frequency difference f2 − f1. Mean values ± 95% confidence interval are shown. Difficulty effect compares easy (±4 Hz) and difficult (±2 Hz) trials in a paired *t* test. Sign effect compares trials with a positive (2 and 4 Hz) and negative (−4 and −2 Hz) frequency difference in a paired *t* test. RTs showed significant effects of difficulty and sign for correct and incorrect trials, however, in opposing directions (cf. interactions in ANOVA of RTs). PCRs were logit-transformed before testing, because of nonnormally distributed residuals. Asterisks indicate statistically significant results.

which indicates an overall response bias toward "f2 > f1" choices (mean criterion shift: 0.0881; $p = .0076$; one-sample *t* test).

An ANOVA (2 × 2 × 2 repeated-measures design with factors Correct/incorrect, Difficulty, and Sign) of the median RTs showed a significant main effect for the factor Accuracy ($p < .001$) and two significant interactions (Accuracy × Sign and Accuracy × Difficulty, all ps $< .001$). More precisely, the median RT with respect to f2 stimulus onset was on average shorter for correct trials (826 msec) than for incorrect trials (927 msec; $p < .001$; paired *t* test). The precise pattern of interaction effects in the RT data is detailed in Table 1.

Bayesian Inference Model Describes Individual Choice Behavior

Assuming that the difference f2 − f1 (both frequencies on logarithmic scale according to Weber's law) describes the comparison of vibrotactile frequencies in our task, one would expect PCRs as illustrated in Figure 1B. That is, PCRs for trials with $|f2 - f1| = 4$ Hz should always be higher than for trials with $|f2 - f1| = 2$ Hz, independent of the specific frequency values of f1 and f2. However, we observed strong and systematic departures from such response behavior (Figure 1D and E). In particular, the proportion of "f2 > f1" choices increased with increasing f1, whereas the proportion of "f1 > f2" choices increased with decreasing f1 (Figure 1D). Both trends intersected at the mean frequency of the stimulus set. This systematic and symmetric bias reflects the characteristic influence of the TOE on choices in sequential 2AFC comparison tasks (cf. Sanchez, 2014; Preuschhof et al., 2010).

In other words, the observed choice pattern suggests that participants showed a tendency to compare f2 with the mean of the stimulus set (i.e., with a representation of f1 that had regressed to the mean of the stimulus set). As a consequence, the mere difference of the physical magnitudes f2 − f1 is not sufficient to account for the comparison process that drives decisions in our task (Figure 2B vs. C; cf. Hellström, 2003). Hence, we used a Bayesian model (cf. Petzschner et al., 2015; Sanchez, 2014; Ashourian & Loewenstein, 2011) that accounts for the influence of the TOE and yields estimates of the subjectively perceived frequency differences (f2 − f1′) for each stimulus pair and participant (see Bayesian model and Figure 2A). In our model, the posterior distribution of f1 is used to describe the representation of f1 by incorporating a priori knowledge about the stimulus set as well as the actual value of f1. Consequently, the posterior (centered on f1′) is closer to the mean of the stimulus set than the true value of f1 (cf. f1 vs. f1′ in Figure 2A). Simulated choices based on comparing f2 with f1′ (i.e., f2 − f1′) approximated the PCR on the test data set for each participant very well (Figure 2B). Furthermore, the estimated model parameters accounted for individual differences in behavioral measures across participants. The estimated precision of stimulus encoding ($1/\sigma^2_{stim}$) was clearly correlated with conventional d′ values ($r = .87$, $p < .001$; Figure 2C), whereas the individual influence of the TOE was well described by the participants' precision of prior knowledge ($1/\sigma^2_{prior}$; $r = .85$, $p < .001$; Figure 2D). In other words, the higher the influence of prior knowledge on the percept of f1, the larger the influence of the TOE on choices (cf. Karim et al., 2012). As anticipated, also the estimated values of the bias term b were highly correlated with individuals' general response bias toward responding "f2 > f1" or "f1 > f2" independent of any stimulus information (i.e., criterion shift; $r = .92$, $p < .001$). Using BFs to quantify the quality of the proposed model (as compared with a "null" model based on the physical differences f2 − f1) provided positive evidence (BF > 3) in favor of the proposed model for each participant (all BFs > 7, strong evidence with BF > 20 for 12 participants; cf. Kass & Raftery, 1995). Furthermore, BFs were also highly correlated with the individual influence of the TOE on choice behavior ($r = .96$, $p < .001$), indicating that accounting for the TOE is the reason for the improved model fit.

Stimulus-evoked Activity and Task-induced TF Modulations

At first, we verified the presence of well-documented somatosensory stimulus effects in the EEG recordings. Figure 3A illustrates the TF representation of steady-state-evoked potentials collapsed across representative electrodes (Fz, F2, FC2, FCz, CP6, CP4, P4, P6; see inset, Figure 3A) during stimulus presentation for an exemplary stimulus pair (f1 = 20 Hz; f2 = 24 Hz). As expected, the evoked TF spectrum prominently mirrors the frequency and duration of the presented stimuli (Figure 3A).

The TF representation of the grand-average induced power (Figure 3B) mimicked the typical pattern reported in previous EEG studies of vibrotactile 2AFC tasks (e.g., Spitzer et al., 2010). Results are shown for illustrative electrodes C3, C4, C5, C6, CP3, CP4, CP5, CP6, and POz (see inset, Figure 3B). Throughout the trial, a marked increase in occipital alpha band activity (8–12 Hz) was evident (Figure 3B). Furthermore, we observed a power decrease over bilateral somatosensory areas during/after f1 presentation in the alpha/mu (8–12 Hz) to beta (15–25 Hz) frequency bands (Figure 3B). This power decrease was followed by a rebound (i.e., a recovery with subsequent increase beyond baseline/previous level) of beta band power in electrodes over contralateral (i.e., right hemispheric) somatosensory areas (~400 to 800 msec after f1; Figure 3B). Finally, in the time interval between f2 stimulus offset and participants' responses, we observed a decrease in beta band power peaking over ipsilateral (left) primary motor cortex (electrode C3; Figure 3B). All effects reported here passed a conservative test on statistical significance (cluster-based permutation test, $p_{\text{threshold}} < .001$, and $p_{\text{cluster}} < .05$, FWE-corrected).

Beta Band Oscillations in Premotor Areas Encode Choice Independent of Response Mapping

To test if the frequency comparison (f1 vs. f2) was reflected in oscillatory EEG activity, we used the subjectively perceived frequency differences as inferred from our Bayesian model (i.e., f2 − f1′) as regressors for a linear regression analysis of each participant's single-trial TF spectra. The analysis revealed a positive relationship between the upper beta band amplitude (~20–30 Hz) and the subjective frequency differences in medial–frontal electrodes (FCz, FC2, and C2; inset Figure 4A) well before responses were given (−750 to −350 msec from response; $p_{\text{cluster}} = .019$, FWE-corrected; Figure 4A, dashed rectangle). More specifically, high values of the signed subjective frequency differences (i.e., the decision-relevant quantity f2 − f1′) were associated with high amplitudes, whereas low (i.e., negative) values were reflected by low amplitudes. The scalp topography (Figure 4B) and 3-D source localization (Figure 4C) of the TF cluster suggest that the beta band modulation originated from premotor areas (Brodmann's area 6, peak coordinates in MNI space: 20, −6, 68). Qualitatively very similar results were obtained when using physical frequency differences (i.e., f2 − f1) for the analysis, which is an expected outcome given that subjective and physical frequency difference values were highly correlated ($r \geq .7$ for every participant).

In a control analysis, we checked whether the observed modulation of upper beta band amplitude could have been explained by the values of f2 alone: We repeated the main analysis as described above on a subset of data in which only trials were considered with f2 values that could lead to either choice (i.e., "f2 > f1" and "f2 < f1"). With this reduced data set, we found the same modulation of upper beta band amplitude (~20–30 Hz) consistent in location (FC2) and time (−850 to −500 msec from response; $p_{\text{cluster}} = .074$, FWE-corrected), indicating that the modulation was indeed decision related. Furthermore, we tested whether the overall response bias in behavior might have contributed to the finding that "f2 > f1" choices are associated with a higher upper beta band amplitude. To this end, we computed another control analysis using only data of participants that showed no substantial response bias (absolute value of criterion shift < 0.1; six participants). Despite the reduced sample size, this analysis still revealed the same tendency of "f2 > f1" choices being reflected in a higher beta band amplitude (for correct and incorrect choices).

Figure 4 (D and E) shows the grand mean time courses of upper beta band amplitude for correct and incorrect trials. Importantly, the definition of correct and incorrect was based on the modeled subjective frequency differences, that is, we classified objectively incorrect trials (e.g., "f2 > f1" choice, but f2 < f1) as subjectively correct (and vice versa) if choices were in accordance with the subjectively perceived frequency difference as inferred from Bayesian modeling (e.g., f2 > f1′; 16 participants showed at least one of these swaps). For subjectively correct trials (Figure 4D), we computed the grand mean time courses for each of the seven subjective difference levels as inferred from Bayesian modeling (see Methods). Note that the aforementioned swaps from objectively incorrect to subjectively correct trials (and vice versa) only occurred in the two subjective difference levels bordering zero (the lightest blue and the lightest red in Figure 4D). Taking these swaps into account led to a significant increase in the difference of beta band amplitude between the two affected levels of subjective difference as compared with using the objective definition of correct and incorrect trials (paired t test, $p = .019$). Overall, beta band amplitude appeared categorically modulated according to the two types of choice, rather than being linearly modulated by the subjective frequency difference values. The black bar in Figure 4D indicates a time window within which pairwise statistical tests of beta band amplitude between choice categories ("f2 > f1" or "f2 < f1") were significantly different (paired one-sided t test, $p < .05$, false discovery rate-corrected), whereas

none of the pairwise tests reached significance within choices ($p > .05$, false discovery rate-corrected). For subjectively incorrect trials (i.e., choices that were not in line with the modeled subjectively perceived frequency differences), we computed the grand mean time courses for two classes only (f2 > f1′ and f1′ > f2; Figure 4E) because of insufficient trial numbers for some levels of subjective frequency differences in individual participants. Importantly, a categorical bifurcation of upper beta band amplitude according to choices was also observed for subjectively incorrect trials (black bar: paired one-sided t test, $p < .05$; Figure 4E). Taken together, the upper beta band activity seems to reflect the internal representation of a subjective quantity (i.e., the subjective comparison outcome) that determines choices (correct and incorrect) in the given task.

Finally, we asked if the choice-related modulation of beta band amplitude depended on a specific mapping of choices onto button presses. Therefore, we divided participants into two groups according to their response mapping (i.e., whether the index or middle finger was used to indicate "f2 > f1"). For each group, we investigated separately whether the medial–frontal beta band amplitude was in the same way choice-modulated as observed for the entire group (i.e., higher beta band activity for "f2 > f1" choices for correct and incorrect trials). On the basis of the results above, we pooled correct and incorrect trials and compared the average beta band amplitude between "f2 > f1" and "f1 > f2" choices for each participant. Figure 5 displays the two group level scalp topographies of the difference in beta band amplitude (between choices) for the previously identified TF cluster (−750 to −350 msec from response, 20–30 Hz). The beta band modulations in the two groups were of the same sign (i.e., higher beta band amplitude for "f2 > f1" choices), showed considerable topographical overlap (cf. white dots in Figure 5A and B span cluster for whole group), and were statistically indistinguishable (independent two-sample t test comparing both scalp topographies revealed no clusters, all $ps > p_{\text{threshold}}$). In other words, the choice-related modulations of beta band amplitude were not systematically linked to the subsequent execution of a specific motor response associated with either choice.

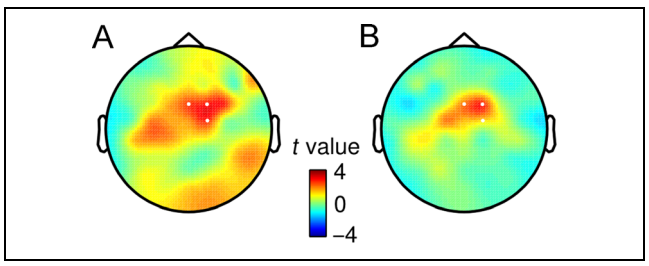

Figure 5. Choice-dependent modulation of premotor upper beta activity was invariant to the individual motor response mapping. (A) Scalp topography of choice modulated beta band activity (20–30 Hz; −750 to −350 msec from button press) for response mapping f1 > f2: index finger; f2 > f1: middle finger. (B) Same as in A for reversed response mapping (f1 > f2: middle finger; f2 > f1: index finger). White dots in A and B mark the significant electrodes identified in main analysis.

DISCUSSION

We investigated oscillatory EEG signatures of perceptual decisions that are based on comparing two sequentially presented vibrotactile frequencies f1 and f2. Medial–frontal upper beta band amplitude (~20–30 Hz) was modulated by participants' choices, regardless of the specific motor response mapping. In particular, choices of "f2 > f1" were always accompanied by higher beta band amplitude than "f1 > f2" choices. Importantly, these choice-related modulations of oscillatory activity were evident clearly before responses were given and were source-localized to premotor areas. Our findings extend previous studies linking neuronal activity in PMC of nonhuman primates to vibrotactile comparisons (Haegens et al., 2011; Hernández et al., 2002, 2010; Romo et al., 2004). Neuronal firing rates in vPMC and mPMC were shown to be modulated by the signed difference between vibrotactile frequencies (i.e., f2 − f1; Hernández et al., 2002, 2010; Romo et al., 2004). Moreover, Haegens et al. (2011) reported a choice-related signal on the population level, that is, in form of amplitude modulations of beta band oscillations in monkey PMC. Here, for the first time, we extend these findings to human observers with remarkable consistency in terms of quality (higher amplitudes for "f2 > f1" choices independent of accuracy and motor response), putative source (PMC), and frequency (beta band). Because we recorded EEG from the whole scalp, our data additionally suggest (within the scope of EEG) that such modulations of beta band amplitude prior to overt responding might in fact be specific to premotor areas. Notably, Haegens et al. (2011) used a delayed response protocol, whereas our task allowed an immediate response. This difference is likely to explain why Haegens et al. (2011) found the choice-related modulation of beta band amplitude accompanied by a beta peak, whereas we see the same effect on top of an overall beta band desynchronization (i.e., power decrease; most likely because of the preparation of the ensuing button press and propagated via volume conductance from left motor cortex to those electrodes that show the choice-related amplitude modulation).

In contrast to previous studies investigating decision processes in the vibrotactile comparison task, we did not use the physical frequency differences (f2 − f1) to characterize choices in this task. Instead, we modeled subjectively perceived frequency differences (f2 − f1′) for each stimulus pair based on individual behavioral data. Thus, we could account for a characteristic bias in choice behavior commonly observed in 2AFC comparison tasks (cf. TOE; Sanchez, 2014; Ashourian & Loewenstein, 2011), while obtaining a proxy for the putative internal representation of the underlying comparison (i.e., the subjectively

perceived frequency difference f2 − f1′). Expanding on classic psychophysical models (cf. Sanchez, 2014; Karim et al., 2012; Hellström, 1979, 1985), subjectively perceived frequency differences in our parsimonious model were defined as the difference between f2 and a weighted average of f1 and the mean of the stimulus set, expressed in terms of Bayesian inference (cf. Petzschner et al., 2015). For each participant, the model based on subjectively perceived frequency differences (f2 − f1′) explained the behavioral data significantly better than a comparable model based only on physical/objective differences (f2 − f1; BF > 7 for all participants). Although both models yielded qualitatively similar results in the EEG analyses, the subjective difference model permitted a considerably more fine-grained scale of individual frequency differences (16 subjective frequency differences vs. 4 physical frequency differences), revealing that the time courses of beta band amplitude clearly separated into only two distinct choice-specific levels. The EEG analysis based on subjectively perceived frequency differences thus indicates more conclusively than an analysis using physical frequency differences that the observed amplitude modulation in the beta band during decision-making is presumably categorical, rather than parametric (monotonic). This suggests that premotor beta band amplitude does not represent the (relative or absolute) decisional evidence per se, but rather the categorical outcome of the internal comparison (see also Haegens et al., 2011). Under this view, additional, potentially more finely graded comparison processes are likely to occur upstream of the large-scale oscillatory signal disclosed in the present analysis.

Notably, the present amplitude modulation in the beta band was inverted for incorrect trials, underpinning the interpretation that this activity corresponds to an internal representation of the subjective decision outcome. In other words, the beta band amplitude reflects whether an observer is about to choose "f2 > f1" or "f1 > f2." Importantly, the choice outcome was disentangled from specific motor responses in our study, in contrast to studies that exploit lateralized EEG signals in preparation for a motor response to predict decisions (e.g., Polanía, Krajbich, Grueschow, & Ruff, 2014; O'Connell, Dockree, & Kelly, 2012; Schurger, Sitt, & Dehaene, 2012; Donner, Siegel, Fries, & Engel, 2009). In the present work, participants indicated decisions by pressing one of two buttons, always with their right hands, using different fingers. We counterbalanced the response mapping across participants and found the same modulation of beta band amplitude no matter which finger was used to respond. Similarly, Haegens and colleagues showed that the choice-related modulation of beta band amplitude in monkeys was absent when no f1-versus-f2 comparison was required, but a prespecified button was pressed (Haegens et al., 2011; see also Romo et al., 2004; Hernández et al., 2002). Both approaches converge on showing that the beta band amplitude modulations in premotor areas are decision related (i.e., choice-selective) and not merely linked to a (specific) motor response (i.e., effector-selective; see e.g., Polanía et al., 2014; O'Connell et al., 2012; Schurger et al., 2012; Donner et al., 2009). Taken together, upper beta band amplitude in PMC seems to represent subjective choices (i.e., the subjectively categorized outcome of a quantitative comparison) that are not yet expressed in specific motor terms.

Besides the choice-related modulations, we also found typical patterns of sensorimotor beta band oscillations (~15–25 Hz) that are routinely observed during somatosensory and motor tasks. That is, when a tactile stimulus is presented or anticipated, beta band activity is known to decrease over somatosensory areas and to rebound ~600 msec afterwards (e.g., Van Ede, de Lange, Jensen, & Maris, 2011; Bauer, Oostenveld, Peeters, & Fries, 2006; Pfurtscheller, 1981; Jasper & Andrews, 1938). In preparation for and during a voluntary hand movement, the same pattern of beta band desynchronization, followed by a rebound, can be observed over contralateral motor areas (e.g., Pfurtscheller, 1981; Jasper & Penfield, 1949). However, it appears unlikely that the choice-related amplitude modulations in the upper beta band we observed over premotor areas are epiphenomena of these classic sensorimotor signals: We confined our analysis to response-locked data to render confounding effects of motor preparation unlikely in the first place. In response-locked data, systematic RT variations should affect beta band amplitude only in form of systematically time-shifted stimulus-locked signals (e.g., a beta band rebound after f2). However, the observed time courses of upper beta band amplitude showed no sign of any time-shifted components (Figure 4D and E). Lastly, we can also rule out that the observed modulations in the upper beta band might be explained by generally higher f2 values in "f2 > f1" choices. When using a subset of data, including only trials in which f2 values could lead to either choice, we still found the same beta band amplitude modulations in electrodes over premotor areas. Taken together, the reported findings are highly unlikely to be the result of a systematic stimulus or response artifact.

In addition to a notable consistency between our results and previous work in nonhuman primates (e.g., Haegens et al., 2011), our findings also connect well with human EEG studies that investigated parametric WM correlates. In vibrotactile comparisons with longer delay periods, Spitzer and colleagues found that upper beta band amplitude (~20–30 Hz) in PFC was systematically modulated by the to-be-maintained vibrotactile frequency information (Spitzer & Blankenburg, 2011; Spitzer et al., 2010). In particular, during the retention interval of the task, the frequency of the first stimulus (f1) was encoded by the upper beta band amplitude. Further work suggests that upper beta band amplitude might encode analogue WM-related quantity information in a supramodal, generalized fashion (Spitzer, Gloel, Schmidt, & Blankenburg, 2014; Spitzer & Blankenburg, 2012). From this perspective, the present results suggest that the upper beta band

amplitude in respective brain areas (PFC and/or PMC) seems to represent task-relevant quantities during the according phases of the vibrotactile comparison task. That is, a detailed representation of absolute quantity during retention (in form of parametric modulations in PFC, see also Barak et al., 2010; Romo et al., 1999) and a categorical representation of the comparison outcome relating to either choice before responding (in form of categorical, choice-dependent modulations in PMC, see also Haegens et al., 2011; Romo et al., 2004; Hernández et al., 2002).

The present finding should be differentiated from a previously reported association of beta band amplitude with the accuracy of a decision (Donner et al., 2007). Donner and colleagues found that in a visual motion detection task beta band amplitude in the dorsal visual pathway was higher for correct trials than for incorrect trials. As discussed by the authors, this finding may relate to the computations that are involved in forming a decision and, in particular, might index the confidence of a decision. In contrast, the results of this study provide evidence for the upper beta band amplitude to represent a quantity on which a perceptual decision is based (see also Siegel, Engel, & Donner, 2011; Donner et al., 2007; deCharms & Zador, 2000). Together with recent studies of WM (see also Spitzer et al., 2014), the present results might suggest beta band activity as a "spectral fingerprint" (see Siegel et al., 2012) of large-scale neural activity involved in the internal evaluation of analogue/quantitative information. However, it remains to be shown in future research how such content representation arises mechanistically in the amplitude of upper beta band oscillations.

To conclude, during vibrotactile frequency comparisons, upper beta band amplitude (~20–30 Hz) in premotor areas was modulated by the choice of participants, independent of a specific motor response and regardless of the correctness of the choice. The topography, timing, and frequency range of the reported signal are in notable agreement with previous findings in nonhuman primates performing an analogue task. In particular, premotor upper beta band amplitude encoded subjective choices prior to translation into an effector-specific motor command. Hence, we suggest that this signal is an internal representation of the subjective categorical outcome of the comparison underlying perceptual decisions in the vibrotactile comparison task.

Acknowledgments

This work was supported by the Deutsche Forschungsgemeinschaft (DFG, GRK1589/1). We thank Simon Ludwig and Sebastian Fleck for help with data acquisition and Jakub Limanowski for useful comments on the manuscript. Moreover, we want to thank Gaëtan Sanchez and Jeremie Mattout for providing the code of their model, on which we based the implementation of our model.

Reprint requests should be sent to Jan Herding, Neurocomputation and Neuroimaging Unit, Department of Education and Psychology, Freie Universität Berlin, Habelschwerdter Allee 45, 14195 Berlin, Germany, or via e-mail: jan.herding@bccn-berlin.de.

Note

1. The expression "f1 > f2" refers to a choice, whereas f1 > f2 describes the relation between the physical values of f1 and f2.

REFERENCES

Ashourian, P., & Loewenstein, Y. (2011). Bayesian inference underlies the contraction bias in delayed comparison tasks. *PLoS One, 6,* e19551.

Barak, O., Tsodyks, M., & Romo, R. (2010). Neuronal population coding of parametric working memory. *Journal of Neuroscience, 30,* 9424–9430.

Bauer, M., Oostenveld, R., Peeters, M., & Fries, P. (2006). Tactile spatial attention enhances gamma-band activity in somatosensory cortex and reduces low-frequency activity in parieto-occipital areas. *Journal of Neuroscience, 26,* 490–501.

Daunizeau, J., Adam, V., & Rigoux, L. (2014). VBA: A probabilistic treatment of nonlinear models for neurobiological and behavioural data. *PLoS Computational Biology, 10,* e1003441.

deCharms, R. C., & Zador, A. (2000). Neural representation and the cortical code. *Annual Review of Neuroscience, 23,* 613–647.

Donner, T. H., Siegel, M., Fries, P., & Engel, A. K. (2009). Buildup of choice-predictive activity in human motor cortex during perceptual decision making. *Current Biology, 19,* 1581–1585.

Donner, T. H., Siegel, M., Oostenveld, R., Fries, P., Bauer, M., & Engel, A. K. (2007). Population activity in the human dorsal pathway predicts the accuracy of visual motion detection. *Journal of Neurophysiology, 98,* 345–359.

Eickhoff, S. B., Stephan, K. E., Mohlberg, H., Grefkes, C., Fink, G. R., Amunts, K., et al. (2005). A new SPM toolbox for combining probabilistic cytoarchitectonic maps and functional imaging data. *Neuroimage, 25,* 1325–1335.

Fechner, G. T. (1860). *Elemente der Psychophysik.* Leipzig: Breitkopf & Härtel.

Friston, K., Harrison, L., Daunizeau, J., Kiebel, S., Phillips, C., Trujillo-Barreto, N., et al. (2008). Multiple sparse priors for the M/EEG inverse problem. *Neuroimage, 39,* 1104–1120.

Friston, K., Henson, R., Phillips, C., & Mattout, J. (2006). Bayesian estimation of evoked and induced responses. *Human Brain Mapping, 27,* 722–735.

Haegens, S., Nácher, V., Hernández, A., Luna, R., Jensen, O., & Romo, R. (2011). Beta oscillations in the monkey sensorimotor network reflect somatosensory decision making. *Proceedings of the National Academy of Sciences, U.S.A., 108,* 10708–10713.

Hellström, Å. (1979). Time errors and differential sensation weighting. *Journal of Experimental Psychology: Human Perception and Performance, 5,* 460–477.

Hellström, Å. (1985). The time-order error and its relatives: Mirrors of cognitive processes in comparing. *Psychological Bulletin, 97,* 35–61.

Hellström, A. (2003). Comparison is not just subtraction: Effects of time- and space-order on subjective stimulus difference. *Perception & Psychophysics, 65,* 1161–1177.

Hernández, A., Nácher, V., Luna, R., Zainos, A., Lemus, L., Alvarez, M., et al. (2010). Decoding a perceptual decision process across cortex. *Neuron, 66,* 300–314.

Hernández, A., Zainos, A., & Romo, R. (2000). Neuronal correlates of sensory discrimination in the somatosensory

cortex. *Proceedings of the National Academy of Sciences, U.S.A., 97,* 6191–6196.
Hernández, A., Zainos, A., & Romo, R. (2002). Temporal evolution of a decision-making process in medial premotor cortex. *Neuron, 33,* 959–972.
Ille, N., Berg, P., & Scherg, M. (2002). Artifact correction of the ongoing EEG using spatial filters based on artifact and brain signal topographies. *Journal of Clinical Neurophysiology, 19,* 113–124.
Jasper, H., & Andrews, H. (1938). Electro-encephalography: III. Normal differentiation of occipital and precentral regions in man. *Archives of Neurology & Psychiatry, 39,* 96–115.
Jasper, H., & Penfield, W. (1949). Electrocorticograms in man: Effect of voluntary movement upon the electrical activity of the precentral gyrus. *Arch Psychiatrie und Z gesamte Neurologie, 183,* 163–174.
Karim, M., Harris, J. A., Morley, J. W., & Breakspear, M. (2012). Prior and present evidence: How prior experience interacts with present information in a perceptual decision making task. *PLoS One, 7,* e37580.
Kass, R. E., & Raftery, A. E. (1995). Bayes factors. *Journal of the American Statistical Association, 90,* 773–795.
Kiebel, S. J., Tallon-Baudry, C., & Friston, K. J. (2005). Parametric analysis of oscillatory activity as measured with EEG/MEG. *Human Brain Mapping, 26,* 170–177.
Kilner, J. M., Kiebel, S. J., & Friston, K. J. (2005). Applications of random field theory to electrophysiology. *Neuroscience Letters, 374,* 174–178.
Litvak, V., & Friston, K. (2008). Electromagnetic source reconstruction for group studies. *Neuroimage, 42,* 1490–1498.
Litvak, V., Mattout, J., Kiebel, S., Phillips, C., Henson, R., Kilner, J., et al. (2011). EEG and MEG data analysis in SPM8. *Computational Intelligence and Neuroscience, 2011,* 852961.
Maris, E., & Oostenveld, R. (2007). Nonparametric statistical testing of EEG- and MEG-data. *Journal of Neuroscience Methods, 164,* 177–190.
O'Connell, R. G., Dockree, P. M., & Kelly, S. P. (2012). A supramodal accumulation-to-bound signal that determines perceptual decisions in humans. *Nature Neuroscience, 15,* 1729–1735.
Petzschner, F. H., Glasauer, S., & Stephan, K. E. (2015). A Bayesian perspective on magnitude estimation. *Trends in Cognitive Sciences, 19,* 285–293.
Pfurtscheller, G. (1981). Central beta rhythm during sensorimotor activities in man. *Electroencephalography and Clinical Neurophysiology, 51,* 253–264.
Polanía, R., Krajbich, I., Grueschow, M., & Ruff, C. C. (2014). Neural oscillations and synchronization differentially support evidence accumulation in perceptual and value-based decision making. *Neuron, 82,* 709–720.
Preuschhof, C., Schubert, T., Villringer, A., & Heekeren, H. R. (2010). Prior information biases stimulus representations during vibrotactile decision making. *Journal of Cognitive Neuroscience, 22,* 875–887.
Romo, R., Brody, C. D., Hernández, A., & Lemus, L. (1999). Neuronal correlates of parametric working memory in the prefrontal cortex. *Nature, 399,* 470–473.
Romo, R., & de Lafuente, V. (2013). Conversion of sensory signals into perceptual decisions. *Progress in Neurobiology, 103,* 41–75.
Romo, R., Hernández, A., & Zainos, A. (2004). Neuronal correlates of a perceptual decision in ventral premotor cortex. *Neuron, 41,* 165–173.
Romo, R., & Salinas, E. (2003). Flutter discrimination: Neural codes, perception, memory and decision making. *Nature Reviews Neuroscience, 4,* 203–218.
Sanchez, G. (2014). *Real-time electrophysiology in cognitive neuroscience: Towards adaptive paradigms to study perceptual learning and decision making in humans*. PhD thesis, Université Claude Bernard Lyon 1, France.
Schurger, A., Sitt, J. D., & Dehaene, S. (2012). An accumulator model for spontaneous neural activity prior to self-initiated movement. *Proceedings of the National Academy of Sciences, U.S.A., 109,* E2904–E2913.
Siegel, M., Donner, T. H., & Engel, A. K. (2012). Spectral fingerprints of large-scale neuronal interactions. *Nature Reviews Neuroscience, 13,* 121–134.
Siegel, M., Engel, A. K., & Donner, T. H. (2011). Cortical network dynamics of perceptual decision-making in the human brain. *Frontiers in Human Neuroscience, 5,* 21.
Spitzer, B., & Blankenburg, F. (2011). Stimulus-dependent EEG activity reflects internal updating of tactile working memory in humans. *Proceedings of the National Academy of Sciences, U.S.A., 108,* 8444–8449.
Spitzer, B., & Blankenburg, F. (2012). Supramodal parametric working memory processing in humans. *Journal of Neuroscience, 32,* 3287–3295.
Spitzer, B., Gloel, M., Schmidt, T. T., & Blankenburg, F. (2014). Working memory coding of analog stimulus properties in the human prefrontal cortex. *Cerebral Cortex, 24,* 2229–2236.
Spitzer, B., Wacker, E., & Blankenburg, F. (2010). Oscillatory correlates of vibrotactile frequency processing in human working memory. *Journal of Neuroscience, 30,* 4496–4502.
Talbot, W., Darian-Smith, I., Kornhuber, H., & Mountcastle, V. (1968). The sense of flutter-vibration: Comparison of the human capacity with response patterns of mechanoreceptive afferents from the monkey hand. *Neurophysiology, 31,* 301–334.
Tobimatsu, S., Zhang, Y. M., & Kato, M. (1999). Steady-state vibration somatosensory evoked potentials: Physiological characteristics and tuning function. *Clinical Neurophysiology, 110,* 1953–1958.
Van Ede, F., de Lange, F., Jensen, O., & Maris, E. (2011). Orienting attention to an upcoming tactile event involves a spatially and temporally specific modulation of sensorimotor alpha- and beta-band oscillations. *Journal of Neuroscience, 31,* 2016–2024.
Woodrow, H. (1935). The effect of practice upon time-order errors in the comparison of temporal intervals. *Psychological Review, 42,* 127–152.

Study 2 - Response-Modality-Specific Encoding of Human Choices in Upper Beta Band Oscillations during Vibrotactile Comparisons

Herding, J., Ludwig, S., and Blankenburg, F. (2017). Response-Modality-Specific Encoding of Human Choices in Upper Beta Band Oscillations during Vibrotactile Comparisons. Frontiers in Human Neuroscience, 11. doi: 10.3389/fnhum.2017.00118

This document is protected by copyright and was first published by Frontiers. All rights reserved. It is reproduced with permission.

frontiers in Human Neuroscience

ORIGINAL RESEARCH
published: 15 March 2017
doi: 10.3389/fnhum.2017.00118

Response-Modality-Specific Encoding of Human Choices in Upper Beta Band Oscillations during Vibrotactile Comparisons

Jan Herding[1,2]*, *Simon Ludwig*[1] and *Felix Blankenburg*[1,2]

[1] Neurocomputation and Neuroimaging Unit, Department of Education and Psychology, Freie Universität Berlin, Berlin, Germany, [2] Bernstein Center for Computational Neuroscience Berlin, Berlin, Germany

Perceptual decisions based on the comparison of two vibrotactile frequencies have been extensively studied in non-human primates. Recently, we obtained corresponding findings from human oscillatory electroencephalography (EEG) activity in the form of choice-selective modulations of upper beta band amplitude in medial premotor areas. However, the research in non-human primates as well as its human counterpart was so far limited to decisions reported by button presses. Thus, here we investigated whether the observed human beta band modulation is specific to the response modality. We recorded EEG activity from participants who compared two sequentially presented vibrotactile frequencies (f1 and f2), and decided whether f2 > f1 or f2 < f1, by performing a horizontal saccade to either side of a computer screen. Contrasting time-frequency transformed EEG data between both choices revealed that upper beta band amplitude (~24–32 Hz) was modulated by participants' choices before actual responses were given. In particular, "f2 > f1" choices were always associated with higher beta band amplitude than "f2 < f1" choices, irrespective of whether the choice was correct or not, and independent of the specific association between saccade direction and choice. The observed pattern of beta band modulation was virtually identical to our previous results when participants responded with button presses. In line with an intentional framework of decision making, the most likely sources of the beta band modulation were now, however, located in lateral as compared to medial premotor areas including the frontal eye fields. Hence, we could show that the choice-selective modulation of upper beta band amplitude is on the one hand consistent across different response modalities (i.e., same modulation pattern in similar frequency band), and on the other hand effector specific (i.e., modulation originating from areas involved in planning and executing saccades).

Keywords: beta band, EEG, decision making, vibrotactile, saccade

OPEN ACCESS

Edited by:
Uta Noppeney,
University of Birmingham, UK

Reviewed by:
Markus Bauer,
University of Nottingham, UK
Vadim Nikulin,
Charité, Germany
Saskia Haegens,
Columbia University, USA

***Correspondence:**
Jan Herding
jan.herding@bccn-berlin.de

Received: *29 September 2016*
Accepted: *24 February 2017*
Published: *15 March 2017*

Citation:
Herding J, Ludwig S and Blankenburg F (2017) Response-Modality-Specific Encoding of Human Choices in Upper Beta Band Oscillations during Vibrotactile Comparisons. Front. Hum. Neurosci. 11:118. doi: 10.3389/fnhum.2017.00118

INTRODUCTION

One of the most complete pictures of neural processes involved in perceptual decision making emerges from the seminal work that has been done in the somatosensory domain over the last years (see Romo and de Lafuente, 2013 for a comprehensive review). Romo and colleagues scrutinized neuronal activity in non-human primates during all stages of a vibrotactile two-alternative forced

choice (2AFC) task. In this task, monkeys had to compare two frequencies (f1 and f2) that were presented one after another, separated by a short working memory (WM) period. Decisions about whether f2 > f1 or f2 < f1 had to be reported via button press after the presentation of f2. Electrophysiological recordings revealed that firing rates in somatosensory cortices (primary and secondary; SI and SII) scaled with the stimulus frequency during presentation (Hernández et al., 2000), whereas prefrontal cortex (PFC) firing rates mirrored f1 (i.e., the frequency) during the WM period (Romo et al., 1999; see also Barak et al., 2010). Most importantly, firing rates in medial and ventral premotor cortex (mPMC and vPMC) encoded the upcoming choices of the monkeys for correct and incorrect decisions (Hernández et al., 2002; Romo et al., 2004).

More recently, Haegens et al. (2011) showed that the monkeys' choices in the vibrotactile 2AFC task were also reflected by amplitude modulations of beta band oscillations (∼18–26 Hz) in premotor local field potentials (LFPs). Applying the same task in a human electroencephalography (EEG) study, we found that this result also translates into beta band oscillations recorded at the scalp (Herding et al., 2016). In particular, the amplitude of upper beta band oscillations (∼20–30 Hz), most likely originating from medial premotor areas, was higher when participants chose "f2 > f1" as compared to "f2 < f1," for correct and for incorrect decisions. These findings match the results of Haegens et al. (2011), and hence, nicely complement the body of work by Romo and colleagues in non-human primates (see above).

According to the notion of an intentional framework of decision making, neural correlates of decisions should be found in brain areas that are involved in the planning and execution of the ensuing motor response (e.g., Cisek, 2007; Shadlen et al., 2008; Cisek and Kalaska, 2010). The work in non-human primates, as well as our recent study, required choices to be reported by a button press. Thus, observing choice-specific neural activity in premotor areas, for planning and informing an ensuing button press, is in line with an intentional framework of decision making. The importance of the intentional framework has been fostered in particular by the extensive body of work compiled by Shadlen and co-workers (reviewed in Gold and Shadlen, 2007). In the visual domain, perceptual decisions that are expressed by saccades, involve those brain areas that are responsible for saccade planning/execution, i.e., lateral intraparietal area (LIP; e.g., Shadlen and Newsome, 1996), frontal eye fields (FEF; e.g., Kim and Shadlen, 1999), and superior colliculus (SC; e.g., Ratcliff et al., 2003).

Taken together, each of the two major lines of research on perceptual decision making in non-human primates (cf. Gold and Shadlen, 2007; Romo and de Lafuente, 2013) appears to converge towards the notion of an intentional framework of decision making. However, the findings from both approaches (vibrotactile button press decisions and visual saccade decisions) have not yet been linked, and thus it is still unclear whether the respective results are directly transferable. In the present study, we aimed to bridge the gap between these two lines of research. We used the vibrotactile 2AFC task typically utilized by Romo and colleagues combined with saccade responses as applied in most of the work by Shadlen and colleagues. In particular, we investigated whether the choice-specific beta band modulation that we observed in our recent study (Herding et al., 2016) would still be present when participants were asked to respond with saccades instead of button presses. If so, can such a modulation be attributed to a brain area that is involved in the planning and execution of saccades as predicted by an intentional framework of decision making? To address these questions, we recorded EEG data of human participants during the vibrotactile 2AFC task, where choices were indicated by horizontal saccades. We contrasted the time-frequency (TF) transformed response-locked EEG data between both alternative choices ("f2 > f1" vs. "f2 < f1") to reveal oscillatory signatures of decision making before responses were given. In line with the results from our previous study with button press responses (Herding et al., 2016), we found again a choice-selective modulation of upper beta band oscillations (∼24–32 Hz) in frontal electrodes. However, source localization of the choice signal suggested more lateral premotor areas as compared to medial premotor areas for the button press responses, importantly, including FEF.

MATERIALS AND METHODS

Participants

Twenty four healthy, right-handed volunteers (20–36 years; nine males) participated in the experiment after giving written informed consent in accordance with the Declaration of Helsinki. The study was approved by the local ethics committee at the Freie Universität Berlin. Two participants (both female) were excluded from the analysis due to near chance-level behavioral performance (<60% correct answers), resulting in 22 data sets for further analysis.

Stimuli and Behavioral Task

Supra-threshold vibrotactile stimuli with constant peak amplitude were applied to the left index finger using a piezoelectric Braille stimulator (QuaeroSys, Schotten, Germany). The stimuli consisted of amplitude-modulated sinusoids with a fixed carrier frequency of 137 Hz. The amplitude-modulation of this carrier signal with frequencies 12–32 Hz created the sensation of tactile 'flutter' (see Talbot et al., 1968; Romo and Salinas, 2003), while the spectrum of the physical driving signal was limited to frequencies above 100 Hz (e.g., Tobimatsu et al., 1999). Thus, the risk of physical artifacts in the EEG analysis range of interest (<100 Hz) was minimized. The sound of the stimulator was masked by white noise of ∼80 dB that was played throughout the experiment (e.g., Spitzer et al., 2010; Spitzer and Blankenburg, 2011). Participants were comfortably seated ∼60 cm in front of a TFT monitor. A fixation cross was displayed at the center of the screen to minimize eye movements. On each trial, two flutter stimuli were successively presented for 250 ms each (with frequencies f1 and f2), interleaved by a retention interval of 1000 ms (see **Figure 1A**). The values of f1 were randomly drawn from 16, 20, 24, or 28 Hz, whereas f2 differed from f1 by ±2 or 4 Hz (**Figure 1B**). After presentation of the second stimulus the central fixation cross vanished and two target dots (diameter of ∼0.5° visual angle) appeared on the left

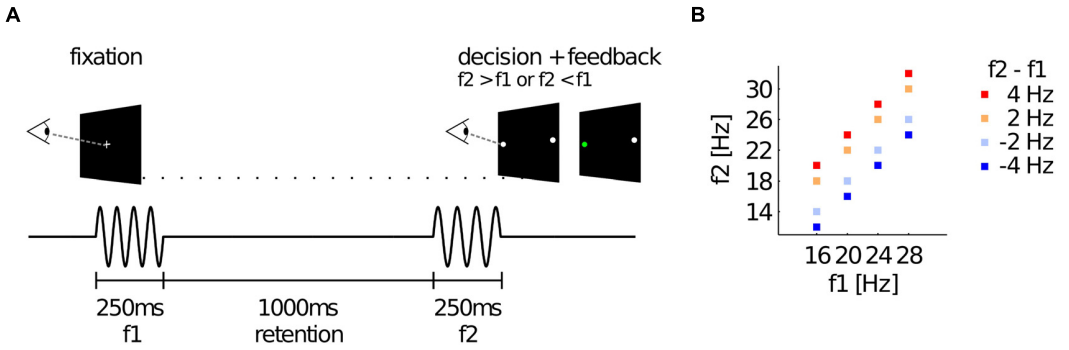

FIGURE 1 | Experimental paradigm and stimulus set. (A) Illustration of a single trial. Participants were presented with two vibrotactile stimuli (with frequencies f1 and f2) at the left index finger, while holding central fixation until the offset of the second stimulus. Afterwards, they decided whether f2 > f1 or f2 < f1 by means of a horizontal saccade. Online feedback was provided immediately after the decision via color change of the selected dot (green for correct, red for incorrect trials). **(B)** The set of all possible frequency combinations of f1 and f2 that were applied in this study. Color-coded squares each indicate one stimulus pair with according f1 and f2 values.

and on the right side of the screen (∼12° visual angle off-center). Participants indicated whether f2 > f1 or f2 < f1 by making a saccade to the right or to the left target, respectively. Importantly, the response assignment of saccade directions was reversed for half of the participants, such that the mapping of choices onto specific saccades (which might have been associated with specific motor preparatory signals) was fully counterbalanced across participants. Responses were registered as soon as participants fixated one of the targets for 200 ms. According choices were evaluated online to provide immediate (with a latency of 20 ms) performance feedback by changing the color of the selected target dot for 200 ms (green for correct, red for incorrect choices). After the feedback, the central fixation cross reappeared and replaced the target dots to indicate the beginning of a new trial. Participants had to fixate the central cross to start the new trial. After a variable time interval (1500–2000 ms) a new stimulus pair was presented. Participants completed seven blocks of 160 f1-vs-f2 comparisons (each block lasted ∼15 min including eye-tracker calibration), for a total of 1120 trials. Before the experiment started, participants performed ∼50 practice trials.

Eye-Tracking

A Tobii T60 eye-tracker was used to record participants' eye movements during each trial (binocular sampling at 60 Hz). The T60 is integrated into a 17″ TFT monitor, and is able to track participants that are comfortably seated in front of the monitor (i.e., no chin rest required). Online evaluation of the participants' gaze directions was implemented with custom code using the Tobii toolbox for MATLAB. Thus, we could check whether participants kept the gaze on the central fixation cross during each trial (with tolerance of ∼3° visual angle), and displayed a warning message if this was not the case ("Please keep fixation throughout the trial"). Additionally, we could read out participants' choices (200 ms fixation on target dot with tolerance of ∼3° visual angle) and provide performance feedback online. To maintain a high tracking accuracy, the eye-tracker was calibrated before the beginning of each block using a standard 5-dot calibration procedure.

Behavioral Analysis Using Bayesian Modeling

We estimated subjectively perceived frequency differences (SPFDs) based on the observation that participants do not compare f2 with the physical value of f1 (cf. Hellström, 1985, 2003), but rather with a value slightly shifted toward the mean of all presented stimulus frequencies (cf. Preuschhof et al., 2010; Ashourian and Loewenstein, 2011; Karim et al., 2012; Sanchez, 2014). Using the framework of Bayesian inference, we introduced this shifted version of f1, which we call f1′, as the expected value of the posterior distribution of f1 when using a Gaussian prior centered over all presented frequencies. Three free parameters (the variance of the likelihood distribution of f1, the variance of the prior distribution, and an overall response bias) were estimated in this model based on each participant's choices (further details in Herding et al., 2016). The SPFDs are then defined as the differences f2–f1′ for each stimulus pair. To assess the quality of the SPFD model, we computed Bayes factors (BFs) comparing the model with a "null" model (based on the physical frequency differences f2–f1) while accounting for differences in model complexities (e.g., Kass and Raftery, 1995).

EEG Recording and Analysis

EEG (ActiveTwo; BioSemi) was recorded at 2048 Hz (offline down-sampled to 512 Hz) from 64 electrodes positioned in an elastic cap according to the extended 10–20 system. Individual electrode locations for each participant were obtained prior to the experiment using a stereotactic electrode-positioning system (Zebris Medical GmbH, Isny, Germany). Four additional electrodes were used to register the horizontal and vertical electrooculogram (hEOG and vEOG). For preprocessing, EEG data were first re-referenced to a common average montage, and then high- and low-pass filtered (with cut-off frequencies of 0.5 and 48 Hz, respectively). Eye blink artefacts in the EEG data were corrected using adaptive spatial filtering based on individual calibration data informed by the vEOG signal (see Ille et al., 2002). The artefact-free EEG data were segmented into

epochs from −2500 to 1000 ms relative to the time of saccade onset (based on the hEOG signal) in order to examine EEG oscillations before choices were reported (i.e., response-locked analysis). Based on visual inspection, noisy trials were excluded from further investigations (10.5% of trials on average). To get a time-resolved representation of spectral power in the EEG signal, Morlet wavelet transforms of short segments of EEG data were computed every 50 ms. The lengths of these segments depended on the frequency of the applied wavelet (i.e., 4–48 Hz resolved with 1 Hz), and always spanned seven cycles (e.g., 700 ms for 10 Hz, 350 ms for 20 Hz). The resulting TF representations of the EEG data were hence resolved at 50 ms and 1 Hz (i.e., TF bin = 50 ms × 1 Hz). All analyses were done in MATLAB (The MathWorks) using the SPM12 toolbox (Wellcome Department of Cognitive Neurology, London[1]), including the FieldTrip toolbox for EEG/MEG data (Radboud University Nijmegen, Donders Institute [2]).

Statistical Analysis

The response-locked single-trial TF data were square root transformed (yielding spectral amplitudes) to approximate normally distributed data (see Kiebel et al., 2005). Additionally, TF data were smoothed with a 3 Hz × 300 ms FWHM (full width at half maximum) Gaussian kernel to decrease inter-subject variability (e.g., Kilner et al., 2005; Litvak et al., 2011). For each participant, we used the smooth TF images of all trials to estimate the average TF maps for either choice category (i.e., f2 < f1 and f2 > f1 trials) separately for correct and incorrect decisions. That is, we implemented a general linear model (GLM) with 2x2 factorial design (factors: "f2 < f1/f2 > f1"; "correct/incorrect"), and estimated the interaction terms. We contrasted the average TF maps within each participant to identify interaction effects between both factors (i.e., between "f2 < f1/f2 > f1" and "correct/incorrect"; contrast vector = [−1 1 1 −1]), as this resulted in contrasting the actual choices of participants disregarding whether choices were correct or incorrect (i.e., chose "f2 > f1" vs. chose "f2 < f1"). The resulting contrast images hence showed the difference in spectral amplitude for each TF bin between both choices (i.e., "f2 > f1" choices minus "f2 < f1" choices) considering correct and incorrect trials. To identify time, frequencies, and channels for which this contrast was consistently different from zero across participants, we used cluster-based permutation testing (Maris and Oostenveld, 2007). We compared the summary statistics of the observed data (one-sample *t*-test across contrast images of all participants in each TF bin) with a distribution of summary statistics obtained from 500 randomly sign-flipped permutations. Consistent with our previous work focusing on strong and focal effects (Herding et al., 2016), a cluster was defined as a group of adjacent TF bins that all exceeded a cluster-defining threshold of $p_{\text{threshold}} < 0.001$ (uncorrected). Clusters that exceeded a family-wise error (FWE) corrected threshold of $p_{\text{cluster}} < 0.05$ (corrected for time, frequency, and channels) were considered to be statistically significant. Additionally, we probed whether a significant modulation by choice was observed individually for correct and incorrect trials within the identified TF cluster. Hence, we computed a conjunction analysis of the choice modulation between correct and incorrect trials (i.e., conjunction of contrasts: [−1 1 0 0] AND [0 0 1 −1]; cf. Friston et al., 2005; Nichols et al., 2005). As described above, we identified significant TF clusters using cluster-based permutation testing separately for correct and incorrect trials, and inspected whether the resulting clusters overlapped. For this analysis, we used a cluster-defining threshold of $p_{\text{threshold}} = 0.01$ (uncorrected), and only corrected for channels that displayed a choice-modulation in the previous analysis of interaction effects.

Source Reconstruction

The cortical sources of choice-modulated beta band activity observed on the scalp-level were localized using the 3D source reconstruction routines provided by SPM12 (Friston et al., 2006). Based on the individually recorded electrode positions for each participant, a forward model was constructed using an 8196-point cortical mesh of distributed dipoles perpendicular to the cortical surface of a template brain (cf. Friston et al., 2006). The lead field of the forward model was computed using the three-shell Boundary Elements Method (BEM) EEG head model available in SPM12. The forward model was inverted using a smoothness prior (called 'COH' in SPM; cf. Litvak et al., 2011), which is similar to the LORETA approach (Pascual-Marqui et al., 1994). That is, the inverse solution preferred source activity with only proximal sources showing correlated activity while the total energy of source activity was minimized. Additionally, we applied group constraints for the model inversion, which effectively restricted the inverse solution to explain individual data using the same set of sources across participants (cf. Litvak and Friston, 2008). Preprocessed response-locked single-trial EEG data before TF transformation (i.e., in the time-domain) were used to invert the forward model. Before model inversion, the single-trial data were additionally tailored to the time interval of the choice modulation identified on the scalp level (i.e., −750 to −450 ms before responses were given). According to the interaction terms of the 2x2 factorial design (see above), the results of the model inversion were summarized in four 3D images that reflected average spectral source power in a representative TF window (i.e., 24–32 Hz; −700 to −500 ms from saccade onset). These images were obtained by computing wavelet transforms of single-trial source activity, and then averaging the source power across trials for each condition of interest. The 3D images were then used to contrast source power between choices for each participant, analogously to the conjunction analysis in sensor space (i.e., conjunction of contrasts: [−1 1 0 0] AND [1 −1 0 0]). The conjunction analysis yielded only sources that exhibited significantly higher beta band power for "f2 > f1" choices than for "f2 < f1" choices in both correct and incorrect trials (i.e., testing the conjunction null; cf. Friston et al., 2005; Nichols et al., 2005). The results of this mass-univariate statistical test are displayed at a significance level of $p < 0.001$ (uncorrected) indicating the most probable sources of the effect observed at the sensor-level. Anatomical reference for source estimates was established on the

[1]http://www.fil.ion.ucl.ac.uk/spm

[2]http://www.fieldtriptoolbox.org

basis of the SPM anatomy toolbox (Eickhoff et al., 2005) where possible.

Time Courses

To get further insights into the effects obtained from the TF analysis, we extracted underlying time courses from the statistically significant TF cluster separately for correct and incorrect trials. For correct trials, we computed the time courses individually for different levels of SPFDs. Based on all observed SPFD values (differences of log-transformed frequency values), we defined six levels of SPFD (i.e., [< −0.18]; [−0.18 to −0.09]; [−0.09 to 0]; [0 to 0.09]; [0.09 to 0.17]; [> 0.17]). We specified the levels symmetrically around a SPFD of zero (corresponding to chance-level performance), and in such a way that each participant had at least one stimulus pair for each level. Based on the identified TF cluster, we computed the grand average time courses of upper beta band amplitude (24–32 Hz) for each level of SPFD. For incorrect trials, we separated the trials only into two classes (due to low trial numbers for some levels of SPFD) with SPFD < 0 and SPFD > 0, i.e., f2 < f1 and f2 > f1, and computed the grand average time courses.

RESULTS

Behavioral Results

On average, participants made correct choices on 74.4% of all stimulus pairs. We performed a within-subject analysis of variance (ANOVA) with the factors "difficulty" (±4 vs. ±2 Hz stimulus differences) and "sign" (positive vs. negative stimulus differences) on proportions of correct responses (PCRs), using a logit-transform to account for non-normality of the residuals. The analysis revealed significant main effects of the factors difficulty ($p < 0.001$) and sign ($p = 0.001$), and a significant interaction of the two factors ($p < 0.001$). As expected, a larger proportion of trials were judged correctly when the physical f2–f1 frequency difference was ±4 Hz (80.9% correct) compared with trials where the difference was only ±2 Hz (67.8%; $p < 0.001$; paired *t*-test; see difficulty effect **Table 1**). We also observed more correct responses for positive (78.1% correct) compared with negative frequency differences (70.6%; $p = 0.006$ paired *t*-test; see sign effect **Table 1**), which indicates an overall response bias toward "f2 > f1" choices (mean criterion shift: 0.12; $p = 0.003$; one-sample *t*-test).

An ANOVA (2x2x2 repeated measures design with factors "correct/incorrect," "difficulty," and "sign") of the median response times (RTs) showed a significant main effect for the factor "correct/incorrect" ($p < 0.001$), and two significant interactions ("correct/incorrect" × "sign", $p = 0.001$ and "correct/incorrect" × "difficulty", $p = 0.004$). More precisely, the median RT with respect to f2 stimulus onset was on average shorter for correct trials (570.4 ms) than for incorrect trials (620.5 ms; $p < 0.001$; paired *t*-test). For correct trials, RTs were faster for trials with f2 > f1 (548.1 ms) as compared to f2 < f1 (599.1 ms; $p = 0.001$; paired *t*-test), whereas for incorrect trials the pattern was reversed (665.1 ms when f2 > f1, and 604.9 ms when f2 < f1; $p = 0.002$; paired *t*-test; all patterns of interaction effects in the RT data are detailed in **Table 1**). Thus, participants were in general faster when choosing "f2 > f1," no matter whether this choice was correct or incorrect. This is in line with the overall response bias toward "f2 > f1" choices (see above). Accordingly, when computing criterion shifts separately for fast and slow trials of each participant (i.e., median split of RTs), fast responses displayed a much stronger bias toward "f2 > f1" choices than slow responses ($p < 0.001$, paired *t*-test). In fact, whereas participants clearly favored "f2 > f1" choices in fast trials (mean criterion shift: 0.31; $p < 0.001$, one sample *t*-test), in slow trials the bias was actually reversed (mean criterion shift: −0.11; $p = 0.009$, one sample *t*-test).

Upper Beta Band Oscillations in Right Frontal Electrodes Encode Choices before Responding

To test if choices were reflected in oscillatory EEG activity before a response was given, we compared average TF maps of f2 < f1 and f2 > f1 trials in response-locked data, while considering that any possible effect of choice should switch sign between correct and incorrect trials (i.e, we checked for an interaction effect of the factors "f2 < f1/f2 > f1" and "correct/incorrect"). The analysis revealed that upper beta band amplitude (∼24–32 Hz) in right frontal electrodes (FC2, FC4; inset **Figure 2A**) was significantly higher for "f2 > f1" choices well before responses were given (−750 to −450 ms from response; $p_{cluster} = 0.034$, FWE corrected; **Figure 2A**, dashed

TABLE 1 | Behavioral data.

	Frequency difference of stimuli (f2–f1) in Hz					
	−4	−2	2	4	Difficulty effect	Sign effect
PCR (%)	75.9 ± 4.4	65.3 ± 3.5	70.5 ± 4.3	86.1 ± 3.7	n/a ($p < 0.001$)*	n/a ($p = 0.002$)*
RT correct (ms)	590.2 ± 44.8	608.0 ± 48.3	554.5 ± 47.1	541.6 ± 44.7	−15.4 ± 9.0 ($p = 0.002$)*	−51.1 ± 28.6 ($p = 0.001$)*
RT incorrect (ms)	615.9 ± 64.9	593.9 ± 60.7	651.5 ± 58.1	678.6 ± 68.2	24.5 ± 19.0 ($p = 0.014$)*	60.2 ± 34.8 ($p = 0.002$)*

Proportion of correct responses (PCRs) and response times (RTs) as a function of the physical frequency difference f2–f1. Mean values ± 95% confidence interval (CI) are shown. 'Difficulty effect' compares easy (±4 Hz) and difficult (±2 Hz) trials in a paired t-test. 'Sign effect' compares between trials with positive (2 and 4 Hz) and negative (−2 and −4 Hz) frequency differences in a paired t-test. PCRs and RTs showed significant effects of difficulty and sign. RTs showed both effects for correct and incorrect trials, however, in opposing directions (cf. interactions in ANOVA of RTs). PCRs were logit-transformed before testing, due to non-normally distributed residuals. We omitted average differences of logit-transformed PCRs for both effects to avoid confusion (indicated by n/a). Asterisks indicate statistically significant results.

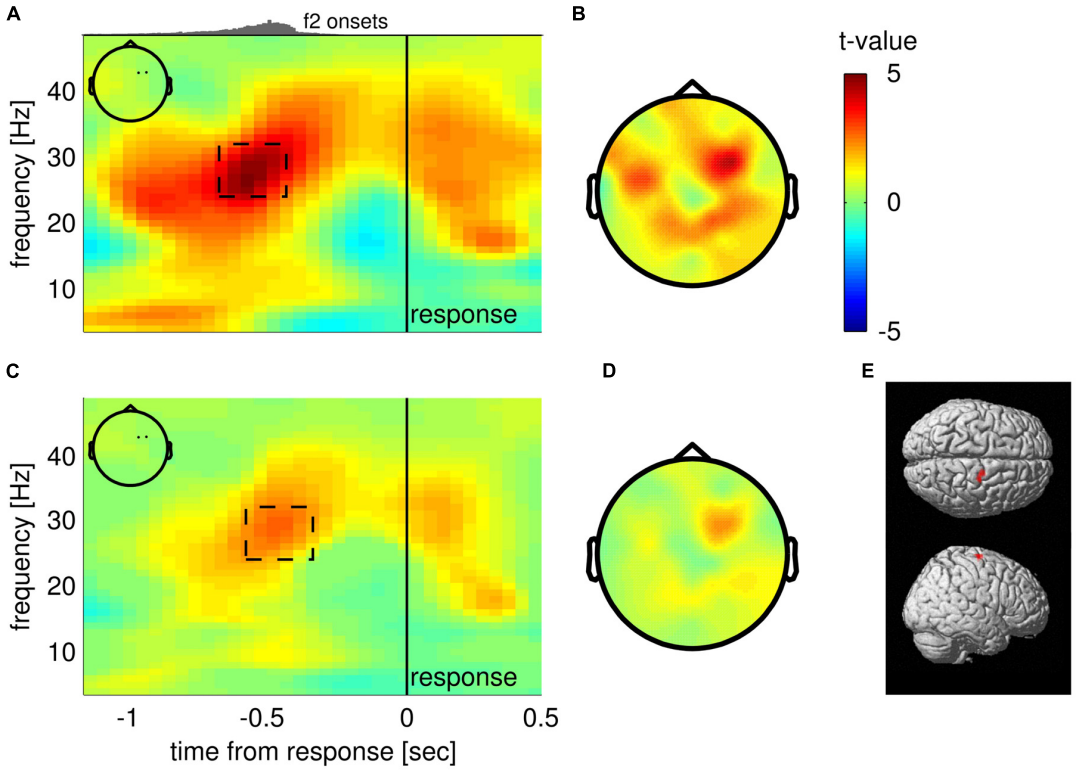

FIGURE 2 | Choice-selective modulation of upper beta band amplitude. (A) Time-frequency (TF) map displaying *t*-values from group analysis of interaction effect ("f2 < f1/f2 > f1" × "correct/incorrect"), averaged over electrodes FC2 and FC4 (see inset) spanning a statistically significant cluster. Histogram on top indicates the distribution of stimulus onset times of the second stimulus. **(B)** Scalp topography of TF window centered on significant cluster as indicated in **(A)**. **(C)** Results of the conjunction analysis between correct and incorrect trials averaged over electrodes FC2 and FC4 (inset). The TF map displays the minimum of *t*-values when combining choice-selective modulation computed separately for correct and incorrect trials. **(D)** Scalp topography corresponding to the TF window indicated in **(C)**. **(E)** Most likely source location of the choice-selective beta band modulation.

rectangle). The scalp topography of the TF cluster shows that the effect also spreads to parietal electrodes and displays a second, weaker peak in left frontal electrodes (**Figure 2B**; the cluster extended to both sites for a lower cluster-defining threshold of $p_{\text{threshold}} = 0.01$). Notably, steady-state evoked potentials (SSEPs) of vibrotactile stimuli are known to lead to a narrow-band power increase in the EEG signal at frequencies corresponding to the stimulus frequency in electrodes contralateral to stimulation (e.g., Tobimatsu et al., 1999). For f2 > f1 trials, f2 was generally higher (25 Hz on average) than for f2 < f1 trials (19 Hz on average). Hence, correct choices of "f2 > f1" were primarily accompanied by SSEPs in the upper beta band, whereas correct choices of "f2 < f1" were mainly associated with SSEPs in lower frequencies. Given that the reported effect partly overlapped with the presentation of f2, we were concerned whether the alleged choice-selective modulation of upper beta band amplitude was driven by the systematic differences in SSEPs between choices. Importantly however, the systematic relationship between SSEPs and choices can only compromise our findings for correct trials. Therefore, we computed a conjunction analysis between correct and incorrect trials to probe whether the observed beta band modulation was the same for both correct and incorrect trials. Indeed, we found overlapping significant TF clusters in the upper beta band (∼25–30 Hz) approximately 500 ms before responses were given in previously identified electrodes FC2 and FC4 (correct: −600 to −400 ms; 26–35 Hz; $p_{\text{cluster}} = 0.044$; incorrect: −1000 to −400 ms; 20–33 Hz; $p_{\text{cluster}} = 0.004$; cf. **Figure 2C**). Remarkably, the effect was even stronger for incorrect trials than for correct trials. Displaying the minimum *t* statistics between correct and incorrect trials reveals that only right frontal electrodes show the choice-selective modulation of upper beta band amplitude consistently for correct and incorrect trials (**Figures 2C,D**). Accordingly, the most probable source of the effect was found in the right precentral gyrus including FEF (MNI coordinates of cluster peak: 18, −12, 70; $p < 0.001$, uncorrected; **Figure 2E**). Taken together, we can largely rule out a major contribution of SSEPs to the observed beta band modulation.

Next, we looked at the choice-selective beta band modulation independently for correct and incorrect choices by separately computing the according grand mean time courses of upper beta band amplitude (24–32 Hz; **Figure 3**). The time courses for correct trials show that beta band amplitudes separate categorically according to choices (**Figure 3**; correct trials). That is, the according choice category modulated upper beta band amplitude, but not the specific values of the SPFD. Notably, the SPFDs described participants' choices more accurately than

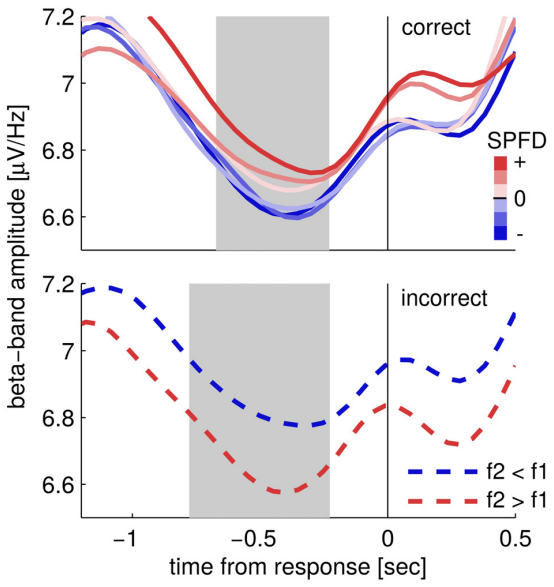

FIGURE 3 | Time courses of upper beta band amplitude (24–32 Hz) separately for correct (upper) and incorrect trials (lower). Correct trials are split into six levels of subjectively perceived frequency differences (SPFDs) as inferred from a Bayesian inference model that describes choice behavior in this task better than physical differences (see text for details). Despite this fine-grained partitioning, time courses are separated solely according to choice categories. Incorrect trials were split only into two classes (according to f2 > f1 and f2 < f1, due to low trial numbers) and still showed a higher beta band amplitude for (incorrect) "f2 > f1" choices (i.e., f2 < f1, blue line) than for "f2 < f1" choices (i.e., f2 > f1, red line). Shaded areas denote the time interval in which the second stimulus was typically presented (central 50%).

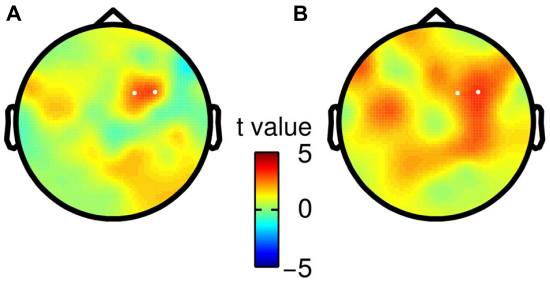

FIGURE 4 | Scalp topographies of choice-selective beta band modulation for both saccade-to-choice mappings. White dots correspond to electrodes spanning the significant TF cluster in the main analysis based on all participants. **(A)** Choices of "f2 > f1" were associated with a rightward saccade, whereas "f2 < f1" choices required a leftward saccade. **(B)** Opposite mapping as described in **(A)**.

the physical differences in each trial (strong evidence in favor of our model, i.e., BFs > 20, for 20/22 participants). For incorrect trials, we only distinguished between SPFD > 0 and SPFD < 0 (i.e., f2 > f1 and f2 < f1), and found that upper beta band amplitude was still higher for (incorrect) choices of "f2 > f1" (**Figure 3**; incorrect trials). Reiterating the results of our conjunction analysis, the identified modulation of beta band amplitude by choices was neither driven solely by correct trials nor solely by incorrect trials. Interestingly, for incorrect trials beta band amplitude was separated according to choices already well before the presentation of the second stimulus. Such a pre-stimulus difference might possibly explain why participants made erroneous choices in according trials (i.e., as the result of a bias), and would foster the interpretation of upper beta band amplitude as a precursor of the ensuing decision report.

In a control analysis, we examined whether the observed modulation of upper beta band amplitude was possibly related to the present variations in RTs according to choices. In particular, RTs for "f2 > f1" choices were always faster as for "f2 < f1" choices, for both correct and incorrect trials. That is, the same interaction as in the EEG data was also present in RTs (see **Table 1**). Thus, if faster RTs were associated with higher beta band amplitude in electrodes FC2 and FC4, the RT variations would be an alternative explanation of the observed modulation in beta band amplitude. We computed correlations between single-trial RTs and beta band amplitude for each participant, however, the obtained correlation coefficients scattered randomly around zero across participants (one sample t-test of correlation coefficients; mean $\rho = -0.021$, $p = 0.245$). Additionally, we checked for the same correlation within each choice category, but again, did not find any connection (one sample t-test of correlation coefficients; "f2 > f1" choices: mean $\rho = -0.013$, $p = 0.463$; "f2 < f1" choices: mean $\rho = -0.018$, $p = 0.408$). Hence, we can largely rule out that the reported modulation of beta band amplitude can be attributed to systematic RT variations. We also probed whether the overall response bias toward "f2 > f1" choices could explain the observed modulation in the beta band. To this end, we repeated the main analysis only using data from participants showing no such bias, or even a bias in the opposite direction (criterion shift < 0.1, 10 participants). These participants did also not show systematic differences in RTs between choices (i.e., "f2 > f1" vs. "f2 < f1" choices) neither for correct nor for incorrect trials (paired t-test between choices, $p = 0.224$ and $p = 0.352$). Despite the markedly reduced sample size, we observed the same pattern of upper beta band amplitude being higher for "f2 > f1" choices than for "f2 < f1" choices.

Finally, we tested whether the observed choice-selective modulation in the beta band was consistent for both specific mappings of choices onto saccade directions. Hence, we split participants according to their response mapping (i.e., right saccade = "f2 > f1" or right saccade = "f2 < f1"), and repeated the analysis of TF data separately for both groups ($N = 11$). We did not find any statistically significant differences between both groups (independent two-sample t-test, no clusters with $p < p_{\text{threshold}}$ before saccade onset), but rather found a considerable agreement in the topography of the choice-selective beta band modulation (**Figure 4**).

DISCUSSION

In the current study we investigated oscillatory EEG signatures of perceptual decisions based on the comparison between two sequentially presented vibrotactile frequencies f1 and f2.

Participants decided whether f2 > f1 or f2 < f1 by performing a horizontal saccade, where the association between saccade direction and choice was counterbalanced across participants. We found that the amplitude of upper beta band oscillations (∼24–32 Hz) in right frontal electrodes was modulated by participants' choices before responses were given, regardless of whether choices were correct or incorrect, and independent of the specific saccade-to-choice mapping. In particular, "f2 > f1" choices were always associated with a higher beta band amplitude than "f2 < f1" choices. Notably, the same modulation pattern of beta band amplitude was recently shown when participants (non-human primates and humans) completed the same task, but reported choices by button presses (Haegens et al., 2011; Herding et al., 2016). In analogy to these studies, we found in the current data that premotor areas were implicated as the most likely source of the choice-selective signal, however, now with a focus on distinct lateral parts, including FEF.

The crucial role of premotor cortex in decision formation during the vibrotactile 2AFC task was established by the seminal work of Romo and colleagues with non-human primates (reviewed in Romo and de Lafuente, 2013). Electrophysiological recordings in mPMC and vPMC showed choice-selective differences in premotor firing rates before actual responses were given by button presses (Hernández et al., 2002, 2010; Romo et al., 2004). Similar to the current data, this modulation was observed as early as during the presentation of the second stimulus (Hernández et al., 2002, 2010; Romo et al., 2004), and was shown to be behaviorally relevant, as the modulation was inverted for incorrect choices (Hernández et al., 2002). Conversely, the choice-selective differences in firing rates disappeared when no comparison of f1 and f2 was necessary in order to respond (i.e., a visual cue guided action), dissociating the finding from mere motor preparation (Hernández et al., 2002, 2010; Romo et al., 2004). To dissociate specific left/right saccade preparation (i.e., lateralized parietal alpha/beta band decrease; see Carl et al., 2016) from choices in the current study, we counterbalanced the mapping from saccade direction to choice across participants. We found that both mappings led to very similar results when according data were analyzed separately (i.e., for either half of the participants). Hence, the reported choice-selective modulation of beta band amplitude is most likely independent of specific saccade preparation. Moreover, we did not find any additional lateralized choice effects (i.e., for neither half of the participants) as a consequence of a consistent mapping between saccade direction and choice (cf. lateralized beta band decrease before decision reports by button presses, e.g., Donner et al., 2009).

Typically, beta band oscillations (∼15–25 Hz) are associated with sensorimotor processing. That is, beta band amplitude is known to decrease over somatosensory areas in anticipation and during the presentation of tactile stimuli, as well as to rebound afterwards (e.g., Jasper and Andrews, 1938; Pfurtscheller, 1981; Bauer et al., 2006; van Ede et al., 2011). In preparation for and during voluntary hand movements like button presses, the same pattern of beta band decrease followed by a rebound over contralateral motor areas is also reliably observed (e.g., Jasper and Penfield, 1949; Pfurtscheller, 1981). Likewise, several studies suggest that a decrease in beta band amplitude over contralateral posterior parietal areas accompanies the execution of saccades (e.g., Pesaran et al., 2002; Brignani et al., 2007; Carl et al., 2016). Moreover, Jo et al. (2016) recently reported a negative correlation between the level of beta band amplitude over motor areas before initiating voluntary button presses and according RTs. Given that in the current study RTs varied systematically in the same way as the (upper) beta band was modulated by choice (i.e., faster responses for "f2 > f1" than for "f2 < f1" choices for correct and incorrect trials), we carefully examined whether the observed beta band modulation could be attributed to these RT variations. However, RTs were not correlated with upper beta band amplitude, neither over all trials, nor within the separate choice categories (i.e., "f2 > f1" or "f2 < f1"). More likely, the variations in RTs are related to the observed response bias toward "f2 > f1" choices, i.e., the preferred choice is also accompanied by faster responses. In favor of this interpretation, fast trials exhibited a stronger bias than slower trials. Moreover, the bias disappears when introducing a response delay to the task (unpublished observation), suggesting that the tendency for choosing "f2 > f1" might be confined to decisions under time pressure. To rule out that the response bias itself accounts for the observed beta band modulation, we additionally analyzed EEG data separately for participants that showed no substantial bias (or even a bias in the opposite direction) and no systematic RT differences between choices. Despite the reduced sample size, we still found the same tendency of "f2 > f1" choices being accompanied by higher beta band amplitude than "f2 < f1" choices, for correct and incorrect trials. Taken together, the reported modulation of upper beta band amplitude by participants' choices is unlikely to be related to systematic shifts of sensorimotor beta band effects due to RT variations or an overall response bias.

Rather, our finding aligns well with previous work that established a link between prefrontal upper beta band oscillations and WM content in the same task (i.e., f1 values; see Spitzer et al., 2010; Spitzer and Blankenburg, 2011), and thus further supports the notion of upper beta band oscillations encoding different task-relevant entities at according processing stages of the vibrotactile 2AFC task (cf. Herding et al., 2016). In the context of decision making, given location (i.e., premotor areas) and characteristics (i.e., representation of content on which choice is based, independent of specific motor response) of the observed effect, we propose that this entity might reflect the input to the (pre)motor system which is in charge of the subsequent response. In particular, beta band amplitude might signal the decision outcome which in turn informs the ensuing action that is planned in effector-specific brain areas. How the beta band modulation might be implemented in detail, however, remains an open question. A recently proposed biophysically principled computational model was able to reproduce beta bursts in human MEG and animal LFPs (monkey and mouse) in great detail (Sherman et al., 2016). Interestingly, the model predicts modulations of the burst amplitudes by changes in the firing rates of some neurons in the network. Hence, this model might provide a new angle on how the firing rate code revealed by Romo and colleagues (e.g., see Romo and de Lafuente, 2013 for review) might be directly translated into

amplitude modulations in the beta band as reported here, and in previous work (Haegens et al., 2011; Herding et al., 2016).

Besides the considerable agreement between our current results and previous work in the vibrotactile 2AFC task, the findings presented here are notably the first ones based on decisions with saccade responses in this paradigm. In the visual domain, however, extensive research has investigated perceptual decision making utilizing saccades for responding in non-human primates (reviewed in Glimcher, 2003; Gold and Shadlen, 2007). The large body of work compiled by Shadlen and colleagues presents coherent evidence that choices, which are expressed by saccades, are reflected in the firing rates of various oculomotor brain areas, i.e., LIP (e.g., Shadlen and Newsome, 1996), FEF (e.g., Hanes and Schall, 1996; Kim and Shadlen, 1999), and SC (e.g., Ratcliff et al., 2003). More precisely, in the random dot motion (RDM) task, LIP activity was shown to reflect the accumulated evidence (i.e., motion information) provided by visual area MT (e.g., Ditterich et al., 2003; Hanks et al., 2006) peaking at RT (e.g., Shadlen and Newsome, 2001). A similar accumulation-to-bound signal was found in FEF (Hanes and Schall, 1996) and SC (Ratcliff et al., 2003) using a visual search task. In general, LIP, FEF, and SC seem to play similar roles in saccade target selection and spatial attention by implementing salience or relevance maps with gradually less abstract representations of the visual field (see e.g., Colby and Goldberg, 1999; Andersen and Buneo, 2002; Fecteau and Munoz, 2006; Schall, 2015). In the visual RDM task, however, Katz et al. (2016) recently questioned the causal role of LIP for decision making by showing that a pharmacological inactivation had no effect on task performance, whereas area MT (i.e., the momentary evidence) proved to be indispensable. Notably, the source reconstruction of the present choice-selective modulation of upper beta band modulation suggested areas in the precentral gyrus including FEF as likely sources. Hence, our findings are remarkably consistent with the work in non-human primates investigating decisions reported by saccades (cf. Hanes and Schall, 1996; Kim and Shadlen, 1999). Contrasting the results from the current study with our previous work, in which participants completed the same task but responded with button presses, reveals that the signal (i.e., choice-selective modulation of upper beta band amplitude) remained the same, however, the topography and the suggested source locations differ considerably. In particular, whereas button press responses implied medial premotor areas as a putative source of the choice signal, saccade responses hinted at source locations including FEF. Hence, both studies observed the same choice-selective signal, however, found sources that are associated with the planning of respective motor responses in an effector specific way.

In line with the aforementioned studies, our findings thus support the notion of an intentional framework of decision making (e.g., Cisek, 2007; Shadlen et al., 2008; Cisek and Kalaska, 2010), which proposes that decisions are expressed in form of intentions to act. As a consequence, neural correlates of decision making should be found in brain areas that are involved in the planning/preparation of the action that is used to express the choice, independent of the specific task at hand. In this light, also the work of Romo and colleagues is in agreement with an intentional framework of decision making. Choices in the vibrotactile 2AFC task were always reported by button presses, and choice-selective neuronal activity was found in mPMC and vPMC (Hernández et al., 2002, 2010; Romo et al., 2004; Haegens et al., 2011). Here, we provide novel evidence that a combination of the vibrotactile 2AFC task with another response modality (i.e., saccades) translates the choice-selective signal to corresponding effector-specific brain areas. Hence, we could effectively bridge the gap between the work of Romo and colleagues (vibrotactile 2AFC) and the work of Shadlen and colleagues (oculomotor responses), and show that their findings are transferable within an intentional framework of decision making.

AUTHOR CONTRIBUTIONS

JH, SL, and FB designed the study. JH and SL collected the data. JH, SL, and FB analyzed the data, interpreted the results, and wrote the manuscript. All authors approved the final version of the manuscript for submission.

FUNDING

This work was supported by the Deutsche Forschungsgemeinschaft (DFG, GRK1589/1).

ACKNOWLEDGMENT

We thank Jakub Limanowski, Alex H. von Lautz, and Lisa Velenosi for valuable comments on this manuscript.

REFERENCES

Andersen, R. A., and Buneo, C. A. (2002). Intentional maps in posterior parietal cortex. *Annu. Rev. Neurosci.* 25, 189–220. doi: 10.1146/annurev.neuro.25.112701.142922

Ashourian, P., and Loewenstein, Y. (2011). Bayesian inference underlies the contraction bias in delayed comparison tasks. *PLoS ONE* 6:e19551. doi: 10.1371/journal.pone.0019551

Barak, O., Tsodyks, M., and Romo, R. (2010). Neuronal population coding of parametric working memory. *J. Neurosci.* 30, 9424–9430. doi: 10.1523/JNEUROSCI.1875-10.2010

Bauer, M., Oostenveld, R., Peeters, M., and Fries, P. (2006). Tactile spatial attention enhances gamma-band activity in somatosensory cortex and reduces low-frequency activity in parieto-occipital areas. *J. Neurosci.* 26, 490–501. doi: 10.1523/JNEUROSCI.5228-04.2006

Brignani, D., Maioli, C., Maria Rossini, P., and Miniussi, C. (2007). Event-related power modulations of brain activity preceding visually guided saccades. *Brain Res.* 1136, 122–131. doi: 10.1016/j.brainres.2006.12.018

Carl, C., Hipp, J. F., König, P., and Engel, A. K. (2016). Spectral signatures of saccade target selection. *Brain Topogr.* 29, 130–148. doi: 10.1007/s10548-015-0426-6

Cisek, P. (2007). Cortical mechanisms of action selection: the affordance competition hypothesis. *Philos. Trans. R. Soc. Lond. B Biol. Sci.* 362, 1585–1599. doi: 10.1098/rstb.2007.2054

Cisek, P., and Kalaska, J. F. (2010). Neural mechanisms for interacting with a world full of action choices. *Annu. Rev. Neurosci.* 33, 269–298. doi: 10.1146/annurev.neuro.051508.135409

Colby, C. L., and Goldberg, M. E. (1999). Space and attention in parietal cortex. *Annu. Rev. Neurosci.* 22, 319–349. doi: 10.1146/annurev.neuro.22.1.319

Ditterich, J., Mazurek, M. E., and Shadlen, M. N. (2003). Microstimulation of visual cortex affects the speed of perceptual decisions. *Nat. Neurosci.* 6, 891–898. doi: 10.1038/nn1094

Donner, T. H., Siegel, M., Fries, P., and Engel, A. K. (2009). Buildup of choice-predictive activity in human motor cortex during perceptual decision making. *Curr. Biol.* 19, 1581–1585. doi: 10.1016/j.cub.2009.07.066

Eickhoff, S. B., Stephan, K. E., Mohlberg, H., Grefkes, C., Fink, G. R., Amunts, K., et al. (2005). A new SPM toolbox for combining probabilistic cytoarchitectonic maps and functional imaging data. *Neuroimage* 25, 1325–1335. doi: 10.1016/j.neuroimage.2004.12.034

Fecteau, J. H., and Munoz, D. P. (2006). Salience, relevance, and firing: a priority map for target selection. *Trends Cogn. Sci.* 10, 382–390. doi: 10.1016/j.tics.2006.06.011

Friston, K., Henson, R., Phillips, C., and Mattout, J. (2006). Bayesian estimation of evoked and induced responses. *Hum. Brain Mapp.* 27, 722–735. doi: 10.1002/hbm.20214

Friston, K. J., Penny, W. D., and Glaser, D. E. (2005). Conjunction revisited. *Neuroimage* 25, 661–667. doi: 10.1016/j.neuroimage.2005.01.013

Glimcher, P. W. (2003). The neurobiology of visual-saccadic decision making. *Annu. Rev. Neurosci.* 26, 133–179. doi: 10.1146/annurev.neuro.25.112701.142900

Gold, J. I., and Shadlen, M. N. (2007). The neural basis of decision making. *Annu. Rev. Neurosci.* 30, 535–574. doi: 10.1146/annurev.neuro.29.051605.113038

Haegens, S., Nácher, V., Hernández, A., Luna, R., Jensen, O., and Romo, R. (2011). Beta oscillations in the monkey sensorimotor network reflect somatosensory decision making. *PNAS* 108, 10708–10713.

Hanes, D. P., and Schall, J. D. (1996). Neural control of voluntary movement initiation. *Science* 274, 427–430. doi: 10.1126/science.274.5286.427

Hanks, T. D., Ditterich, J., and Shadlen, M. N. (2006). Microstimulation of macaque area LIP affects decision-making in a motion discrimination task. *Nat. Neurosci.* 9, 682–689. doi: 10.1038/nn1683

Hellström, A. (2003). Comparison is not just subtraction: effects of time- and space-order on subjective stimulus difference. *Percept. Psychophys.* 65, 1161–1177. doi: 10.3758/BF03194842

Hellström, Å. (1985). The time-order error and its relatives: mirrors of cognitive processes in comparing. *Psychol. Bull.* 97, 35–61. doi: 10.1037/0033-2909.97.1.35

Herding, J., Spitzer, B., and Blankenburg, F. (2016). Upper beta band oscillations in human premotor cortex encode subjective choices in a vibrotactile comparison task. *J. Cogn. Neurosci.* 28, 668–679. doi: 10.1162/jocn

Hernández, A., Nácher, V., Luna, R., Zainos, A., Lemus, L., Alvarez, M., et al. (2010). Decoding a perceptual decision process across cortex. *Neuron* 66, 300–314. doi: 10.1016/j.neuron.2010.03.031

Hernández, A., Zainos, A., and Romo, R. (2000). Neuronal correlates of sensory discrimination in the somatosensory cortex. *Proc. Natl. Acad. Sci. U.S.A.* 97, 6191–6196. doi: 10.1073/pnas.120018597

Hernández, A., Zainos, A., and Romo, R. (2002). Temporal evolution of a decision-making process in medial premotor cortex. *Neuron* 33, 959–972. doi: 10.1016/S0896-6273(02)00613-X

Ille, N., Berg, P., and Scherg, M. (2002). Artifact correction of the ongoing EEG using spatial filters based on artifact and brain signal topographies. *J. Clin. Neurophysiol.* 19, 113–124. doi: 10.1097/00004691-200203000-00002

Jasper, H., and Andrews, H. (1938). Electro-encephalography: III. Normal differentiation of occipital and precentral regions in man. *Arch. Neurol. Psychiatry* 39, 96–115. doi: 10.1001/archneurpsyc.1938.02270010106010

Jasper, H., and Penfield, W. (1949). Electrocorticograms in man: effect of voluntary movement upon the electrical activity of the precentral gyrus. *Eur. Arch. Psychiatry Clin. Neurosci.* 183, 163–174. doi: 10.1007/bf01062488

Jo, H. G., Hinterberger, T., Wittmann, M., and Schmidt, S. (2016). Rolandic beta-band activity correlates with decision time to move. *Neurosci. Lett.* 616, 119–124. doi: 10.1016/j.neulet.2016.01.051

Karim, M., Harris, J. A., Morley, J. W., and Breakspear, M. (2012). Prior and present evidence: how prior experience interacts with present information in a perceptual decision making task. *PLoS ONE* 7:e37580. doi: 10.1371/journal.pone.0037580

Kass, R. R. E., and Raftery, A. E. A. (1995). Bayes factors. *J. Am. Stat. Assoc.* 90, 773–795. doi: 10.1080/01621459.1995.10476572

Katz, L., Yates, J., Pillow, J. W., and Huk, A. (2016). Dissociated functional significance of choice-related activity across the primate dorsal stream. *Nature* 535, 285–288. doi: 10.1038/nature18617

Kiebel, S. J., Tallon-Baudry, C., and Friston, K. J. (2005). Parametric analysis of oscillatory activity as measured with EEG/MEG. *Hum. Brain Mapp.* 26, 170–177. doi: 10.1002/hbm.20153

Kilner, J. M., Kiebel, S. J., and Friston, K. J. (2005). Applications of random field theory to electrophysiology. *Neurosci. Lett.* 374, 174–178. doi: 10.1016/j.neulet.2004.10.052

Kim, J. N., and Shadlen, M. N. (1999). Neural correlates of a decision in the dorsolateral prefrontal cortex of the macaque. *Nat. Neurosci.* 2, 176–185. doi: 10.1038/5739

Litvak, V., and Friston, K. (2008). Electromagnetic source reconstruction for group studies. *Neuroimage* 42, 1490–1498. doi: 10.1016/j.neuroimage.2008.06.022

Litvak, V., Mattout, J., Kiebel, S., Phillips, C., Henson, R., Kilner, J., et al. (2011). EEG and MEG data analysis in SPM8. *Comput. Intell. Neurosci.* 2011:852961. doi: 10.1155/2011/852961

Maris, E., and Oostenveld, R. (2007). Nonparametric statistical testing of EEG- and MEG-data. *J. Neurosci. Methods* 164, 177–190. doi: 10.1016/j.jneumeth.2007.03.024

Nichols, T., Brett, M., Andersson, J., Wager, T., and Poline, J. B. (2005). Valid conjunction inference with the minimum statistic. *Neuroimage* 25, 653–660. doi: 10.1016/j.neuroimage.2004.12.005

Pascual-Marqui, R. D., Michel, C. M., and Lehmann, D. (1994). Low resolution electromagnetic tomography: a new method for localizing electrical activity in the brain. *Int. J. Psychophysiol.* 18, 49–65. doi: 10.1016/0167-8760(84)90014-X

Pesaran, B., Pezaris, J. S., Sahani, M., Mitra, P. P., and Andersen, R. A. (2002). Temporal structure in neuronal activity during working memory in macaque parietal cortex. *Nat. Neurosci.* 5, 805–811. doi: 10.1038/nn890

Pfurtscheller, G. (1981). Central beta rhythm during sensorimotor activities in man. *Electroencephalogr. Clin. Neurophysiol.* 51, 253–264. doi: 10.1016/0013-4694(81)90139-5

Preuschhof, C., Schubert, T., Villringer, A., and Heekeren, H. R. (2010). Prior Information biases stimulus representations during vibrotactile decision making. *J. Cogn. Neurosci.* 22, 875–887. doi: 10.1162/jocn.2009.21260

Ratcliff, R., Cherian, A., and Segraves, M. (2003). A comparison of macaque behavior and superior colliculus neuronal activity to predictions from models of two-choice decisions. *J. Neurophysiol.* 90, 1392–1407. doi: 10.1152/jn.01049.2002

Romo, R., Brody, C. D., Hernández, A., and Lemus, L. (1999). Neuronal correlates of parametric working memory in the prefrontal cortex. *Nature* 399, 470–473. doi: 10.1038/20939

Romo, R., and de Lafuente, V. (2013). Conversion of sensory signals into perceptual decisions. *Progress Neurobiol.* 103, 41–75. doi: 10.1016/j.pneurobio.2012.03.007

Romo, R., Hernández, A., and Zainos, A. (2004). Neuronal correlates of a perceptual decision in ventral premotor cortex. *Neuron* 41, 165–173. doi: 10.1016/S0896-6273(03)00817-1

Romo, R., and Salinas, E. (2003). Flutter discrimination: neural codes, perception, memory and decision making. *Nat. Rev. Neurosci.* 4, 203–218. doi: 10.1038/nrn1058

Sanchez, G. (2014). Real-Time Electrophysiology in Cognitive Neuroscience: Towards Adaptive Paradigms to Study Perceptual Learning and Decision Making in Humans. Villeurbanne: Université Claude Bernard-Lyon.

Schall, J. D. (2015). Visuomotor functions in the frontal lobe. *Annu. Rev. Vis. Sci.* 1, 469–498. doi: 10.1146/annurev-vision-082114-035317

Shadlen, M., and Newsome, W. (1996). Motion perception: seeing and deciding. *PNAS* 93, 628–633. doi: 10.1073/pnas.93.2.628

Shadlen, M. N., Kiani, R., Hanks, T. D., and Churchland, A. K. (2008). "Neurobiology of decision making: an intentional framework," in *Better*

Than Conscious? Decision Making, the Human Mind, and Implications For Institutions, eds C. Engel and W. Singer (Cambridge: MIT Press), 71–101.

Shadlen, M. N., and Newsome, W. T. (2001). Neural basis of a perceptual decision in the parietal cortex (area LIP) of the rhesus monkey. *J. Neurophysiol.* 86, 1916–1936.

Sherman, M. A., Lee, S., Law, R., Haegens, S., Thorn, C. A., Hämäläinen, M. S., et al. (2016). Neural mechanisms of transient neocortical beta rhythms: converging evidence from humans, computational modeling, monkeys, and mice. *PNAS* 113, E4885–E4894. doi: 10.1073/pnas.1604135113

Spitzer, B., and Blankenburg, F. (2011). Stimulus-dependent EEG activity reflects internal updating of tactile working memory in humans. *PNAS* 108, 8444–8449. doi: 10.1073/pnas.1104189108

Spitzer, B., Wacker, E., and Blankenburg, F. (2010). Oscillatory correlates of vibrotactile frequency processing in human working memory. *J. Neurosci.* 30, 4496–4502. doi: 10.1523/JNEUROSCI.6041-09.2010

Talbot, W., Darian-Smith, I., Kornhuber, H., and Mountcastle, V. (1968). The sense of flutter-vibration: comparison of the human capacity with response patterns of mechanoreceptive afferents from the monkey hand. *Neurophysiology* 31, 301–334.

Tobimatsu, S., Zhang, Y. M., and Kato, M. (1999). Steady-state vibration somatosensory evoked potentials: physiological characteristics and tuning function. *Clin. Neurophysiol.* 110, 1953–1958. doi: 10.1016/S1388-2457(99)00146-7

van Ede, F., de Lange, F., Jensen, O., and Maris, E. (2011). Orienting attention to an upcoming tactile event involves a spatially and temporally specific modulation of sensorimotor alpha- and beta-band oscillations. *J. Neurosci.* 31, 2016–2024. doi: 10.1523/JNEUROSCI.5630-10.2011

Conflict of Interest Statement: The authors declare that the research was conducted in the absence of any commercial or financial relationships that could be construed as a potential conflict of interest.

Copyright © 2017 Herding, Ludwig and Blankenburg. This is an open-access article distributed under the terms of the Creative Commons Attribution License (CC BY). The use, distribution or reproduction in other forums is permitted, provided the original author(s) or licensor are credited and that the original publication in this journal is cited, in accordance with accepted academic practice. No use, distribution or reproduction is permitted which does not comply with these terms.

Study 3 - Oscillatory EEG Signatures of Postponed Somatosensory Decisions

Ludwig, S.*, **Herding, J.***, and Blankenburg, F. (submitted). Oscillatory EEG Signatures of Postponed Somatosensory Decisions. Human Brain Mapping.

HUMAN BRAIN MAPPING

Oscillatory EEG Signatures of Postponed Somatosensory Decisions

Journal:	*Human Brain Mapping*
Manuscript ID	HBM-17-0458
Wiley - Manuscript type:	Research Article
Date Submitted by the Author:	26-Apr-2017
Complete List of Authors:	Ludwig, Simon; Freie Universität Berlin, Neurocomputation and Neuroimaging Unit, Department of Education and Psychology Blankenburg, Felix; Freie Universität Berlin, Neurocomputation and Neuroimaging Unit, Department of Education and Psychology; Bernstein Center for Computational Neuroscience Berlin Herding, Jan; Freie Universität Berlin, Neurocomputation and Neuroimaging Unit, Department of Education and Psychology; Bernstein Center for Computational Neuroscience Berlin
Keywords:	decision making, beta band, somatosensory, postponed decision, vibrotactile

SCHOLARONE™
Manuscripts

Oscillatory EEG Signatures of Postponed Somatosensory Decisions

Simon Ludwig[1*], Jan Herding[1, 2,*], & Felix Blankenburg[1, 2,]

[1]*Neurocomputation and Neuroimaging Unit, Freie Universität Berlin;* [2]*Bernstein Center for Computational Neuroscience, Berlin*

* *The authors contributed equally to this work*

Correspondence:

Simon Ludwig (simon.ludwig@fu-berlin.de)

Freie Universität Berlin

FB Erziehungswissenschaften und Psychologie

Habelschwerdter Allee 45

Raum JK 25/212

14195 Berlin

Tel. +49 (0) 30 838 56693

Running title: Postponed Somatosensory Decisions

For Peer Review

Abstract

In recent EEG studies, the vibrotactile frequency comparison task has been used to study oscillatory signatures of perceptual decision making in humans, revealing a choice-selective modulation of premotor upper beta band power shortly before decisions were reported. Importantly, these studies focused on decisions that were indicated immediately after stimulus presentation, and for which a direct motor mapping was provided. Here, we investigated whether these effects also extend to postponed decisions, and how a response mapping that is dissociated from a specific motor command influences the putative beta-band choice signal. We recorded EEG data in two separate experiments, both employing the vibrotactile frequency comparison task with delayed decision reports. In the first experiment, delayed choices were associated with a fixed motor mapping, whereas in the second experiment, choices were mapped onto a color code concealing a specific motor response until the end of the delay phase. In between stimulus presentations, as well as after the second stimulus, prefrontal beta band power indexed stimulus information held in working memory. Beta band power also encoded choices during the response delay, notably, in different cortical areas depending on the provided response mapping. In particular, when decisions were associated with a specific motor mapping, choices were represented in premotor cortices, whereas the color mapping resulted in a choice-selective modulation of beta band power in parietal cortices. Together, our findings imply that *how* a choice is expressed (i.e., the decision consequence) determines *where* in the cortical sensorimotor hierarchy an according decision signal is processed.

Keywords

beta band, decision making, response context, vibrotactile, intentional decisions

For Peer Review

Introduction

A key question regarding perceptual decision making concerns the functional role of sensory cortices, association cortices, and motor cortices in the transformation of sensory information into motor actions. Besides the highly influential studies on perceptual decisions in the visual domain (for reviews see Heekeren et al., 2008; Gold and Shadlen, 2007), intensive research in the *somatosensory* domain has yielded seminal insights into the processes underlying a sensorimotor transformation from perception via decision to action (see Romo and de Lafuente, 2013, for a comprehensive review). In particular, employing a vibrotactile sequential frequency comparison (SFC) task, in which monkeys had to decide whether the second of two serially presented vibrations had a higher or a lower frequency than the first one, Romo and colleagues revealed specific activity patterns of single neurons during sensory processing, working memory (WM), and decision making. That is, during stimulus presentation, single neurons in the primary somatosensory cortex encoded the stimulus frequencies (f1 or f2) by a monotonically increasing rate code (Salinas et al., 2000). In the retention interval, i.e., during WM maintenance, neurons in prefrontal cortices showed a sustained parametric in- or decrease in firing rates as a function of f1 (Brody et al., 2003; Romo et al., 1999). In the decision phase of the task, firing rates (Hernández et al., 2002) recorded from medial premotor cortex (MPC), as well as the power of beta band oscillations in corresponding local field potentials (LFPs, Haegens et a., 2011), finally encoded the monkeys' upcoming choices. Further research investigated whether stimulus information (i.e. stimulus frequencies, f1 and f2) and choice information (i.e., the signed differences, f2-f1) was also maintained in the corresponding brain structures when decisions had to be postponed (Lemus et al., 2007). Indeed, both stimulus frequencies and the signed differences informing choices were indexed by neuronal firing rates of MPC neurons until monkeys' reported their choices.

For Peer Review

Recent work has started to translate the findings from monkey electrophysiology recordings during the different stages of the SFC task to human Electroencephalography (EEG) studies (Spitzer et al., 2010, 2012; Spitzer and Blankenburg, 2011, 2014; Herding et al., 2016; 2017). In particular, during the retention interval of the task, prefrontal beta band power (20 – 25 Hz) has been found to scale with the frequency that had to be maintained in WM (i.e., f1) in analogy to the monkey data (Spitzer et al., 2010; Spitzer and Blankenburg, 2011). Notably, the same modulation of beta band power during WM processing has also been observed for other sensory modalities and different analogue stimulus properties (Spitzer et al., 2012; Spitzer and Blankenburg, 2014), drawing a coherent picture of beta band power representing quantitative WM content in a generic way. Also during the decision phase of the task, beta band power has been suggested to convey task-relevant information, namely, the subjectively perceived outcome of the comparison between f2 and f1 (i.e., f2 < f1 or f2 > f1; Herding et al., 2016, 2017). Importantly, this choice-indicative signal originated from effector-specific premotor structures, i.e., from MPC when responses were reported by button presses (Herding et al., 2016), and from the frontal eye fields (FEF) when saccades were required to indicate decisions (Herding et al., 2017). Together, these findings are well in line with an intentional framework of decision making, which proposes that decisions are formed as intentions to act in those brain structures, which are also involved in the execution of the according action (see Shadlen et al., 2008).

In the current study, we investigated the role of oscillatory EEG signals in the SFC task when decision reports were postponed. In particular, we aimed at extending previous findings concerning WM processing and decision making also to a delayed response setting. We recorded EEG data in two separate experiments. Both experiments deployed the vibrotactile SFC task with delayed decision reports, however, decisions were either associated with a fixed motor mapping or with a mapping onto a color code. With the delayed

For Peer Review

response design, we intended to probe whether the response delay might constitute an additional retention interval of the task. That is, we asked the following questions: (i) Does sensory information vanish once a decision has been made, or do we find reactivations of stimulus information during the delay period, as suggested by monkey data? (ii) Are participants' choices indexed by upper beta band power just as observed for immediate decision reports (i.e., in an intentional space), or is this information referenced by the usual (generic) prefrontal WM signatures? Additionally, we wanted to pursue the idea of an intentional framework of decision making and contrasted clearly intentional decisions (i.e., associated with a fixed motor mapping) with more abstract decisions (i.e., based on a color mapping), leading to the final question: (iii) How are perceptual decisions processed if no fixed motor mapping is associated with a choice, i.e., if subjects cannot prepare a specific action as a consequence of their decision, but have to decide in a more abstract space?

Materials & Methods

Participants

We acquired EEG data from a total of 35 (23 female; 21 – 40 years old) right-handed participants completing the delayed SFC tasks (17 in the first experiment, and 18 in the second experiment; see Figure 1). Informed consent was obtained from each participant prior to the experiment, and the study was approved by the local ethics committee at the Freie Universität Berlin and was in accordance with the Declaration of Helsinki.

Stimuli & Task

Both experiments consisted of the same SFC task but varied in the way subjects were instructed to report their decisions (see below). Supra-threshold vibrotactile stimuli with a constant peak amplitude were presented to the left index finger using a 16-dot piezoelectric

For Peer Review

Braille display (4x4 quadratic matrix; 2.5 mm spacing) controlled by a programmable stimulator (Piezostimulator; Quaerosys, Schotten, Germany). The driving signals of the stimuli were generated by modulating the amplitude of a sinusoidal carrier signal (fixed at 133 Hz) using frequencies in the flutter range (i.e., 12 – 32 Hz). Thereby, subjects only perceived tactile flutter (i.e., the modulation frequency corresponding to the envelope of the stimulus function; e.g., see Tobimatsu et al., 1999), while possible artifacts in the EEG data, associated with the physical driving signal, were constrained to frequencies above 100 Hz, well outside the frequency range of interest (5 – 45 Hz). The sound of the Braille display was masked by white noise (~ 80 dB), presented via loudspeakers, throughout the experiments. The experiments were implemented in Matlab (The MathWorks), using the Psychophysics Toolbox extensions (Brainard, 1997; Kleiner et al, 2007) and custom Matlab code.

- Figure 1 about here -

In each trial, two vibrotactile stimuli (250 ms each), separated by a short retention period (1000 ms), were presented to the subjects' left index finger, while they fixated a cross in the center of a computer screen. The first stimulus could take one of four possible frequencies (f1: 16, 20, 24, or 28 Hz; randomly varied). In 75% of the trials, the frequency of the second stimulus (f2) differed by +/- 2 or 4 Hz from f1. In the remaining 25% of trials, f2 was identical to f1 (f2 = f1). These trials were introduced to study decisions independent from any sensory evidence. We did not inform subjects that both stimuli could be identical, and asked them to always respond whether f2 < f1 or f2 > f1. In both experiments, 2000 ms after the offset of f2, two colored target dots (diameter of 1° visual angle) were displayed to the left and to the right of the fixation cross (12° of visual angle off-center). One of the targets was blue, whereas the other one was yellow (counterbalanced over sides across trials). After another 500 ms, a response cue was provided (i.e., the fixation cross disappeared), and

For Peer Review

subjects reported their choices (i.e., "f2 < f1" or "f2 > f1"). In Experiment 1, the colors of the targets were irrelevant and subjects were instructed to ignore them. Instead, choices were associated with the spatial location of targets (i.e., select left vs. right target), and consequently, subjects indicated their decisions by applying a fixed motor mapping, allowing to prepare a specific action during the response delay (e.g., if "f2 < f1", press left-arrow button). Conversely, in Experiment 2, subjects reported their decisions by selecting a target based on its color (i.e., select blue vs. yellow target). Since the colored targets only appeared at the end of the response delay (i.e., 2000 ms after f2) and the specific spatial configuration was unpredictable (i.e., blue dot was equally likely on either side of the screen), the color mapping prevented the preparation of a specific motor response during the delay phase. Importantly, the association between the specific locations/colors (i.e., left/right and blue/yellow) and choices (i.e., "f2 < f1" or "f2 > f1") was counterbalanced across participants in both experiments to dissociate decisions from the *specific* decision consequence. Of note, subjects fixated the center of the screen during the whole trial, even during responding, although the fixation cross disappeared to cue a response. The raw EEG signal was scrutinized by careful visual inspection. All trials exhibiting saccades were excluded from the analysis. After a short training session of 20 trials, subjects performed eight full experimental blocks, each containing 128 trials resulting in a total of 1024 frequency comparisons.

EEG recording

EEG was recorded using a 64-channel active electrode system (ActiveTwo; BioSemi) with electrodes placed according to the extended 10-20 system. Three additional electrodes were used to record the vertical and horizontal electrooculogram (vEOG and hEOG, respectively). Single electrode locations were registered using a stereotactic electrode positioning system (Zebris Medical) prior to recording.

For Peer Review

EEG analysis

EEG analyses were performed using SPM8 (Wellcome Department of Cognitive Neurology, London, UK; www.fil.ion.ucl.ac.uk/spm/), FieldTrip (Oostenveld et al., 2011) and custom Matlab code.

Preprocessing included co-registration of the channels to the individual electrode positions, rejection of noisy channels, average referencing, adaptive spatial filtering to correct for eye-blink artifacts (based on templates obtained from the vEOG; see Ille et al., 2002), as well as high-pass filtering (0.5 Hz). The continuous recordings were segmented into epochs from 2250 ms before the onset of the second stimulus (i.e. 1000 ms before the onset of the first stimulus) to 500 ms after the response cue. Artifact rejection was done by careful visual inspection of the entire EEG-data in addition to automatically marking epochs with amplitudes greater than 150 μV.

Induced Activity: To examine purely induced, i.e. non-phase locked responses, the event-related potential (ERP) of each stimulus pair was subtracted from every trial. Time-frequency (TF) representations of corresponding single-trial spectral power between 5 and 45 Hz (resolved in steps of 1 Hz) were computed every 50 ms by applying a Morlet wavelet-transformation with a sliding window of seven cycles length (i.e., TF bin = 50 ms x 1 Hz). Changes of spectral power are reported as event-related (de)synchronizations (ERD/ERS) in individual frequencies (Pfurtscheller and Aranibar, 1977). That is, ERD/ERS provide a measure for the percentage change in spectral power relative to a pre-stimulus baseline (-2000 ms to -1300 ms, for parametric effects by f1; -1000 ms to 0 ms, for parametric effects of f2, f2 – f1, & choice). To restrain inter-trial and inter-subject variability, time frequency data were convolved with a 3 Hz x 300 ms Gaussian smoothing kernel (Kilner et al., 2005).

Statistical analysis: We used the framework of general linear models (GLM) to implement

For Peer Review

different single-trial factorial designs for repeated measures, depending on the factors of interest (i.e., f1, f2, f2 – f1, or choices). The resulting parameter estimates (i.e., TF maps of average spectral power for each factor of interest) were weighted with specific contrast weights. To analyze parametric effects of f1, we implemented a one-factorial design with four factor levels representing the four possible f1 conditions (16, 20, 24, and 28 Hz), and tested for a parametric modulation in the resulting TF maps using a linear contrast vector (f1-contrast: [-0.75 -0.25 0.25 0.75]). Possible parametric effects of f2 were investigated analogously (i.e., one-factorial design; five factor levels for possible f2: 18, 20, 22, 24 and 26 Hz; linear contrast vector: [-1 -0.5 0 0.5 1]), however, this analysis was performed only on a subset of trials in which f2 and f2-f1 were independent, because in the full stimulus set factors f2 and f2-f1 were somewhat correlated. Analyzing only data from this subset prevented us from confounding the signed differences (f2-f1) with f2-stimulus information and vice versa. To investigate decision effects, i.e. oscillatory signals coding the difference between f2 and f1, we estimated subjectively perceived frequency differences (SPFDs) as a refined measure for the quantity on which decisions are based in the SFC task (see Herding et al., 2016, 2017). In brief, we modeled subjects' choices in the framework of Bayesian inference, motivated by the observation that participants do not seem to compare f2 with the physical value of f1 (cf. Hellström, 1985, 2003), but rather with a value slightly shifted toward the mean of all presented stimulus frequencies (cf. Preuschhof et al., 2010; Ashourian and Loewenstein, 2011; Karim et al., 2012; Sanchez, 2014). We introduced this shifted version of f1, which we call f1′, as the expected value of the posterior distribution of f1 when using a Gaussian prior centered over all presented frequencies. Three free parameters (the variance of the likelihood distribution of f1, the variance of the prior distribution, and an overall response bias) were estimated in this model based on each participant's choices (further details in Herding et al., 2016). The SPFDs were then defined as the differences f2–

For Peer Review

f1′ for each stimulus pair, yielding 16 individually refined difference measures for each participants (as compared to four objective differences: -4, -2, 2, and 4 Hz). Based on all observed SPFD values (differences of log-transformed frequency values), we defined six levels of SPFD (i.e., [< −0.18]; [−0.18 to −0.09]; [−0.09 to 0]; [0 to 0.09]; [0.09 to 0.17]; [> 0.17]) to allow for a sensible grouping of data across subjects while maintaining subjective information. We specified the levels symmetrically around a SPFD of zero (corresponding to chance-level performance), and in such a way that each participant had at least one stimulus pair for each level. For incorrect trials, we separated trials only into two classes (due to low trial numbers for some levels of SPFD) with SPFD < 0 and SPFD > 0, i.e., f2 < f1 and f2 > f1. We used these discrete levels of SPFDs to implement a one-factorial design with six factor levels corresponding to the above-defined levels of SPFDs. The six TF maps resulting from GLM estimation (i.e., average spectral power per SPFD level) were contrasted using subject-specific contrast vectors defined by the median of individual SPFDs per factor level.

Up to this point, all analyses were calculated using correct trials from comparisons with f2 ≠ f1, and all trials with f2=f1 (no correct/incorrect judgment possible). To investigate effects of choices on spectral power, we also included incorrect trials as an additional factor into the analysis, leading to a one-factorial design with eight levels (i.e. six levels for correct trials + two levels for incorrect trials, see above). We contrasted the resulting TF maps using a categorical choice contrast, instead of a linear contrast as before, in order to reveal true choice effects (i.e., chose “f2 > f1” vs. chose “f2 < f1”). In particular, since such a choice modulation should be expressed as opposing modulations by SPFDs in correct and incorrect trials, we assessed choice effects by applying a categorical interaction contrast between both factors (i.e., SPFDs x correct/incorrect: [-1/3 -1/3 -1/3 1/3 1/3 1/3 1 -1]).

On the group-level, contrast images were tested for significant effects using a cluster based permutation test (Maris and Oostenveld, 2007). For effects of f1, f2, and f2-f1’ we compared

For Peer Review

the summary statistics of the observed data (one-sample t-test pooling across participants from all four experiments; n = 35) with a distribution of summary statistics obtained from 1000 randomly sign-flipped permutations. For choice effects we followed the same procedure, but computed the respective tests for each experiment individually. A cluster was defined as a group of adjacent TF bins that all exceeded a cluster-defining threshold of $p_{threshold} < .005$ (uncorrected). Clusters that exceeded a family-wise error (FWE)-corrected threshold of $p_{cluster} < .05$ (corrected for time, frequency, and channels) were considered to be statistically significant. Due to strong a priori assumptions on the topographical distribution of signals encoding quantity information (Spitzer et al., 2010, Spitzer and Blankenburg 2011), for parametric WM (or delay activity) effects of f1, f2 and f2-f1', we applied FWE-correction only for right frontal electrodes (AF4, F2, F4, F6, FC6, FC4, FC2). For choice effects, we corrected over all electrodes.

Source reconstruction The cortical sources of amplitude modulations observed on the scalp level were localized using the 3-D source reconstruction routines provided by SPM8 (Friston et al., 2006). On the basis of the individually recorded electrode positions for each participant, a forward model was constructed using an 8196-point cortical mesh of distributed dipoles perpendicular to the cortical surface of a template brain (cf. Friston et al., 2008). The lead field of the forward model was computed using the three-shell boundary elements method EEG head model available in SPM8. Conventional minimum norm priors under group constraints (Litvak and Friston, 2008) were used to invert the forward model. For each condition, the results of model inversion were summarized in a 3-D image that reflected spectral source amplitude in the TF window of interest. Relevant contrasts of these 3-D images served as an estimate for subject-specific source locations and were used for group level statistical analysis (see Litvak et al., 2011). The signal was localized using the preprocessed stimulus-locked EEG data (i.e., in the time domain). Additionally, the data were

For Peer Review

bandpass filtered in the frequency range of the TF cluster identified on the scalp level (±1 Hz to ensure that no information is lost at the cluster borders). The 3-D images summarizing each condition were computed over a representative TF window. To identify cortical sources in which the respective amplitude was modulated by f1, f2, f2-f1', or by choice, the 3-D images were weighted by a contrast vector in analogy to the sensor space analysis. Source estimates were statistically analyzed on the group level using conventional t-tests and displayed at a threshold of $p < .05$ (uncorrected). Anatomical reference for source estimates was established on the basis of the SPM anatomy toolbox (Eickhoff et al., 2005).

For Peer Review

Results

Behavior

Proportions of correct responses (PCRs) were analyzed using a two factorial 2 x 4 ANOVA including the between-subject factor *Experiment* (2 levels) and the within-subject factor *f1-frequency* (4 levels). We used Greenhouse-Geisser correction to correct for degrees of freedom and hence p-values for violated assumptions of sphericity. Table 1 shows the PCRs across f1-frequencies for the two experiments. There was no main effect for the factor *Experiment* ($F(1, 33) = 1.56$, $p = 0.22$), but a significant main effect for *f1-frequency* ($F(2.11, 69.63) = 12.28$, $p < 0.001$). Within-subject contrasts revealed that performance accuracy was significantly lower for f1 = 16 and 28 Hz compared to f1 = 20 and 24 Hz. No interaction between both factors was observed ($F(2.11, 69.63) = 0.05$, $p = 0.96$).

- Table 1 about here -

EEG

Parametric effects of f1 Figure 2 A shows parametric effects of f1 during the retention interval and the response delay pooled over both experiments. Here, we identified two significant clusters. First, in the retention interval after the offset of f1 and before the onset of f2, beta band power (15 – 20 Hz) exhibited a parametric modulation by f1 from -800 to -400 ms in electrodes AF4, F2, and F4 ($p_{cluster}$ = 0.04, FWE-corrected over a priori defined set of electrodes). That is, the higher the f1-frequency, the higher the beta band power. During the response delay, we found a similar modulation 650 to 900 ms after the onset of f2 in electrodes AF4, F4, F6, FC6, and FC4 ($p_{cluster}$ = 0.02, FWE-corrected over a priori defined set of electrodes). The topographical distributions (extracted from the marked time-frequency windows) show that the signal for both of these parametric effects was mostly carried by right frontal electrodes. Source reconstruction revealed that this modulation most likely originated from the right IFG, area 45.

Parametric effects of f2 Figure 2 D shows parametric effects of f2 during the response delay pooled over the two experiments. Including all trials of the orthogonal subset in the analysis, we did not find any effect of f2. To increase the signal to noise ratio we excluded trials with f2 ≠ f1 from further analysis (as in these trials frequencies cannot be successfully discriminated). We identified a significant cluster indicating a positive parametric modulation by f2 in electrodes AF4, F2, F4, and F6 ($p_{cluster}$ = 0.04, FWE-corrected over a priori defined set of electrodes) in the frequency range from 30 to 35 Hz, 1600 to 1800 ms after the onset of f2. As shown in Figure 2 E, this effect is mainly driven by an overall lower beta band power for f2 = 18 Hz. However, the significant cluster seems to indeed be the result of a parametric modulation by f2. Source reconstruction localized the modulation by f2 also within right IFG, area 45.

Parametric effects of SPFDs Figure 2 G shows parametric effects of subjectively perceived

For Peer Review

frequency differences (SPFDs) between f2 and f1 (f2-f1') pooled over all participants from both experiments. We identified a significant cluster ($p_{cluster} < 0.04$, FWE-corrected over a priori defined set of electrodes) in the response delay in the frequency range from 16 to 29 Hz, 600 to 900 ms after the offset of f2 in electrodes F6, FC4, and FC2, indexing a positive modulation of beta band power by SPFDs.

- Figure 2 about here -

Choice Effects Figure 3 shows the effects of choices for either experiment. In the beginning, we sought to find effects in trials with f2 ≠ f1, and to confirm any observed modulation by choices in trials with f2 = f1. The analysis of trials with f2 = f1, however, did not reveal any significant choice modulations, possibly because this analysis only comprised 25% of all trials (max. 256 trials per subject), which was likely not enough data to find significant effects of this kind. Nevertheless, as our Bayesian model predicted small but non-zero SPFDs, even for trials with f2 = f1 (i.e., no physical difference), we were able to divide these trials as well into correct and incorrect trials (i.e. trials with positive SPFDs and choice f2>f1/f2<f1 were classified as correct/incorrect, whereas trials with negative SPFDs and choice f2>f1/f2<f1 were classified as incorrect/correct). These trials could thus also be grouped into the known SPFD classes, allowing for a combined analysis with all the other trials (i.e., f2 ≠ f1), choice effects reported in the following were computed on all trials, irrespective of whether they were correct or incorrect. That is, the time-frequency maps display the group statistics of the interaction contrast between the sign of the frequency difference (f2<f1/f2>f1) and correct/incorrect decisions.

In *Experiment 1,* there was a significant cluster ($p_{cluster} = 0.01$, FWE-corrected) in eleven (pre)frontal electrodes (see Figure 3 C), strongest in F1 and F2, highlighting a positive

For Peer Review

modulation by choices in frequencies from 30 to 40 Hz at a time around 750 to 1050 ms after the onset of f2. In particular, the power in this frequency range was higher for "f2 > f1" choices as compared with "f2 < f1" choices. A source reconstruction localized this choice modulation to the left medial premotor cortex (MPC).

In *Experiment 2,* we found a significant cluster ($p_{cluster}$ = 0.04, FWE-corrected) with positive effects in seven parietal electrodes (see Figure 3 F), strongest in CP1, CPz, and CP2 (higher power for response "f2 > f1"). This cluster was evident in a frequency range between 27 to 32 Hz around 1200 to 1550 ms after the offset of f2. A source reconstruction suggested the posterior parietal cortex (PPC) in the left hemisphere as the most likely origin of the choice modulation in this experiment.

- Figure 3 about here -

Discussion

In the present study we investigated oscillatory EEG correlates of decision making in the vibrotactile SFC task with delayed responses. We introduced different response mappings in two separate experiments to explore the influence of decision consequences on relevant choice signals. We also focused on oscillatory signatures of WM processing, and probed whether individual stimulus information, alongside of choice information, was maintained during the delay phase of this task. During the main retention interval, i.e. between f1 and f2, we observed a parametric modulation of spectral power in right prefrontal beta band oscillations (15 - 25 Hz) by the frequency of the first stimulus (f1). During the ensuing response delay (or "second retention interval"), parametric power modulations by f1, f2, as well as by the estimated subjectively perceived frequency differences (SPFDs; f2-f1') were also evident in right prefrontal electrodes, spanning similar frequencies (15 – 35 Hz).

For Peer Review

Depending on the response mapping, we moreover found different cortical sources of choice-selective modulations in the upper beta band (~25 - 40 Hz). These sources indicated that choices mapped onto a specific action (Experiment 1) were represented in premotor areas. In contrast, choices associated with a mapping onto a color code (Experiment 2) were processed in parietal areas. Notably in contrast, all observed choice-related power modulations were inverted for *incorrect* trials, underpinning the behavioral relevance of the respective signals.

Maintenance of stimulus information throughout the task

Memory-based perceptual decisions entail the comparison of an active representation of sensory information with previously presented sensory information maintained in WM (Hayden and Pasternak, 2013). For memory-based decisions in the somatosensory domain, a vibrotactile SFC task has been extensively used to study the underlying neural processes in monkeys (Romo et al., 1999; Hernández et al., 2010; for review see Romo and de Lafuente, 2013) and in humans (Li Hegner et al., 2010; Pleger et al., 2006; Spitzer et al., 2010; 2012; Spitzer and Blankenburg, 2011; 2014). Specifically, during the retention phase of the task, the PFC has been implicated by animal work (e.g., Romo et al., 1999), as well as by several human EEG studies (e.g., Spitzer et al., 2010; Spitzer and Blankenburg, 2011), to index the content that has to be maintained in WM, i.e., f1. In overall agreement with the monkey literature, and directly replicating the previous EEG studies, we found that the power of beta band oscillations in prefrontal electrodes was modulated by f1 during the retention interval of the task. Other studies have generalized this effect to visual and auditory WM (Spitzer and Blankenburg, 2012) as well as to different analogue stimulus features (Spitzer et al., 2014). Taken together, these findings suggest that the large-scale oscillatory beta band effect in the human EEG signal might reflect an internal estimate of an abstract quantity ascribed to the relevant stimulus feature held in WM (Spitzer et al., 2011; Spitzer and Blankenburg, 2014).

For Peer Review

In previous studies, subjects usually reported their decision right after the presentation of the second stimulus. Only a few studies in monkeys investigated how stimulus information and decision evidence are further processed in cases where the decision report is delayed, i.e. when a decision has to be stored in WM (e.g., Lemus et al., 2007; Hernández et al., 2010; Haegens et al., 2011). Here, an interesting question is whether only information about the decision is maintained in WM or if stimulus information, on which the decision was based, is stored alongside, e.g., to reevaluate the decision. If such stimulus information was also retained during the decision delay, one could expect to observe similar effects as indexing the maintenance of f1 (see above). Indeed, we observed a parametric modulation of prefrontal beta band power as a function of f1 and f2 during the response delay. Further, a ROI-based analysis indicated that decisional evidence in the form of SPFDs (f2-f1') was also represented in right prefrontal beta band power. The present findings thus complement earlier studies of the delayed SFC task, in which firing rates in monkeys' medial premotor cortex (MPC) monotonically encoded f1, f2, and f2-f1 (Lemus et al., 2007). Our results further extend the original findings by Spitzer et al. (2010) in multiple ways: we show that the maintenance of f2 and a reactivation of f1 during the forced response delay induced the same parametric modulations of beta band power as f1 in the (initial) retention interval. Further, we show that this modulation was not only evident for single stimulus features but also for dynamic combinations of quantitative estimates such as the subjectively perceived differences between f2 and f1. From an ecological perspective, maintaining stimulus information over the course of the response delay is an appealing concept (even though decisions have been already formed after the presentation of f2, and responses can possibly be prepared), because time resources are exploited, and the flexibility to adapt to changing affordances is preserved (Lemus et al., 2007).

For Peer Review

Oscillatory choice signals are represented in the space of their consequences

In the field of perceptual decision making, two main hypotheses about the neural implementation of decision formation have evolved over the last decades. On the one hand, the intentional framework views decision making as a selection between a limited set of affordances or intentions, processed in areas related to motor planning (Cisek and Kalaska 2010; Shadlen et al. 2008). On the other hand, a modality-transcending general decision module is assumed, supposedly located in the dorsolateral prefrontal cortex (Heekeren et al., 2008) or in the anterior insular (Ho et al., 2009; Lui and Pleskac, 2011). Curiously, the findings obtained in the vibrotactile SFC paradigm (reviewed in Romo and de Lafuente, 2013) have rarely been linked to either of these two conceptual frameworks, possibly because most of the work with the SFC task focused exclusively on decision reports by button presses. In the context of button press responses, however, the available results appear to be in favor of an intentional framework of decision making. Choice-selective signals were consistently reported in recordings from premotor areas that are known to be involved in the preparation of the according decision reports (e.g., Hernández et al., 2002, 2010; Romo et al., 2004; Haegens et al., 2011; Herding et al., 2016). Conversely, firing rates in PFC were shown to reflect upcoming choices (Jun et al. 2010; Hernández et al., 2010), which might be interpreted in favor of a general decision module. However, in two recent EEG studies, we provided more evidence for an intentional interpretation of perceptual decisions by showing that the same choice signal appears to originate from different effector-specific premotor structures, depending on the response modality (Herding et al., 2016, 2017). That is, we found a choice-indicative modulation of upper beta band power (i.e., increased beta band power for “f2 > f1” choices as compared to “f2 < f1” choices; see also Haegens et al., 2011) most likely originating from MPC when responses were reported by button presses, and with a source in FEF when saccades were used to indicate responses. In the current study, we

For Peer Review

further corroborated the idea of an intentional framework of decision making and extended these findings to postponed decision reports in the vibrotactile SFC task, but notably, only when choices were associated with a fixed motor mapping (Experiment 1). In line with previous animal studies (Lemus et al., 2007; Haegens et al., 2011), we could hence show that choice information was also maintained in premotor areas during a forced response delay. In particular, we found the same choice signal in upper beta band power that was previously only associated with immediate decision reports in the vibrotactile SFC task (see Haegens et al., 2011; Herding et al., 2016, 2017). Interestingly, a recent study in rats also substantiated a causal role of frontal motor cortices for maintaining choice information (Goard et al., 2016). In a memory-guided visual decision task, the authors showed that after optogenetic inhibition of frontal motor cortices, but not of parietal or sensory areas, maintenance of choice information was disrupted.

Besides premotor structures, the PPC has been strongly implicated in the formation of perceptual decisions, especially in the visual domain, and when responses were reported by saccades (for review see Shadlen and Gold, 2007). Specifically, firing rates of single neurons in PPC (i.e., in lateral intraparietal area; LIP) were shown to reflect accumulating evidence for oculomotor decisions, peaking at the time of the decision report (e.g., Shadlen & Newsome, 2001; Roitman & Shadlen, 2002). Recently, Bennur and Gold (2011) demonstrated that LIP appears to index evidence for subsequent choices also when decisions are dissociated from a specific oculomotor action. The authors applied a variant of the classic random dot motion (RDM) task, in which choices (i.e., perceived motion direction) were associated with a color mapping similar to the one used in the current study (e.g., if leftward motion, chose red target). Monkeys were trained to make a saccade to one of two visual targets based on the targets' colors, which were only revealed either before, during, or after stimulus presentation. Crucially, firing rates of LIP neurons encoded sensory evidence for a

For Peer Review

decision (i.e., perceived net motion) even before the colors of the targets were disclosed, i.e., before a specific action could be prepared. Only after the motor mapping was clear, firing rates in LIP started to encode the direction of the subsequent saccade as known from previous work (e.g., Shadlen & Newsome, 2001; Roitman & Shadlen, 2002). In line with these insights, we found that the usual choice-indicative modulation of upper beta band power with a most-likely source in PPC was observed when choices were associated with a color mapping that concealed a specific motor action (Experiment 2). That is, the lack of a specific motor mapping led to a relocation of a known choice signal from premotor cortices (Experiment 1) to PPC (Experiment 2). Whereas the signal in MPC lends itself to a straightforward interpretation (i.e., informing a subsequent button press), an interpretation of the choice-informative signal in PPC is a bit speculative. Since the color mapping arguably also conveyed some spatial information about the ensuing choice (i.e., target dots were always at same locations), we suggest that a choice-informative signal in PPC can possibly be interpreted with respect to the idea of PPC implementing intentional or saliency maps (e.g., see Andersen and Buneo, 2003).

Together, our findings suggest that the information that determines a decision (here, the categorized comparison outcome) is processed in cortical areas that implement the consequences of that decision, i.e., in PMC when a motor mapping is provided, and in PPC when a non-motor (i.e., color) mapping is required. In other words, the sensorimotor transformation at the heart of perceptual decision making appears to proceed as far as possible, constrained by the given circumstances. Accordingly, monkeys' FEF seem to have access to evolving decisional evidence only when a specific motor mapping is provided for a decision report (Shadlen and Gold, 2003): microstimulation of FEF reliably evoked an involuntary saccade of the monkeys before they could indicate their choices in a RDM task. Importantly, this evoked saccade was deflected towards the later chosen response targets,

For Peer Review

only when a specific motor mapping was provided in advance. Conversely, Katz et al. (2016) questioned the causal role of LIP for decisions under these circumstances. The authors showed that a pharmacological inactivation of LIP had no effect on decision performance in a RDM task, whereas area MT (i.e., source of the sensory evidence) proved to be indispensable. Hence, when a specific action is associated with a choice, LIP activity seems to be largely redundant for a decision (Katz et al., 2016), whereas FEF appears to encode choices solely under these conditions (Gold and Shadlen, 2003). Taken together, these results suggest that premotor areas (i.e., FEF) and PPC (i.e., LIP) play distinct roles in decision making, dissociated by the level of abstractness in the resulting action consequence. In line with previous monkey data (Bennur and Gold, 2011), we here provide first evidence for a similar dissociation in the opposite direction when a non-motor mapping is required (i.e., a choice signal in PPC but not in premotor structures).

To conclude, we systematically investigated the influence of different response mappings (motor mapping vs. color mapping) in postponed decisions based on vibrotactile frequency comparisons. We found that overall, stimulus information, decisional evidence, and choices were represented in beta band power throughout the task, i.e., also after the presentation of the second stimulus. We found that choices that could be mapped onto specific actions were encoded in premotor areas involved in the planning and preparation of the according motor response. Conversely, choices that were not associated with a specific action, but rather required a more abstract response mapping, were encoded in posterior parietal regions. In sum, our findings are well in line with an intentional framework of decision making, and clearly emphasize that the consequences of a decision (i.e., how it is expressed) determine where the crucial information that informs this decision (i.e., what is it based on) is processed.

For Peer Review

For Peer Review

References

Andersen RA, Buneo CA (2002): Intentional maps in posterior parietal cortex. Annual review of neuroscience 25:189–220.

Ashourian P, Loewenstein Y (2011): Bayesian Inference Underlies the Contraction Bias in Delayed Comparison Tasks. PLOS ONE 6:e19551.

Bennur S, Gold JI (2011): Distinct representations of a perceptual decision and the associated oculomotor plan in the monkey lateral intraparietal area. J Neurosci 31:913–921.

Brainard DH (1997): The Psychophysics Toolbox. Spat Vis 10:433–436.

Brody CD, Hernández A, Zainos A, Romo R (2003): Timing and Neural Encoding of Somatosensory Parametric Working Memory in Macaque Prefrontal Cortex. Cereb Cortex 13:1196–1207.

Cisek P, Kalaska JF (2010): Neural Mechanisms for Interacting with a World Full of Action Choices. Annual Review of Neuroscience 33:269–298.

Eickhoff SB, Stephan KE, Mohlberg H, Grefkes C, Fink GR, Amunts K, Zilles K (2005): A new SPM toolbox for combining probabilistic cytoarchitectonic maps and functional imaging data. NeuroImage 25:1325–1335.

Friston K, Henson R, Phillips C, Mattout J (2006): Bayesian estimation of evoked and induced responses. Hum Brain Mapp 27:722–735.

Goard MJ, Pho GN, Woodson J, Sur M (2016): Distinct roles of visual, parietal, and frontal motor cortices in memory-guided sensorimotor decisions. eLife 5:e13764.

Gold JI, Shadlen MN (2003): The influence of behavioral context on the representation of a perceptual decision in developing oculomotor commands. J Neurosci 23:632–651.

Gold JI, Shadlen MN (2007): The neural basis of decision making. Annu Rev Neurosci 30:535–574.

For Peer Review

Haegens S, Nácher V, Hernández A, Luna R, Jensen O, Romo R (2011): Beta oscillations in the monkey sensorimotor network reflect somatosensory decision making. PNAS 108:10708–10713.

Hayden B, Pasternak T (2013): Linking neural activity to complex decisions. Vis Neurosci 30:331–342.

Heekeren HR, Marrett S, Ungerleider LG (2008): The neural systems that mediate human perceptual decision making. Nat Rev Neurosci 9:467–479.

Hellström Å (1985): The time-order error and its relatives: Mirrors of cognitive processes in comparing. Psychological Bulletin 97:35–61.

Hellström Å (2003): Comparison is not just subtraction: Effects of time- and space-order on subjective stimulus difference. Perception & Psychophysics 65:1161–1177.

Herding J, Ludwig S, Blankenburg F (2017): Response-Modality-Specific Encoding of Human Choices in Upper Beta Band Oscillations during Vibrotactile Comparisons. Front Hum Neurosci 11. http://journal.frontiersin.org/article/10.3389/fnhum.2017.00118/abstract.

Herding J, Spitzer B, Blankenburg F (2016): Upper Beta Band Oscillations in Human Premotor Cortex Encode Subjective Choices in a Vibrotactile Comparison Task. J Cogn Neurosci:1–12.

Hernández A, Nácher V, Luna R, Zainos A, Lemus L, Alvarez M, Vázquez Y, Camarillo L, Romo R (2010): Decoding a perceptual decision process across cortex. Neuron 66:300–314.

Hernández A, Zainos A, Romo R (2002): Temporal evolution of a decision-making process in medial premotor cortex. Neuron 33:959–972.

Ho TC, Brown S, Serences JT (2009): Domain general mechanisms of perceptual decision making in human cortex. J Neurosci 29:8675–8687.

Ille N, Berg P, Scherg M (2002): Artifact correction of the ongoing EEG using spatial filters based on artifact and brain signal topographies. Journal of clinical neurophysiology 19:113–124.

For Peer Review

Jun JK, Miller P, Hernández A, Zainos A, Lemus L, Brody CD, Romo R (2010): Heterogenous population coding of a short-term memory and decision task. J Neurosci 30:916–929.

Katz LN, Yates JL, Pillow JW, Huk AC (2016): Dissociated functional significance of decision-related activity in the primate dorsal stream. Nature 535:285–288.

Kilner JM, Kiebel SJ, Friston KJ (2005): Applications of random field theory to electrophysiology. Neurosci Lett 374:174–178.

Kleiner M, Brainard D, Pelli D, Ingling A, Murray R, Broussard C, others (2007): What's new in Psychtoolbox-3. Perception 36:1.

Lafuente V de, Jazayeri M, Shadlen MN (2015): Representation of Accumulating Evidence for a Decision in Two Parietal Areas. J Neurosci 35:4306–4318.

Lemus L, Hernández A, Luna R, Zainos A, Nácher V, Romo R (2007): Neural correlates of a postponed decision report. PNAS 104:17174–17179.

Li Hegner Y, Lee Y, Grodd W, Braun C (2010): Comparing tactile pattern and vibrotactile frequency discrimination: a human FMRI study. J Neurophysiol 103:3115–3122.

Litvak V, Friston K (2008): Electromagnetic source reconstruction for group studies. Neuroimage 42:1490–1498.

Litvak V, Mattout J, Kiebel S, Phillips C, Henson R, Kilner J, Barnes G, Oostenveld R, Daunizeau J, Flandin G, Penny W, Friston K (2011): EEG and MEG Data Analysis in SPM8. Computational Intelligence and Neuroscience 2011:e852961.

Liu T, Pleskac TJ (2011): Neural correlates of evidence accumulation in a perceptual decision task. J Neurophysiol 106:2383–2398.

Maris E, Oostenveld R (2007): Nonparametric statistical testing of EEG- and MEG-data. Journal of neuroscience methods 164:177–190.

For Peer Review

Oostenveld R, Fries P, Maris E, Schoffelen J-M (2010): FieldTrip: Open Source Software for Advanced Analysis of MEG, EEG, and Invasive Electrophysiological Data. Computational Intelligence and Neuroscience 2011:e156869.

Pfurtscheller G, Aranibar A (1977): Event-related cortical desynchronization detected by power measurements of scalp EEG. Electroencephalogr Clin Neurophysiol 42:817–826.

Pleger B, Ruff CC, Blankenburg F, Bestmann S, Wiech K, Stephan KE, Capilla A, Friston KJ, Dolan RJ (2006): Neural coding of tactile decisions in the human prefrontal cortex. J Neurosci 26:12596–12601.

Roitman JD, Shadlen MN (2002): Response of neurons in the lateral intraparietal area during a combined visual discrimination reaction time task. J Neurosci 22:9475–9489.

Romo R, Brody CD, Hernández A, Lemus L (1999): Neuronal correlates of parametric working memory in the prefrontal cortex. Nature 399:470–473.

Romo R, Hernández A, Zainos A (2004): Neuronal correlates of a perceptual decision in ventral premotor cortex. Neuron 41:165–173.

Romo R, Hernández A, Zainos A, Lemus L, Brody CD (2002): Neuronal correlates of decision-making in secondary somatosensory cortex. Nat Neurosci 5:1217–1225.

Romo R, de Lafuente V (2013): Conversion of sensory signals into perceptual decisions. Progress in Neurobiology 103:41–75.

Salinas E, Romo R (1998): Conversion of sensory signals into motor commands in primary motor cortex. J Neurosci 18:499–511.

Salinas E, Hernández A, Zainos A, Romo R (2000): Periodicity and Firing Rate as Candidate Neural Codes for the Frequency of Vibrotactile Stimuli. J Neurosci 20:5503–5515.

Sanchez G, Daunizeau J, Maby E, Bertrand O, Bompas A, Mattout J (2014): Toward a New Application of Real-Time Electrophysiology: Online Optimization of Cognitive Neurosciences Hypothesis Testing. Brain Sci 4:49–72.

For Peer Review

Shadlen MN, Newsome WT (2001): Neural basis of a perceptual decision in the parietal cortex (area LIP) of the rhesus monkey. J Neurophysiol 86:1916–1936.

Shadlen MN, Kiani R, Hanks TD, Churchland AK (2008): Neurobiology of Decision Making. In: Engel, C, Singer, W, editors. Better Than Conscious? Cambridge: The MIT Press. pp 71–102. http://mitpress.universitypressscholarship.com/view/10.7551/mitpress/9780262195805.001.0001/upso-9780262195805-chapter-4.

Spitzer B, Blankenburg F (2012): Supramodal Parametric Working Memory Processing in Humans. Journal of Neuroscience 32:3287–3295.

Spitzer B, Wacker E, Blankenburg F (2010): Oscillatory Correlates of Vibrotactile Frequency Processing in Human Working Memory. Journal of Neuroscience 30:4496–4502.

Spitzer B, Blankenburg F (2011): Stimulus-dependent EEG activity reflects internal updating of tactile working memory in humans. PNAS 108:8444–8449.

Spitzer B, Gloel M, Schmidt TT, Blankenburg F (2014): Working memory coding of analog stimulus properties in the human prefrontal cortex. Cereb Cortex 24:2229–2236.

Tobimatsu S, Zhang YM, Kato M (1999): Steady-state vibration somatosensory evoked potentials: physiological characteristics and tuning function. Clin Neurophysiol 110:1953–1958.

For Peer Review

Tables

Table 1

Behavioral Results

PCR

f1 (Hz)	16	20	24	28
Experiment 1	63.9±5.3	72.0±4.4	72.1±4.7	67.4±3.9
Experiment 2	67.5±5.2	75.1±4.3	74.6±4.5	70.9±3.8

Note: Percent of correct responses (PCRs) and 95% confidence intervals for each f1 condition in Experiments 1 and 2.

For Peer Review

Captions to figures

- Figure 1

Schematic of the task and the overall experimental design. F1 was presented for 250 ms, followed by a retention interval of 1000 ms. Subsequently, f2 was presented for 250 ms, followed by a 2000 ms response delay. Thereafter, the response mapping (RM) in form of two colored targets was presented lateral to the fixations cross. Note, that the response mapping was only relevant in Experiment 2. In Experiment 1 the dots were also presented to ensure consistency over the experiments. After another 500 ms the fixation cross disappeared (response cue; RC) and the subject reported its decision.

For Peer Review

- Figure 2

Induced parametric activity as a function of f1 and f2 stimulus frequencies and their subjectively perceived differences. **A** Statistical parametric map of the effect of oscillatory power as a function of f1 averaged over a priori defined electrodes. The significant clusters ($p_{retention}$ = 0.04; p_{delay} = 0.02; FWE-corrected over a priori defined set of right frontal electrodes) are marked by dashed rectangles. **B** Time-courses of oscillatory power in a frequency range from 15 Hz to 20 Hz for the four f1 stimulus frequencies (16, 20, 24, and 28 Hz) averaged over electrodes showing a significant effect. **C** Upper part: Topographical scalp distributions of the two marked time-frequency windows in the retention interval and the delay (dashed rectangles). Lower Part: 3D source localization for the parametric modulation by f1 for the indicated time-frequency window (dashed rectangle). **D** Same as **A** for effects as a function of f2 ($p_{cluster}$ = 0.04; FWE-corrected over a priori defined right frontal electrodes). **E** Time-courses of oscillatory power in a frequency range between 30 Hz and 35 Hz for the five f2 stimulus frequencies of the orthogonal subset (18, 20, 22, 24, and 16 Hz) **F** Same as **C** for effects of f2. **G** Same as **A** for effects as a function of f2-f1' ($p_{cluster}$ = 0.04; FWE-corrected over a priori defined right frontal electrodes). **H** Time-courses of oscillatory power in a frequency range between 15 Hz and 25 Hz for the four f2-f1 stimulus frequency differences (-4, -2, 2, and 4 Hz) **I** Same as **C** for effects of f2-f1.

For Peer Review

- Figure 3

Statistical parametric maps, topographical distributions, and estimated sources of the choice contrast and the significant clusters in Experiments 1 and 2. **A** Significant cluster for choices with a fixed motor mapping (Experiment 1; $p_{cluster} = 0.01$, FWE-corrected) **B** Time-courses of oscillatory power in a frequency range between 30 Hz and 40 Hz for the six SPFD classes **C** Upper part: Topographical scalp distributions of the marked time-frequency windows for Experiment 1 (dashed rectangles). Lower part: 3D source reconstructions of the modulations by choice for the respective experiments. **D** Significant cluster for choices with flexible decision-to-response mapping (Experiment 2; $p_{cluster} = 0.04$, FWE-corrected) **E** Time-courses of oscillatory power in a frequency range between 29 Hz and 32 Hz for the six SPFD classes. **F** Same as C for Experiment 2.

For Peer Review

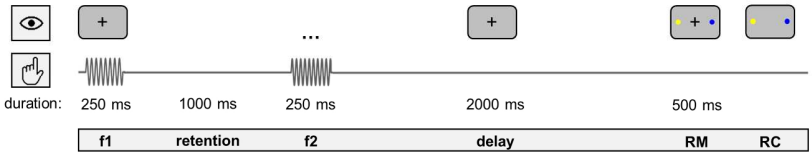

Schematic of the task and the overall experimental design. F1 was presented for 250 ms, followed by a retention interval of 1000 ms. Subsequently, f2 was presented for 250 ms, followed by a 2000 ms response delay. Thereafter, the response mapping (RM) in form of two colored targets was presented lateral to the fixations cross. Note, that the response mapping was only relevant in Experiment 2. In Experiment 1 the dots were also presented to ensure consistency over the experiments. After another 500 ms the fixation cross disappeared (response cue; RC) and the subject reported its decision.

180x29mm (300 x 300 DPI)

For Peer Review

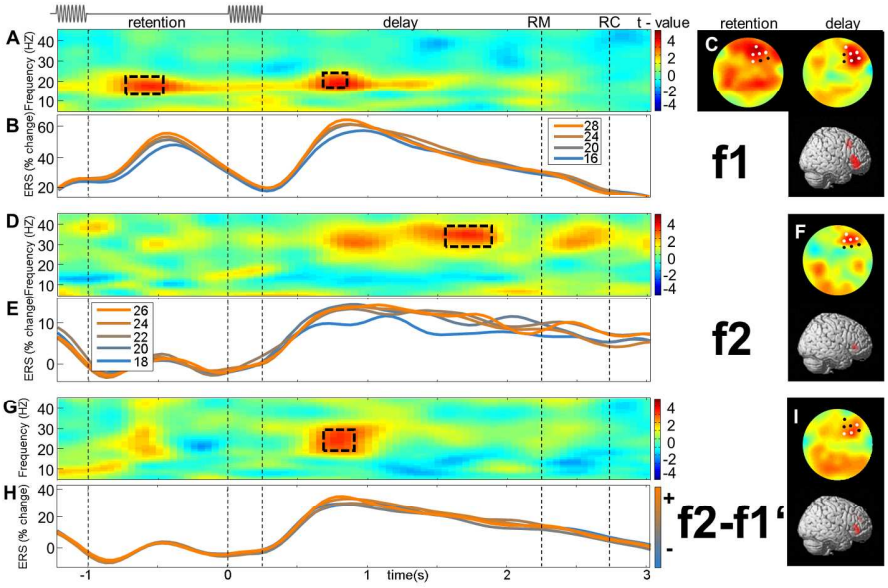

Induced parametric activity as a function of f1 and f2 stimulus frequencies and their subjectively perceived differences. A Statistical parametric map of the effect of oscillatory power as a function of f1 averaged over a priori defined electrodes. The significant clusters (pretention = 0.04; pdelay = 0.02; FWE-corrected over a priori defined set of right frontal electrodes) are marked by dashed rectangles. B Time-courses of oscillatory power in a frequency range from 15 Hz to 20 Hz for the four f1 stimulus frequencies (16, 20, 24, and 28 Hz) averaged over electrodes showing a significant effect. C Upper part: Topographical scalp distributions of the two marked time-frequency windows in the retention interval and the delay (dashed rectangles). Lower Part: 3D source localization for the parametric modulation by f1 for the indicated time-frequency window (dashed rectangle). D Same as A for effects as a function of f2 (pcluster = 0.04; FWE-corrected over a priori defined right frontal electrodes). E Time-courses of oscillatory power in a frequency range between 30 Hz and 35 Hz for the five f2 stimulus frequencies of the orthogonal subset (18, 20, 22, 24, and 16 Hz) F Same as C for effects of f2. G Same as A for effects as a function of f2-f1' (pcluster = 0.04; FWE-corrected over a priori defined right frontal electrodes). H Time-courses of oscillatory power in a frequency range between 15 Hz and 25 Hz for the four f2-f1 stimulus frequency differences (-4, -2, 2, and 4 Hz) I Same as C for effects of f2-f1.

180x114mm (300 x 300 DPI)

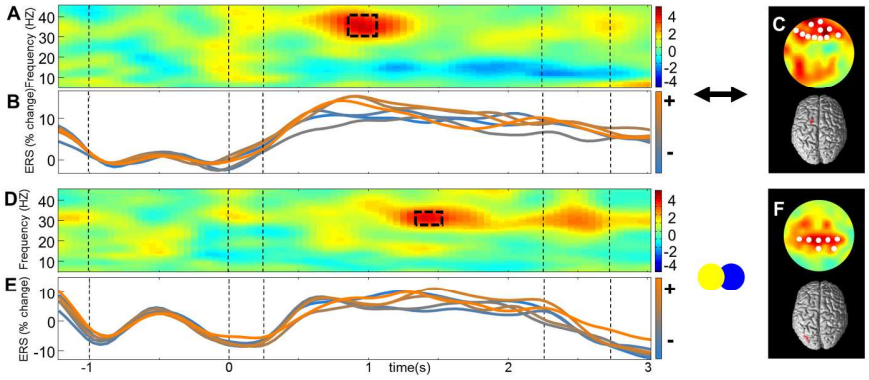

Statistical parametric maps, topographical distributions, and estimated sources of the choice contrast and the significant clusters in Experiments 1 and 2. A Significant cluster for choices with a fixed motor mapping (Experiment 1; pcluster = 0.01, FWE-corrected) B Time-courses of oscillatory power in a frequency range between 30 Hz and 40 Hz for the six SPFD classes C Upper part: Topographical scalp distributions of the marked time-frequency windows for Experiment 1 (dashed rectangles). Lower part: 3D source reconstructions of the modulations by choice for the respective experiments. D Significant cluster for choices with flexible decision-to-response mapping (Experiment 2; pcluster = 0.04, FWE-corrected) E Time-courses of oscillatory power in a frequency range between 29 Hz and 32 Hz for the six SPFD classes. F Same as C for Experiment 2.

180x75mm (300 x 300 DPI)

Review

Study 4 - Centro-parietal EEG Potentials in Perceptual Decision Making: From Subjective Evidence to Confidence

Herding, J., Ludwig, S., Spitzer, B., and Blankenburg, F. (submitted). Centro-parietal EEG Potentials in Perceptual Decision Making: From Subjective Evidence to Confidence. Journal of Neuroscience.

The Journal of Neuroscience

https://jneurosci.msubmit.net

JN-RM-1132-17

Centro-parietal EEG potentials in perceptual decision making: from subjective evidence to confidence

Jan Herding, Freie Universität Berlin
Simon Ludwig, Freie Universität Berlin
Bernhard Spitzer, University of Oxford
Felix Blankenburg, Charité

Commercial Interest:

This is a confidential document and must not be discussed with others, forwarded in any form, or posted on websites without the express written consent of The Journal for Neuroscience.

Section: Behavioral/Cognitive

Centro-parietal EEG potentials in perceptual decision making: from subjective evidence to confidence

Abbreviated title: Subjective evidence and confidence in the CPP

Authors: Jan Herding[1,2] , Simon Ludwig[1], Bernhard Spitzer[1,3], Felix Blankenburg[1,2]

[1]Neurocomputation and Neuroimaging Unit, Department of Education and Psychology, Freie Universität Berlin, Habelschwerdter Allee 45, 14195 Berlin

[2] Bernstein Center for Computational Neuroscience Berlin, Philippstr. 13, 10115 Berlin

[3]Department of Experimental Psychology, University of Oxford, Oxford OX1 3UD, UK.

Corresponding author: Jan Herding (jan.herding@bccn-berlin.de), Neurocomputation and Neuroimaging Unit, Department of Education and Psychology, Freie Universität Berlin, Habelschwerdter Allee 45, 14195 Berlin

Number of figures: 8
Number of tables: 1
Number of words: ~7850 (Abstract: 244, Introduction: 631, Discussion: 1462)
Acknowledgements: This work was supported by the Deutsche Forschungsgemeinschaft (DFG, GRK1589/1). We thank Ulf Toelch for useful comments on the manuscript.

Abstract

Recent studies suggest that a centro-parietal positivity (CPP) in the human EEG signal tracks the absolute (i.e. unsigned) strength of accumulated evidence for choices that require the integration of noisy sensory input. Here, we investigated whether the CPP might also reflect the evidence for decisions that are based on a quantitative comparison between two sequentially presented stimuli (i.e., a signed quantity). We recorded EEG data while participants decided whether the latter of two vibrotactile frequencies was higher or lower than the former in six different variants of this task (n = 116). To account for known biases in sequential comparisons, we applied a behavioral model based on Bayesian inference that allowed us to estimate subjectively perceived frequency differences as well as statistical decision confidence. We used the perceived differences as a measure of subjective evidence. The sign indicated which alternative was favored, and its absolute value reflected the strength of evidence for that alternative. Immediately after the second stimulus, the signed value of subjective evidence was reflected in the CPP. Strikingly, this early modulation was even seen in trials without any objective evidence for either choice. After the modulation by signed evidence, the CPP represented the absolute strength of perceived evidence. Notably, this late modulation exhibited all features of statistical decision confidence. Finally, the CPP was also correlated with previously identified choice-selective premotor beta band amplitudes. Together, our data suggest that the CPP first indexes choice-relevant (signed) evidence, and later a measure of confidence.

Significance statement

How is decisional evidence represented by neural signals? Recent studies suggested that a well-known EEG signature might actually index this long sought signal. In particular, the P300 wave – now often termed centro-parietal positivty (CPP) – was found to track the evolving evidence for various perceptual decisions that required temporal accumulation of evidence. Here, we show that the CPP also indexes instantaneous evidence driving decisions based on quantitative comparisons. Additionally, we revealed that the CPP conveys more information than previously assumed. That is, the CPP first indexed the signed quantity on which choices were based, and then reflected decision confidence. Hence, our data support the idea of the CPP as a decision signal, however, demand for refinements in its interpretation.

Introduction

Recent studies have suggested a centro-parietal positivity (CPP) in the EEG signal (arguably identical to the classic P300 component) as a modality-independent proxy of accumulated evidence in perceptual decision making tasks (e.g., Kelly & O'Connell, 2015; Philiastides et al., 2014). In particular, when classifying a noisy sensory stimulus interval into one of two categories, the CPP increased faster and peaked earlier the weaker the interfering noise was, i.e., the clearer the presented evidence (e.g., random dot motion (RDM) discrimination: Kelly & O'Connell, 2013; face-vs-car discrimination: Philiastides et al., 2014). Moreover, the CPP reached a fixed threshold at the time of the decision report, suggesting a threshold-crossing for response initiation (e.g., O'Connell et al., 2012; but see Philiastides et al., 2014). Together, these findings capture the hallmarks of popular sequential-sampling models of evidence accumulation (e.g., see Smith and Ratcliff, 2004), and may relate to similar, or even homologue neuronal processes as identified in the parietal cortex of non-human primates (e.g., Roitman and Shadlen, 2002; Gold and Shadlen, 2007; Shadlen and Kiani, 2013).

The link between decisional evidence and the CPP is not limited to decisions that require the accumulation of noisy sensory input over time. In an auditory four-stimulus oddball paradigm, the differences between 'deviant' and 'standard' stimuli (i.e., the evidence for a 'deviant' detection) modulated the CPP in the very same way as it was modulated by the strength of evidence in accumulation-based decisions (Twomey et al., 2015). Notably, the three 'deviant' stimuli in this task were always higher in pitch than the 'standard' stimulus, eliminating the necessity to evaluate the sign of the difference (i.e., higher or lower) between 'deviant' and 'standard'.

In all of the aforementioned EEG studies, a parietal potential tracked the strength of evidence during perceptual decision making, however, without indicating for which choice alternative (i.e., unsigned evidence; e.g., Kelly and O'Connell, 2013; Philiastides et al., 2014). In the RDM task for instance, only

77 the proportion of coherently moving dots modulated the CPP, without differentiating between the
78 directions in which the dots moved (Kelly and O'Connell, 2013). Here, we examined whether the CPP
79 might also index the choice alternative, in addition to the amount of evidence, if we apply a
80 sequential comparison task. In particular, does the CPP indicate the decision-relevant signed evidence
81 for choices that involve a quantitative comparison? We used a classic vibrotactile two-alternative
82 forced choice (2-AFC) task, in which participants compare two stimulus frequencies (f1 and f2), and
83 decide whether the second one was higher or lower than the first one (comprehensive review on
84 monkey electrophysiology in Romo and de Lafuente, 2013). In this paradigm, a choice-specific (i.e.,
85 binary) modulation of upper beta band (~20 – 30 Hz) amplitude in premotor cortex, decoupled from
86 the motor response, was recently observed in human EEG recordings (Herding et al., 2016, 2017),
87 replicating previous findings from monkey LFPs (Haegens et al., 2011). A representation of the graded
88 differences between f1 and f2 (i.e., the signed evidence), however, has not yet been identified in the
89 human EEG. For the current study, we pooled EEG data over six experiments, utilizing the same
90 vibrotactile 2-AFC task while varying response modality, response timing, and response mapping (N =
91 116). We estimated subjective evidence and difficulty (i.e., the subjectively perceived signed and
92 absolute difference between f1 and f2, respectively) using a Bayesian inference model of choice
93 behavior. This way, we accounted for known biases in sequential comparisons due to the so-called
94 time-order effect/error (TOE; cf. Fechner, 1861; Woodrow, 1935; Hellström, 1985, 2003). Moreover,
95 the behavioral model allowed us to derive a measure of confidence grounded in statistical decision
96 theory (i.e., statistical decision confidence). Using the behavioral model, we found that the CPP was
97 first modulated by the subjectively perceived signed difference, and later by its absolute value (i.e.,
98 the absolute strength of evidence).

Materials and Methods

Experimental Design

Participants: A total of 129 datasets were obtained from healthy, right-handed volunteers (21 – 40 years; 76 females) who participated in six different variants of the experiment. Most participants were students from the Freie Universität Berlin, and some participated in more than one variant of the experiment. All studies were approved by the local ethics committee at the Freie Universität Berlin, and participants gave written informed consent before an experiment started. Thirteen datasets were excluded due to chance-level behavioral performance (<55% correct answers) and/or excessive EEG artifacts, leaving 116 datasets for further analyses.

Stimuli and behavioral task: In all six variants of the experiment, stimuli and comparison task were identical. Only the response modality and response timing varied across experiments (Figure 1). Supra-threshold vibrotactile stimuli with constant peak amplitude were applied to the left index finger using a piezoelectric Braille stimulator (QuaeroSys Medical Devices, Schotten, Germany). The stimuli consisted of amplitude-modulated sinusoids with a fixed carrier frequency of 133 Hz (n.b., 137 Hz in Experiment 2). Amplitude-modulation of this carrier signal with frequencies between 12 – 32 Hz was used to create the sensation of tactile 'flutter' (see Talbot et al., 1968; Romo and Salinas, 2003), while limiting the spectrum of the physical driving signal to frequencies above 100 Hz (e.g., Tobimatsu et al., 1999). Thus, the risk of physical artifacts in the EEG analysis range of interest (<100 Hz) was minimized. The sound of the stimulator was masked by white noise of ~80 dB that was played throughout the experiment (e.g., Spitzer et al., 2010; Spitzer and Blankenburg, 2011). Participants were comfortably seated ~60 cm in front of a TFT monitor. A fixation cross was displayed at the

center of the screen to minimize eye movements. On each trial, two flutter stimuli were successively presented for 250 ms each (with frequencies f1 and f2), interleaved by a retention interval of 1000 ms (see Figure 1). The frequencies of the first stimulus (f1) were randomly drawn from 16, 20, 24 or 28 Hz, whereas f2 differed from f1 by +/- 2 or 4 Hz. In four variants of the experiment (Experiments 3 - 6), f2 was identical to f1 in 25% of the trials, without participants knowing. Participants were instructed to always decide whether f2 > f1 or f2 < f1.

In Experiments 1 and 2, participants indicated choices immediately after presentation of the second stimulus either by pressing one of two buttons with the right index or middle finger (Experiment 1), or by making a saccade to one of two target dots (Experiment 2). The target dots (diameter of ~0.5° visual angle) appeared on the left and on the right side of the screen (~12° visual angle off-center). Importantly, the response assignment of the two buttons and of the two saccade directions was reversed for half of the participants. This way, the mapping of choices onto specific motor responses (which might have been associated with specific motor preparatory signals) was fully counterbalanced across participants (see also Herding et al., 2016, 2017). In Experiments 3 and 4, participants reported choices analogously to Experiments 1 and 2, however, only after a delay of 2500 ms. In Experiments 5 and 6, an additional mapping of choices onto a color-code (blue vs. yellow) was required to report decisions after the delay. In the experiments with delayed responses (Experiments 3 – 6), 2000 ms after the presentation of f2, a blue and a yellow target dot (diameter of ~1° visual angle) appeared on the left and on the right side of the screen (fully counterbalanced across trials; ~12° visual angle off-center). In Experiments 3 and 4, the colors of the dots were irrelevant, and participants selected targets based on a fixed association between direction and choices (counterbalanced across participants). In Experiments 5 and 6, each color was associated with one of the two choice options (counterbalanced across participants). Participants selected a target based on its location

(Experiments 3 and 4) or color (Experiments 5 and 6) after another 500 ms either by pressing the left-arrow or right-arrow button with the right index or middle finger (Experiments 3 and 5), or by making a saccade onto the target (Experiments 4 and 6). See Figure 1 for a graphical summary of the experimental designs.

In Experiments 1 and 2, participants received performance feedback after each trial, and completed seven blocks of 160 f1-vs-f2 comparisons (each block lasted ~15 minutes including eye-tracker calibration) for a total of 1120 trials. In Experiments 3 – 6, feedback based on the performance for trials with f1 ≠ f2 was provided after each block, and participants completed eight blocks of 128 frequency comparisons (each block lasted ~12 minutes including eye-tracker calibration) for a total of 1024 trials. Before each experiment, participants performed ~50 practice trials.

Note that the influence of the different response conditions was not subject to the current study. Oscillatory signatures in the EEG signal that are related to these response manipulations have been reported elsewhere (Experiment1: Herding et al., 2016; Experiment 2: Herding et al., 2017), or the according manuscripts are in preparation (Experiment 3 – 6).

Eye-tracking: In Experiment 2, a Tobii T60 eye-tracker (Tobii Technology, Danderyd, Sweden) was used to record eye movements of participants during each trial (binocular sampling at 60 Hz). The T60 is integrated into a 17'' TFT monitor, and is able to track participants that are comfortably seated in front of the monitor (i.e., no chin rest required). In Experiments 4 and 6, eye movements were recorded (monocular sampling at 500 Hz) using an EyeLink 1000 Desktop Mount with a chin rest (SR Research, Ottawa, Canada). Online evaluation of the participants' gaze directions was implemented with custom code using the Tobii toolbox and psychtoolbox 3 for MATLAB (Brainard, 1997; Cornelissen et al., 2002). Thus, we were able to monitor that participants kept the gaze on the central

fixation cross during each trial (with tolerance of ~3° visual angle), and displayed a warning message if this was not the case ("Please keep fixation throughout the trial"). Additionally, we read out participants' choices (200 ms fixation on target dot with tolerance of ~3° visual angle) and provided performance feedback online, either after each trial (experiment 2) or after each block (experiments 4 and 6). To maintain a high tracking accuracy, the eye-tracker was calibrated before the beginning of each block using a standard 5-dot (Tobii T60) or 9-dot (EyeLink 1000) calibration procedure.

Statistical Analysis

Behavioral model of choices and confidence: In order to explain the observed choice pattern, we fitted a Bayesian inference model to individual behavioral data, and thereby, estimated subjectively perceived frequency differences (SPFDs; Figure 2A, for details see Herding et al., 2016; see also Ashourian and Loewenstein, 2011; Sanchez, 2014). In brief, the model targets to account for a known bias in sequential comparisons (cf. Hellström, 1985, 2003). That is, participants tend to compare f2 not only with the physical value of f1, but also with the average frequency of all presented stimuli (e.g., Preuschhof et al., 2010; Ashourian and Loewenstein, 2011; Karim et al., 2012; see time-order effect for core principle: e.g., Fechner, 1820; Woodrow, 1935, Hellström, 1985). In other words, the quantity that drives choices in the given task is best described by the difference between f2 and a representation of f1 that deviates from its physical value toward the mean frequency of the stimulus set. In our model, we introduce this shifted quantity – which we will call f1' – as a weighted average of the mean of all stimulus frequencies and the physical value of f1 – implemented in terms of Bayesian inference. In particular, f1' is the expected value of the Gaussian posterior distribution of f1, assuming a Gaussian prior centered on the frequencies of the stimulus set (cf. Figure 2A). The model was fitted to the choices of individual participants by optimizing three free parameters (i.e., variance of stimulus

likelihood σ^2_{stim}, prior variance σ^2_{prior}, and a decision criterion *c*) using variational Bayes as implemented in the VBA toolbox (Daunizeau et al., 2014). In order to assess the model's goodness-of-fit, we computed Bayes Factors (BFs) to compare each model fit with a "null" model in which decisions were based on the physical stimulus differences (i.e., f2 – f1). Notably, the model of SPFDs as well as the "null" model followed Weber-Fechner's law and implemented the representation of frequency values on a logarithmic scale (cf. Herding et al., 2016).

Based on the individual model fits, we quantified the SPFD for each stimulus pair by the difference f2 – f1', yielding 16 SPFD values for Experiments 1 and 2, and 20 SPFD values for Experiments 3 – 6. At the same time, the difference distribution between the likelihood of f2 and the posterior of f1 (centered on f1') additionally allowed us to compute a measure of confidence based on statistical decision theory (e.g., Sanders et al., 2015, Hangya et al., 2016; Figure 2B). The difference distribution describes the distribution of percepts that are associated with a given stimulus pair, i.e., with the SPFD between both stimuli. According to statistical decision theory (or signal detection theory), a single percept can be conceived as a sample *d* from this distribution, and a choice based on this very percept depends on where the sample is located with respect to a decision criterion *c* (i.e., choose f2 > f1 if $d > c$). The distance between the sample and the criterion (i.e., $|d - c|$) can be transformed into the probability of a correct response given the percept *d*, which in turn is a measure for confidence (Lak et al., 2014; Urai et al., 2017; Figure 2B). For each participant, we estimated average confidence based on this approach for SPFDs on the interval [-0.4, 0.4]. For each SPFD on this interval, we drew 100,000 samples from the individual difference distributions (i.e., based on the estimated parameters), and computed the associated confidence for each sample. Confidence values were then averaged separately for correct and incorrect trials. Since results were roughly symmetric across zero, the average confidence was grouped according to absolute values of SPFDs (e.g., -0.2 and 0.2), and

214 respective mean values were computed. The illustration in Figure 2B was obtained by simulating data
215 from an unbiased observer (c=0) with $\sigma^2_{stim} = 0.05$ and $\sigma^2_{prior} = 0.347$.
216
217 **EEG recording and analysis:** In all experiments, EEG (ActiveTwo; BioSemi) was recorded at 2048 Hz
218 (offline down-sampled to 512 Hz) from 64 electrodes positioned in an elastic cap according to the
219 extended 10-20 system. Individual electrode locations for each participant were obtained prior to the
220 experiments using a stereotactic electrode-positioning system (Zebris Medical GmbH, Isny, Germany).
221 Additional electrodes were used to register the horizontal and vertical electrooculogram (hEOG and
222 vEOG). For preprocessing, EEG data were high- and low-pass filtered using a non-causal FIR filter (with
223 cut-off frequencies of 0.1 and 30 Hz, respectively), and re-referenced to a common average montage.
224 Eye blink artifacts in the EEG data were corrected using adaptive spatial filtering based on individual
225 calibration data informed by the vEOG signal (see Ille et al., 2002). For experiment 2, in which
226 participants gave immediate responses by saccades, we used the same approach informed by the
227 hEOG signal to remove artifacts of horizontal saccades from the EEG signal. The artifact-free EEG data
228 were segmented into epochs from -2250 to 2000 ms relative to the presentation time of the second
229 stimulus in order to examine evoked EEG responses after the second stimulus as well as to compute
230 control analyses after the first stimulus. Noisy trials were identified by careful visual inspection, and
231 were excluded from further analysis (14.8 % of trials on average). The remaining single-trial data were
232 baseline-corrected relative to the 100 ms preceding stimulus onset. All analyses were done in
233 MATLAB (The MathWorks) using custom code, functions of the SPM12 toolbox (Wellcome
234 Department of Cognitive Neurology, London; www.fil.ion.ucl.ac.uk/spm), and the FieldTrip toolbox for
235 EEG/MEG data (Radboud University Nijmegen, Donders Institute; fieldtrip.fcdonders.nl).
236

Multiple regression and group-level analysis: For each participant, we implemented a multiple regression analysis of the preprocessed single-trial EEG data. At each time point, we regressed the EEG data onto the SPFDs (i.e., f2 – f1') and their absolute values (i.e., |f2 – f1'|) over trials, separately for correct and incorrect choices. The resulting regression coefficients quantified how strongly the trial-specific values of the regressors (i.e., f2 – f1' and |f2 – f1'|) were related to trial-by-trial variability in the EEG data. To identify time periods and channels for which this relation was consistently different from zero across participants, we used cluster-based permutation testing (Maris and Oostenveld, 2007). We compared the summary statistics of the observed data (one-sample t-test of regression coefficients across all data sets at each time point) with a distribution of summary statistics obtained from 500 randomly sign-flipped permutations. A cluster was defined as a group of adjacent time points that all exceeded a cluster-defining threshold of $p_{threshold} < 0.005$ (uncorrected). Clusters that exceeded a cluster-based family-wise error (FWE) corrected threshold of $p_{FWE} < 0.05$ (corrected for time and channels) were considered to be statistically significant.

Event-related potentials (ERPs): To visualize the effects identified in the statistical analysis as classic ERPs, we binned the individual 16 values of SPFDs (i.e., differences of log-transformed stimulus frequencies; one per stimulus pair with f1 ≠ f2) into six discrete levels across participants (i.e., [< -0.18]; [-0.18 to -0.09]; [-0.09 to 0]; [0 to 0.09]; [0.09 to 0.17]; [> 0.17]). The grand average ERPs were computed separately for each level. We defined the six levels symmetrically around a SPFD of zero (corresponding to chance-level performance), and in such a way that each participant had at least one stimulus pair per level. Since SPFDs were generally small for trials with identical stimuli (i.e., f1 = f2), we used only four levels for the computation of ERPs in these trials (i.e., [< -0.09]; [-0.09 to 0]; [0 to 0.09]; [> 0.09]).

Source reconstruction: The cortical sources of the observed modulations on the scalp-level were localized using the 3D source reconstruction routines provided by SPM12 (Friston et al., 2006). Based on the individually recorded electrode positions for each participant, a forward model was constructed using an 8196-point cortical mesh of distributed dipoles perpendicular to the cortical surface of a template brain (cf. Friston et al., 2006). The lead field of the forward model was computed using the three-shell Boundary Elements Method (BEM) EEG head model available in SPM12. Multiple sparse priors (Friston et al., 2008) under group constraints (Litvak and Friston, 2008) were applied to invert the forward model. For model inversion, we used a representative time interval (i.e., -200 to 1500 ms relative to f2) of ERPs that were computed separately for each level of SPFDs (see ERPs above) drawing on all trials including those with identical stimuli (i.e., f1 = f2). The results of the inversion were summarized in six corresponding 3D images (i.e., one for each level of SPFDs) that reflected source activity averaged over a time window of interest. In particular, summary images were computed for an early (250 to 500 ms) and a late (500 to 800 ms) time window capturing the two effects observed at the scalp level (i.e., modulation by signed evidence and strength of evidence, respectively). For each time window, contrasting the 3D images within each participant analogously to the sensor space analysis served as an estimate for subject-specific source locations of both effects. The results of conventional group-level statistical analyses of these source images (see Litvak et al., 2011) are displayed at a significance level of $p < 0.001$ (uncorrected). Anatomical references for source estimates were established on the basis of the SPM anatomy toolbox (Eickhoff et al., 2005) where possible.

Single-trial correlation of CPP and upper beta band amplitude: In order to explore the relationship

between the CPP and premotor choice-specific upper beta band amplitude (cf. Herding et al., 2016, 2017), single-trial correlations between these two measures were computed. Notably, only for experiments 1 and 2; only these experiments required immediate responses, and hence, a direct transformation of evidence into a motor response. For each participant, the magnitude of the CPP in every trial was specified by a single value for the early and for the late effect, respectively. In particular, the single-trial EEG signal from electrode CPz was averaged over a brief time period during which a modulation of the CPP by the signed values of SPFDs (i.e., 250 – 500 ms) or by its absolute values (i.e., 500 – 800 ms) was observed. Additionally, a measure of the upper beta band amplitude in electrodes over premotor areas was computed for each trial. Using response-locked time-frequency representations of the single-trial data (reported in Herding et al., 2016, 2017), average beta band amplitude was computed over a time-frequency cluster that exhibited a significant modulation by participants' choices (i.e., electrodes FC2, FCz, and C2; 20 – 30 Hz; -750 to -350 ms from responses for experiment 1, cf. Herding et al., 2016; electrodes FC2 and FC4, 24 – 32 Hz, -750 to -450 ms from responses for experiment 2, cf. Herding et al., 2017). We used correct and incorrect trials to compute the single-trial correlations for each participant. The correlation coefficients from both experiments were pooled (N = 45), and a one-sample t-test was computed to assess whether a consistent correlation was present across participants.

Results

Behavioral Results

Pooled over all experiments, participants made on average 72.5% correct choices. To test whether performance varied across the six experiments and across the different frequency differences, we performed a two-way repeated measures ANOVA on proportions of correct responses (PCRs) with between-subject factor 'Experiment' (experiments 1 – 6), and within-subject factor 'Frequency Difference' (-4, -2, 2, and 4 Hz stimulus difference). We used logit-transformed PCRs to account for non-normally distributed residuals. The analysis revealed no significant performance differences between experiments (main effect 'Experiment', $p = 0.125$; interaction 'Experiment' x 'Frequency Difference', $p = 0.182$). Within each experiment, PCRs varied significantly with the factor 'Frequency Difference' ($p < 0.001$). For further insights into this effect, we computed post-hoc paired t-tests for each study separately to evaluate the influence of difficulty (+/- 4 Hz vs. +/- 2 Hz differences), and sign of the frequency differences (positive vs. negative differences). As expected, a larger proportion of trials were judged correctly when the (physical) f2 − f1 frequency difference was ±4 Hz compared with trials where the difference was only ±2 Hz in all experiments (all $p < 0.001$; paired t-test; see difficulty effect, Table 1). In experiments 1 and 2, we additionally observed more correct responses for positive compared with negative frequency differences ($p = 0.03$, and $p = 0.002$; paired t-test; see sign effect, Table 1), which indicated an overall response bias toward "f2 > f1" choices only in these experiments that required immediate responses (mean criterion shifts: 0.116 and 0.126 with $p = 0.029$ and $p = 0.002$; one-sample t test).

Bayesian inference model yields good approximations for signed subjective evidence and experienced difficulty

As known from many 2-AFC studies that require the comparison of two sequentially presented stimuli, participants often show a particular choice pattern (e.g., Preuschhof et al., 2010; Ashourian et al., 2011; Karim et al., 2012; see squares in Figure 3A and B). For trials with f2 > f1 (i.e., f2 - f1 = 2 Hz or 4 Hz), participants performed better with increasing f1, whereas for trials with f2 < f1 (i.e., f2 - f1 = -2 Hz or -4 Hz), the opposite is seen (Figure 3A). In other words, the probability to choose f1 decreases with increasing f1 for all frequency differences (interestingly also for those trials with no frequency difference; Figure 3B). Our previously proposed Bayesian inference model (Herding et al., 2016) can account for this choice pattern (lines in Figures 3A and B). Moreover, with the individually estimated SPFDs (i.e., f2 – f1') we obtained a subjective, fine-grained measure that reliably predicted participants' choices. Hence, we used the signed SPFDs as a proxy for signed subjective evidence towards a decision in this task (Figure 3C). Computing BFs to formally assess the quality of our Bayesian model provided positive evidence (BF > 3) in favor of the SPFD model for 91.4 % of the participants (106/116), and strong evidence (BF > 20) for 87.9 % (102/116; Figure 3E). Accordingly, the absolute values of the SPFDs (i.e., |f2 - f1'|) correlated significantly more with participants PCRs than the absolute values of the physical differences (i.e., |f2 – f1|), rendering SPFDs also an improved predictor of subjectively experienced difficulty (paired t-test, $p < 0.001$; Figure 3D).

CPP first reflects signed subjective evidence and then absolute strength of evidence

We computed a multiple regression analysis on the epoched EEG data using the signed SPFDs (i.e., f2 – f1') as well as their absolute values (i.e., |f2 – f1'|) as single-trial regressors. This way, we could independently assess correlations of scalp potentials with signed subjective evidence and with the absolute strength of evidence. For a first analysis, we only used trials in which objective sensory evidence was present (i.e., physically different stimuli with f2 ≠ f1). For correct decisions, we found

346 that a centro-parietal positive ERP after the second stimulus was positively correlated with the signed
347 subjective evidence early on (168 – 709 ms, 35 electrodes, strongest in P1, Pz, CPz, CP4, CP2, and P2
348 with $p_{FWE} = 0.002$). Later, however, the same ERP was positively correlated with the absolute strength
349 of the evidence (273 – 953 ms, 33 electrodes, strongest in P1, CPz, Cz, C2, CP2, and P2 with $p_{FWE} =$
350 0.002; scalp topographies in Figure 4). The overall profile of the underlying ERP strongly resembled
351 the classic P300 or CPP (see time courses in Figure 4). For incorrect decisions, the above mentioned
352 modulations by subjective evidence vanished, however, the overall profile of the ERP remained
353 unchanged conforming to the shape of a typical P300 or CPP (not shown). Directly comparing the
354 modulations between correct and incorrect decisions revealed significant differences (i.e., interaction
355 effects) in both the modulation by signed subjective evidence (326 – 367 ms and 418 – 455 ms,
356 electrodes P1, P3, P5, PO7, and PO3 with $p_{FWE} = 0.022$ and $p_{FWE} = 0.032$) and in the modulation by
357 absolute strength of evidence (723 – 750 ms, electrodes CP5, P7, PO7, O1, Iz, and O2 with $p_{FWE} =$
358 0.028). In sum, the CPP reflected the signed and absolute subjective evidence only for correct trials –
359 even significantly more than for incorrect trials. Hence, a faithful representation of the subjective
360 evidence is tightly linked to correct decisions, implying the behavioral relevance of the CPP.
361 The significant positive correlations in centro-parietal electrodes were accompanied by significant
362 negative correlations in bilateral fronto-temporal electrodes for all described effects, hinting at the
363 rough orientation of underlying dipole generators (see scalp topographies in Figure 4). In general
364 agreement with the scalp topographies, the reconstructed source locations suggest that the
365 modulation by signed subjective evidence originates from left superior parietal lobule (SPL; Brodman
366 area 7A; MNI peak coordinates: -24, -62, 54) in the posterior parietal cortex (PPC; Figure 5). On a
367 considerably lower significance level ($p < 0.05$; uncorrected), also the right SPL is implicated as a likely
368 source. The modulation by the absolute strength of subjective evidence additionally suggested

probable sources in bilateral inferior frontal gyrus (IFG, Brodman area 44/45, MNI peak coordinates: -54/+48, 14, 12; Figure 5).

We challenged our findings in a series of control analyses to exclude confounding factors as the driving forces behind the observed effects. First and foremost, we examined whether the observed modulations of the CPP were driven by the outer most stimulus pairs alone. That is, in the given stimulus set, some choices could have been based on exceptionally high or low f2 alone, possibly associated with qualitatively distinct percepts. We excluded these outer most stimuli from the stimulus set and repeated the multiple regression analysis on the remaining subset of data (inset Figure 6). In particular, the subset only included trials in which f2 could lead to either choice (i.e., f2 alone did not predict the correct decision in these trials), leading to markedly reduced trial numbers for the analysis (i.e., 400 and 288 trials per subject were dismissed for experiments with immediate and delayed responses, respectively). Nevertheless, the results were qualitatively identical to those obtained when using the full set (Figure 6). After the presentation of f2, the CPP was first modulated by the signed subjective evidence (295 – 578 ms, 24 electrodes, strongest in Pz, CPz, CP1, CP2, P1, and P3 with $p_{FWE} = 0.002$) and then by the absolute strength of evidence for correct decisions (486 – 676 ms, 14 electrodes, strongest in CPz, Pz, POz, CP1, CP2, and P1 with $p_{FWE} = 0.002$), but not for incorrect decisions (no clusters). A significant interaction between correct and incorrect trials was only observed for the late modulation by absolute strength of evidence (602 – 654 ms, electrodes P1, P3, PO7, PO3, POz, and PO4 with $p_{FWE} = 0.026$). With respect to the computation of ERPs, excluding the outer most stimuli, led to fewer trials falling into the most extreme bins of SPFDs (cf. ERPs in Material and Methods). In particular, this concerned large negative and large positive SPFDs (dark blue and dark red in upper panel of Figure 6) with 26 and 78 participants respectively contributing data to the grand average ERPs (i.e., 35 trials per individual ERPs on average). For comparison, all 116 participants

392 contributed individual ERPs (based on 67 trials on average) to the grand average for the remaining
393 levels of SPFDs. Note, however, that the computation of ERPs only served displaying purposes. The
394 statistical analysis was based on single-trials (i.e., not binned into discrete levels of SPFDs), and hence
395 unaffected by any imbalances in trial numbers per discrete levels of SPFDs. Taken together, this
396 analysis ruled out that the outer most stimulus pairs alone accounted for the observed modulations in
397 the EEG signal.
398 In a further control analysis we focused on the observation that for some participants SPFDs were
399 distributed asymmetrically around zero due to an overall response bias. Hence, the corresponding
400 absolute values were not fully independent from the signed SPFDs. We therefore orthogonalized the
401 absolute values with respect to the signed SPFDs before computing the multiple regression once
402 more, and again obtained qualitatively identical results (modulation by signed SPFDs: 264 – 537 ms,
403 29 electrodes, strongest in Pz, CPz, POz, CP2, CP4, and P1 with $p_{FWE} = 0.002$; modulation by absolute
404 values of SPFDs: 279 – 947 ms, 32 electrodes, strongest in Pz, CPz, CP1, CP2, P1, and P3 with $p_{FWE} =$
405 0.002). Next, we explored whether the EEG signal was possibly also affected after the first stimulus by
406 the quantity that had to be kept in working memory (i.e., in analogy to the presumed subjective
407 difference quantity on which the decision is based). That is, we studied whether we could find a
408 parietal potential that was modulated by f1 in a similar way as the CPP was modulated by SPFDs after
409 the second stimulus. We did not find any comparable effect (i.e., no cluster with comparable spatial
410 and temporal configuration). Finally, when examining the data from each experiment (cf. Materials
411 and Methods) separately, we found the same pattern of modulations by subjective evidence as with
412 the pooled data. In all experiments, the CPP was first modulated by the signed subjective evidence,
413 and then by the strength of subjective evidence for correct (all effects with $p_{FWE} < 0.014$, except for
414 Experiment 3, with $p_{FWE} = 0.178$ and $p_{FWE} = 0.248$ for the early and late modulation, respectively), but

not for incorrect decisions (no clusters in parietal electrodes, except for Experiment 2 showing a negative modulation by the absolute strength of evidence with $p_{FWE} = 0.018$).

Signed subjective evidence modulates CPP even during judgements of physically identical stimulus pairs

We repeated the multiple regression analysis with signed SPFDs and their absolute values as regressors, this time, however, only using trials without any physical evidence for a decision. In particular, we only used trials with two identical stimuli (i.e., f1 = f2: 12 Hz vs 12 Hz, 16 Hz vs 16 Hz, 20 Hz vs 20 Hz, 24 Hz vs 24 Hz). Although the physical difference f2 – f1 is always zero for these trials, crucially, the individually estimated SPFDs yielded non-zero values for each stimulus pair. This is a direct consequence of the known biases in choice behavior that are typically observed in sequential comparison tasks (i.e., comparing f2 with mean-biased f1' instead of the physical value of f1). Based on the non-zero SPFDs, we were hence able to divide trials according to decisions that were in line with the estimated SPFDs (i.e., SPFD < 0: f1 chosen, and SPFD > 0: f2 chosen), and those that were not (i.e., SPFD < 0: f2 chosen, and SPFD > 0: f1 chosen). This way, we could divide trials into "consistent" and "inconsistent" with respect to the model outcome. Remarkably, for "consistent" decisions, we found the same positive correlation of the CPP with signed SPFDs as for correct trials in which physical evidence for a decision was actually present (236 – 246 ms, electrodes PO3, POz, Pz, CP6, CP4, CP2, P2, P4, P6, P8, and PO8, $p_{cluster} = 0.016$, FWE corrected, Figure 7). For decisions identified as "inconsistent", no such correlation was found. A comparison between "consistent" and "inconsistent" trials revealed that the modulation of the CPP by signed subjective evidence was significantly different (i.e., an interaction effect) between both sets of trials (322 – 338 ms, electrodes P3, P5, PO3, Oz, POz, Pz, P2, P8, PO8, and PO4, $p_{cluster} = 0.044$, FWE corrected). Notably, the separation of trials

into these two sets was solely based on the modeled SPFDs, and yet, we were able to observe a significant difference in the EEG signal. On the other hand, the absolute values of the SPFDs did not modulate the CPP in trials with identical stimuli. Only a more anterior cluster became statistically significant for "consistent" decisions (268 – 279 ms, electrodes F1, F3, Fz, F2, F4, FC2, and FCz, $p_{cluster}$ = 0.03, FWE corrected), however, not in the interaction between "consistent" and "inconsistent" trials.

Late modulation by absolute strength of evidence conforms with statistical decision confidence

That the CPP was correlated with the absolute values of SPFDs faintly suggested that this late modulation might index the level of confidence in a decision. However, in order to make a more convincing point, we sought further evidence in support of this idea. In particular, we checked whether the late CPP conforms with the predictions of statistical decision confidence (cf. Sanders et al., 2016, Hangya et al., 2016). In this framework, confidence exhibits four key characteristics that can be tested without the need for explicit confidence ratings, simply based on statistical decision theory (or signal detection theory): (1) confidence is positively correlated with PCRs; (2) confidence increases with evidence strength for correct choices, but decreases for incorrect choices (see Figure 2B for intuition); (3) when (almost) no evidence is available (i.e., in very hard trials), confidence exhibits the same intermediate level for correct and incorrect choices; (4) for the same strength of evidence, high-confidence trials still yield higher PCRs than low-confidence trials.

Concerning (1), as reported in our main results, we found that the late CPP was positively correlated with the absolute values of SPFDs, which in turn were highly correlated with PCRs (Figure 3D). For (2) and (3) we extracted single-trial amplitudes of the CPP (mean amplitude between 500 and 800 ms after f2 in electrode CPz), and grouped these amplitudes according to the discrete levels of absolute SPFDs separately for correct and incorrect trials (i.e., three levels for trials with f2 ≠ f1: [0 to 0.09];

[0.09 to 0.17]; [> 0.17]; two levels for trials with f2 = f1: [0 to 0.09]; [> 0.09]). As predicted by statistical decision confidence, we found that the CPP amplitude increased with evidence strength for correct trials, and (initially) decreased for incorrect trials, in remarkable alignment with the average confidence computed from individual model fits (Figure 8). Moreover, for the most difficult trials (i.e., least evidence strength), the CPP amplitude was at the same intermediate level for correct and incorrect trials (Figure 8B). Notably, predictions (2) and (3) were also reflected in CPP amplitudes when considering only trials with f2 = f1 (Figure 8B, right panel). Lastly, we did a median split of our data based on CPP amplitudes to simulate a division into high- and low-confidence trials (4). We compared PCRs between high- and low-amplitude trials for each of the three levels of evidence strength (i.e., [0 to 0.09]; [0.09 to 0.17]; [> 0.17]), and found that for the intermediate and high level of evidence strength, PCRs were significantly higher in trials with a high CPP amplitude as compared to trials with a low CPP amplitude (paired t-test, both $p < 0.001$). Taken together, the late CPP mirrors all aspects of a measure of confidence as defined by statistical decision theory.

CPP correlates with upper beta band amplitude over effector-specific premotor areas

Finally, we explored whether the observed modulation of the CPP was related to previously identified choice-specific modulations of upper beta band amplitude over premotor areas in the same data (i.e., experiments 1 and 2 as reported in Herding et al., 2016, 2017). That is, beta band power was shown to be higher for “f2 > f1” choices as compared to “f2 < f1” choices, regardless of whether the choice was correct or incorrect. Indeed, we found a positive correlation between the amplitude of the CPP during the early modulation by signed SPFDs and the beta band amplitude (one-sample t-test across single-trial correlations of participants, mean rho = 0.03, $p < 0.001$). Notably, we obtained the same positive correlation when considering data from both experiments separately (experiment 1: mean

rho = 0.03, p = 0.016; experiment 2: mean rho = 0.02, p = 0.002). The late CPP (i.e., during the modulation by absolute SPFDs) was also positively correlated with single-trial beta band amplitudes (mean rho = 0.02, p = 0.006). However, when considering both experiments separately, only data from experiment 1 showed a significant positive correlation (mean rho = 0.02, p = 0.02), but not data from experiment 2 (mean rho = 0.01, p = 0.15). Importantly, average response times in experiments 1 and 2 (~ 862 ms and ~ 603 ms) render a causal relation between the late CPP (i.e., 500 – 800 ms after f2) and choice-specific upper beta band amplitude unlikely. For the early CPP (i.e., 250 – 500 ms after f2), on the other hand, a causal role in choice selection seems chronologically possible, nevertheless, remains to be thoroughly investigated.

Discussion

In the current study, we investigated human ERP signals during the comparison of two sequentially presented vibrotactile stimuli (with frequencies f1 and f2). We pooled a sizeable amount of data (N = 116) over six different variants of this task, varying in response modality, response timing, and response mapping, whereas stimuli and comparison task remained unchanged. Despite the variations, we consistently found that the CPP after the second stimulus was first modulated by the signed subjective evidence in favor of the ensuing decision (i.e., signed SPFDs), and later by the absolute strength of evidence (i.e., absolute values of SPFDs). Notably, both modulations were only observed for correct decisions, linking a successful discrimination of f1 and f2 with a faithful representation of the perceived stimulus difference (i.e., SPFDs) in the CPP. Even in the absence of any objective differences between f1 and f2 (i.e., f1 = f2), the CPP indexed the signed values of SPFDs, but not its absolute values. This observation implies that the CPP indexes endogenous evidence for subsequent decisions (see CPP in the absence of stimuli in O'Connell et al., 2012). Accordingly, we found a correlation between the early CPP and choice-selective upper beta band amplitudes in effector-specific premotor areas. The late modulation by the absolute values of SPFDs on the other hand seems to index the confidence in a decision. The putative neuronal sources of both early and late CPP modulation were located in SPL (Brodman area 7A; primarily in the left hemisphere), whereas the late modulation by absolute differences additionally exhibited likely sources in bilateral IFG (Brodman area 44/45).

Several studies of the broadband human EEG signal have shown that the CPP reflects the accumulated evidence for perceptual decisions which require the integration of noisy sensory input over time for immediate and delayed responses (e.g., O'Connoll et al., 2012; Kelly and O'Connell, 2013; Philiastides et al., 2014, Twomey et al., 2016). These findings might be directly linked to seminal work on visual

perceptual decision making in monkeys that implicated the PPC as a key site for evidence accumulation (see Shadlen and Kiani, 2013). A recent study showed that also in other tasks, i.e., in a classic oddball paradigm, the CPP, or rather the P300, was modulated by the evidence in favor of a successful 'deviant' detection (i.e., a modulation by the difference between 'deviant' and 'standard' stimulus; Twomey et al., 2015). Our findings are in general agreement with these reports of the CPP, and in particular, extend the latter observation beyond the limits of a mere detection task. Moreover, we were able to trace the modulations of the CPP by subjective evidence back to a source in PPC, consistent with the results from monkey electrophysiology.

On closer inspection, our results are, however, crucially different from previous reports of the CPP in perceptual decision making. Until now, all studies that associated the CPP with decisional evidence, found a modulation of the CPP by the evidence *within* a single choice category, but never a modulation by evidence *across* choice alternatives (e.g., O'Connell et al., 2012; Kelly and O'Connell, 2013; Philiastides et al., 2014; Twomey et al., 2015; Twomey et al., 2016). That is, the CPP was shown to track the strength of available evidence, albeit concealing for which choice alternative. In particular, Kelly and O'Connell (2013) showed that only the proportion of coherent motion, independent of direction (i.e., leftward or rightward), modulated the CPP in a RDM task (see also Twomey et al., 2016). Moreover, Philiastides et al. (2014) were able to discriminate different levels of presented evidence based on a parietal potential (i.e., likely the CPP), no matter whether an image of a face or a car was shown. However, a classification between faces and cars was not possible. In the current study, we report for the first time that the CPP was modulated by both the amount of evidence and the choice alternative at the same time (i.e., by signed evidence in form of SPFDs). Only later, the absolute strength of evidence alone (i.e., absolute values of SPFDs; independent of the specific choice category) was reflected by the CPP as known from previous work. We propose that the

early modulation by the signed values of SPFDs indexes the evidence on which a decision was based. The late modulation by the absolute values of SPFDs, on the other hand, might refer to the confidence in the decision.

Interpreting the late CPP modulation by absolute values of SPFDs as confidence is based on the observation that the late CPP complies in all respects with the definition of statistical decision confidence (see Sanders et al., 2016, Hangya et al., 2016). Importantly, according to the classic definition of confidence, statistical decision confidence refers to the probability that a choice is correct (given the evidence), and was recently shown to align with human confidence judgements (Sanders et al., 2016). That is, this framework allows to infer confidence levels even in the absence of explicit confidence ratings. That the CPP, or rather the P300, might indicate confidence has been suggested for a long time (e.g., Squires et al., 1973; Sutton et al., 1982; Curran, 2004), and also more recent work reiterated this idea. Gherman and Philiastides (2015), for instance, reported a higher amplitude of the CPP for choices that were made with high certainty as compared to choices with low certainty (see also Philiastides et al., 2014). Moreover, although the CPP has been typically reported to reach a fixed level at the time of the response report (see Kelly and O'Connell, 2015, but Philiastides et al., 2014), when considering false alarm trials, a clearly lower amplitude was observed, possibly indexing lower confidence in those trials (Figure 2C in O'Connell et al., 2012). The lack of differences in CPP amplitudes at response time for the remaining results might be related to the task demands per se. By applying continuous task designs (e.g., O'Connell et al., 2012, Kelly and O'Connell, 2013), decision-unrelated stimulus evoked EEG signals were elegantly avoided, however, an additional level was added to the task, requiring the detection of stimuli. This might have led to a rather constant level of confidence before committing to a decision (see Discussion in Philiastides et al., 2014). The reconstructed sources of the confidence signal in bilateral IFG appear unusual at first

562 glance, however, recent fMRI studies also implicated the IFG in the processing of confidence (Hebart
563 et al., 2016; Sherman et al., 2016).
564 Finally, the present vibrotactile 2-AFC task has been used extensively by Romo and colleagues during
565 electrophysiological recordings from monkeys (reviewed in Romo and deLafuente, 2013). In this
566 research, premotor areas were identified as one of the first sites to show decision-related firing rate
567 patterns that encoded the differences between f1 and f2 (Hernández et al., 2002, 2010; Romo et al.,
568 2004). Furthermore, a choice-specific (i.e., binary) amplitude modulation of large-scale upper beta
569 band oscillations (~20 – 30 Hz) in premotor areas was recently identified in monkey local field
570 potentials (Haegens et al., 2011) as well as in human EEG data (Herding et al., 2016, 2017). With the
571 current results, we provide first evidence for a previously missing EEG signature that indexes the fine-
572 grained subjective evidence in favor of the ensuing choices. Given the stimulus-locked early onset of
573 the CPP modulation by signed evidence, the response-locked character of the beta band modulation,
574 the conceptually reasonable gradient (i.e., choices are based on evidence), and the source locations of
575 both findings (i.e., evidence in parietal cortex and choice in premotor cortex), we presume that the
576 CPP precedes and potentially drives the beta band effect. In fact, using the data from Experiments 1
577 and 2 with immediate responses (i.e., with a direct translation from evidence to choices), we found a
578 positive correlation between single-trial CPP magnitude (during the early modulation by signed
579 evidence) and the level of beta band amplitude (during the choice modulation). This observation
580 indeed hints at a connection between CPP and beta band amplitude, and deserves a more thorough
581 investigation in future research.
582 To conclude, our data corroborate the notion of the CPP tracking evidence in perceptual decision
583 making (see Kelly and O'Connell, 2015). Using a vibrotactile 2-AFC comparison task, we could show,
584 however, that the interpretation of this signal is not as simple as previously assumed. Our results

revealed that the CPP first indexes signed subjective evidence, and only later the absolute strength of evidence. We propose that the early modulation reflects the quantity on which a decision is based, whereas the late modulation might index decision confidence. In the context of the vibrotactile 2-AFC task, our findings suggest that the fine-grained signed evidence that is reflected early in the CPP might index the input to more categorical choice representations, e.g., in effector-specific premotor areas (see Haegens et al., 2011; Herding et al., 2016, 2017).

References

Ashourian P, Loewenstein Y (2011) Bayesian inference underlies the contraction bias in delayed comparison tasks. PLoS One 6.

Baranski J V, Petrusic WM (1998) Probing the locus of confidence judgments: experiments on the time to determine confidence. J Exp Psychol Hum Percept Perform 24:929–945.

Brainard DH (1997) The Psychophysics Toolbox. Spat Vis 10:433–436.

Cornelissen FW, Peters EM, Palmer J (2002) The Eyelink Toolbox: Eye tracking with MATLAB and the Psychophysics Toolbox. Behav Res Methods, Instruments, Comput 34:613–617.

Curran T (2004) Effects of attention and confidence on the hypothesized ERP correlates of recollection and familiarity. Neuropsychologia 42:1088–1106.

Daunizeau, J., Adam, V., & Rigoux, L. (2014). VBA: A Probabilistic Treatment of Nonlinear Models for Neurobiological and Behavioural Data. *PLoS Computational Biology*, *10*, e1003441.

Eickhoff SB, Stephan KE, Mohlberg H, Grefkes C, Fink GR, Amunts K, Zilles K (2005) A new SPM toolbox for combining probabilistic cytoarchitectonic maps and functional imaging data. Neuroimage 25:1325–1335.

Fechner, G. T. (1860). Elemente der Psychophysik. Leipzig: Breitkopf & Härtel.

Festinger L (1943) Studies in decision: I. Decision-time, relative frequency of judgment, and subjective confidence as related to physical stimulus difference. J Exp Psychol 32:291–306.

Friston K, Harrison L, Daunizeau J, Kiebel S, Phillips C, Trujillo-Barreto N, Henson R, Flandin G, Mattout J (2008) Multiple sparse priors for the M/EEG inverse problem. Neuroimage 39:1104–1120.

Friston K, Henson R, Phillips C, Mattout J (2006) Bayesian estimation of evoked and induced responses. Hum Brain Mapp 27:722–735.

Gherman S, Philiastides MG (2015) Neural representations of confidence emerge from the process of decision formation during perceptual choices. Neuroimage 106:134–143.

Gold JI, Shadlen MN (2007) The neural basis of decision making. Annu Rev Neurosci 30:535–574.

615 Haegens S, Nácher V, Hernández A, Luna R, Jensen O, Romo R (2011) Beta oscillations in the monkey sensorimotor
616 network reflect somatosensory decision making. PNAS 108:10708–10713.

617 Hangya B, Sanders JI, Kepecs A (2016) A mathematical framework for statistical decision confidence. Neural Computation
618 28:9, 1840-1858.

619 Hebart MN, Schriever Y, Donner TH, Haynes JD (2016) The Relationship between Perceptual Decision Variables and
620 Confidence in the Human Brain. Cereb Cortex 26:118–130.

621 Hellström A (2003) Comparison is not just subtraction: effects of time- and space-order on subjective stimulus difference.
622 Percept Psychophys 65:1161–1177.

623 Hellström Å (1985) The time-order error and its relatives: Mirrors of cognitive processes in comparing. Psychol Bull 97:35–
624 61.

625 Herding J, Spitzer B, Blankenburg F (2016) Upper Beta Band Oscillations in Human Premotor Cortex Encode Subjective
626 Choices in a Vibrotactile Comparison Task. J Cogn Neurosci 28:668–679.

627 Herding J, Ludwig S, Blankenburg F (2017) Response-modality-specific encoding of human choices in upper beta-band
628 oscillations during vibrotactile comparisons. Frontiers in Human Neuroscience.

629 Hernández A, Nácher V, Luna R, Zainos A, Lemus L, Alvarez M, Vázquez Y, Camarillo L, Romo R (2010) Decoding a
630 perceptual decision process across cortex. Neuron 66:300–314.

631 Hernández A, Zainos A, Romo R (2002) Temporal evolution of a decision-making process in medial premotor cortex.
632 Neuron 33:959–972.

633 Ille N, Berg P, Scherg M (2002) Artifact correction of the ongoing EEG using spatial filters based on artifact and brain signal
634 topographies. J Clin Neurophysiol 19:113–124.

635 Karim M, Harris J a., Morley JW, Breakspear M (2012) Prior and present evidence: How prior experience interacts with
636 present information in a perceptual decision making task. PLoS One 7.

637 Kelly SP, O'Connell RG (2013) Internal and external influences on the rate of sensory evidence accumulation in the human
638 brain. J Neurosci 33:19434–19441.

639 Kelly SP, O'Connell RG (2015) The neural processes underlying perceptual decision making in humans: Recent progress and
640 future directions. J Physiol 109:27–37.

641 Litvak V, Friston K (2008) Electromagnetic source reconstruction for group studies. Neuroimage 42:1490–1498.

642 Litvak V, Mattout J, Kiebel S, Phillips C, Henson R, Kilner J, Barnes G, Oostenveld R, Daunizeau J, Flandin G, Penny W,
643 Friston K (2011) EEG and MEG data analysis in SPM8. Comput Intell Neurosci 2011:852961.

644 Maris E, Oostenveld R (2007) Nonparametric statistical testing of EEG- and MEG-data. J Neurosci Methods 164:177–190.

645 Mazurek ME, Roitman JD, Ditterich J, Shadlen MN (2003) A Role for Neural Integrators in Perceptual Decision Making.
646 Cereb Cortex 13:1257–1269.

647 O'Connell RG, Dockree PM, Kelly SP (2012) A supramodal accumulation-to-bound signal that determines perceptual
648 decisions in humans. Nat Neurosci 15.

649 Philiastides MG, Heekeren HR, Sajda P (2014) Human Scalp Potentials Reflect a Mixture of Decision-Related Signals during
650 Perceptual Choices. J Neurosci 34:16877–16889.

651 Preuschhof C, Schubert T, Villringer A, Heekeren HR (2010) Prior Information biases stimulus representations during
652 vibrotactile decision making. J Cogn Neurosci 22:875–887.

653 Roitman JD, Shadlen MN (2002) Response of neurons in the lateral intraparietal area during a combined visual
654 discrimination reaction time task. J Neurosci 22:9475–9489.

655 Romo R, de Lafuente V (2013) Conversion of sensory signals into perceptual decisions. Prog Neurobiol 103:41–75.

656 Romo R, Hernández A, Zainos A (2004) Neuronal correlates of a perceptual decision in ventral premotor cortex. Neuron
657 41:165–173.

658 Romo R, Salinas E (2003) Flutter discrimination: neural codes, perception, memory and decision making. Nat Rev Neurosci
659 4:203–218.

660 Sanchez G (2014) Real-time electrophysiology in cognitive neuroscience: towards adaptive paradigms to study perceptual
661 learning and decision making in humans.

662 Sanders JI, Hangya B, Kepecs A (2016) Signatures of a Statistical Computation in the Human Sense of Confidence. Neuron

90: 499-506.

Shadlen MN, Kiani R (2013) Decision making as a window on cognition. Neuron 80:791–806.

Sherman MT, Seth AK, Kanai R (2016) Predictions Shape Confidence in Right Inferior Frontal Gyrus. J Neurosci 36:10323–10336.

Singer T, Critchley HD, Preuschoff K (2009) A common role of insula in feelings, empathy and uncertainty. Trends Cogn Sci 13:334–340.

Smith PL, Ratcliff R (2004) Psychology and neurobiology of simple decisions. Trends Neurosci 27:161–168.

Spitzer B, Blankenburg F (2011) Stimulus-dependent EEG activity reflects internal updating of tactile working memory in humans. PNAS 108:8444–8449.

Spitzer B, Wacker E, Blankenburg F (2010) Oscillatory correlates of vibrotactile frequency processing in human working memory. J Neurosci 30:4496–4502.

Squires KC, Hillyard S a, Lindsay PH (1973) Vertex potentials evoked during auditory signal detection : Relation to decision criteria *. Percept Psychophys 14:265–272.

Sutton S, Rouchkin DS, Munson R, Kietzman ML, Hammer M (1982) Event related potentials in a two-interval forced choice decision task. Percept Psychophys 32:360–374.

Talbot W, Darian-Smith I, Kornhuber H, Mountcastle V (1968) The sense of flutter-vibration: comparison of the human capacity with response patterns of mechanoreceptive afferents from the monkey hand. Neurophysiology 31:301–334.

Tobimatsu S, Zhang YM, Kato M (1999) Steady-state vibration somatosensory evoked potentials: physiological characteristics and tuning function. Clin Neurophysiol 110:1953–1958.

Twomey DM, Kelly SP, O'Connell RG (2016) Abstract and Effector-Selective Decision Signals Exhibit Qualitatively Distinct Dynamics before Delayed Perceptual Reports. J Neurosci 36:7346–7352.

Twomey DM, Murphy PR, Kelly SP, O'Connell RG (2015) The classic P300 encodes a build-to-threshold decision variable. Eur J Neurosci 42:1636–1643.

Urai AE, Braun A, Donner TH (2017) Pupil-linked arousal is driven by decision uncertainty and alters serial choice bias.

687 Nature Communications 8:14637.

688 Vickers D (1979) *Decision processes in visual perception*. New York, NY: Academic Press.

689 Woodrow H (1935) The effect of practice upon time-order errors in the comparison of temporal intervals. Psychol Rev

690 42:127–152.

Table 1. Behavioral data

	Frequency difference of stimuli (f2 – f1) in Hz					
	-4	-2	2	4	difficulty effect	sign effect
Exp.1	74.8 ±6.3	63.4 ±5.5	68.9 ±4.0	85.0 ±2.9	p < 0.001	p = 0.030
Exp. 2	75.9 ±4.4	64.7 ±3.5	70.8 ±4.4	86.1 ±4.3	p < 0.001	p = 0.002
Exp. 3	74.3 ±6.1	64.2 ±6.0	65.2 ±5.2	78.1 ±5.7	p < 0.001	p = 0.615
Exp. 4	77.7 ±8.8	65.4 ±7.7	66.2 ±5.5	79.8 ±6.6	p < 0.001	p = 0.871
Exp. 5	78.8 ±5.5	66.6 ±4.2	67.8 ±4.5	81.1 ±5.8	p < 0.001	p = 0.388
Exp. 6	74.2 ±5.9	63.1 ±4.3	66.9 ±5.3	80.6 ±5.0	p < 0.001	p = 0.067
pooled	**75.9 ±2.4**	**64.5 ±2.0**	**67.7 ±1.9**	**81.8 ±2.0**	**p < 0.001**	**p < 0.001**

Proportion of correct responses (PCRs) in % as a function of the physical frequency difference f2 – f1 for each experiment. Mean values ± 95% confidence interval are shown. 'Difficulty effect' compares easy (+/- 4 Hz) and difficult (+/- 2 Hz) trials in a paired t-test. 'Sign effect' compares trials with a positive (2 and 4 Hz) and negative (-4 and -2 Hz) frequency difference in a paired t-test. PCRs were logit-transformed before testing, due to non-normally distributed residuals.

Figure 1: Task and stimuli. One after another, two vibrotactile stimuli with frequencies f1 and f2 were briefly presented to the left index finger of participants who had to decide whether f2 > f1 or f2 < f1. Response timing (immediate / delayed), response modality (saccade / button press), and response mapping (direction / color) varied over six variants of the task (exp. 1 – exp. 6). **Inset**, The stimulus set that was used in all experiments, with the exception of zero-difference trials (gray) which were not used in exp. 1 and exp. 2. Each square represents one stimulus pair with f1 (x-axis) and f2 (y-axis). The color-code denotes the physical stimulus differences f2 – f1.

Figure 2: Behavioral model for choices and confidence. **A**, Graphical illustration of the behavioral model based on Bayesian inference. Y-axes display frequencies on a logarithmic scale. Top: Representation of f1 during different stages of the task. Pink distribution represents the likelihood function of f1. Black distribution is the prior centered on the stimulus set. Purple distribution is the posterior of f1 with shifted mean f1'. Lower: The likelihood of f2 (pink distribution) is used for the comparison with the posterior of f1. Subtracting the posterior of f1 from the likelihood of f2, yields a difference distribution which is used to fit the probability to chose f1 to the behavioral data of each participant by optimizing σ^2_{stim}, σ^2_{prior}, and decision criterion *c.* **B**, Intuition of statistical decision confidence. The distance between perceived evidence and decision criterion is proportional to confidence. Average perceived evidence is displayed separately for correct and incorrect trials (green and red bar, respectively). Difference distribution for hard (f2 – f1' = 0.1) and easy (f2 – f1' = 0.3) trials illustrate that confidence increases with evidence strength for correct trials, but decreases for incorrect trials.

Figure 3: Behavioral and modeling results. **A**, Grand average of observed (squares) and modeled (lines) proportions of correct responses (PCRs) plotted separately for each f1 (x-axis) and each physical stimulus difference f2 – f1 (color-code). **B**, Same as in A, but for probabilities to chose f1. Note that the blue squares/lines are identical as in A, and the red squares/lines correspond to 1-PCRs from A. **C**, Probabilities to chose f1 for each stimulus pair of each participant (dots), color-coded for physical stimulus differences (f2 – f1), and plotted against subjectively perceived frequency differences (SPFD; f2 – f1'). The solid black line represents the modeled probability to chose f1, averaged over all participants +/- 95% confidence interval (dashed lines). **D**, Histogram of correlation coefficients from all participants obtained from correlating absolute physical differences (|f2-f1|) with PCRs (gray), and from correlating absolute values of SPFDs (|f2-f1'|) with PCRs (black). **E**, Histogram of Bayes factors (BFs), comparing the SPFD model with a "null" model (based on physical stimulus differences) for each participant. Red line marks threshold for positive evidence in favor of SPFD model (BF > 3).

Figure 4: CPP is first modulated by signed subjective evidence and then by the absolute value, displayed for trials with available physical evidence (i.e., f2 ≠ f1). **Lower**, Scalp topographies of t-values reflecting group-level statistics for modulations by signed subjective evidence (f2 - f1') and by the absolute strength of evidence (|f2 – f1'|). Displayed topographies are averages over 250 ms windows, starting at 0 with the onset of the second stimulus. The modulation by signed subjective evidence peaks clearly earlier (250 – 500 ms topography) than the modulation by the absolute strength of evidence (500 – 750 ms topography). **Upper**, ERPs from electrode CPz (white dot in scalp topographies), are computed separately for six levels of SPFDs, and display a modulation by the signed values of the SPFDs and then by the absolute values of the SPFDs. Black dots denote samples at which the electrode was part of a statistically significant cluster ($p < 0.05$; FWE corrected) indicating a modulation by signed subjective evidence (upper) or by the absolute strength of evidence (lower).

732 **Figure 5:** Source reconstructions for the early CPP modulation by signed subjective evidence (red), and the late
733 modulation by the absolute strength of evidence (blue).

734 **Figure 6:** CPP modulation persists when using a subset of trials in which f2 alone does not predict decision outcome (i.e.,
735 f2 and f2 – f1 are orthogonal). Inset in upper left corner highlights the stimulus pairs that were used for this analysis (see
736 also Figure 1). Same conventions as in Figure 3. Note that only the grand average ERPs for the most negative and most
737 positive level of SPFDs (dark blue and dark red) were affected by using a reduced dataset (see text for details).

Figure 7: CPP is modulated by signed subjective evidence even in the absence of physical evidence (i.e., f2 = f1). Same conventions as in Figure 3. **Lower**, The modulation by subjective evidence peaks in the same time window as the modulation for trials with f2 ≠ f1 (250 – 500 ms topography), and displays a similar topography (cf. Figures 3 and 4). A modulation by the absolute strength of evidence is not observed. Note the different scale of t-values. **Upper**, ERPs from electrode Pz (white dot in scalp topographies) are computed separately for four levels of SPFDs, and display a weak modulation by the signed values of the SPFDs. The black dots denote the brief interval at which the electrode was part of a statistically significant cluster indicating a modulation by signed subjective evidence. Gray dots additionally mark samples at which a significant modulation by signed subjective evidence was observed without correcting for multiple testing (one-sample t-test, $p < 0.05$). Note that a considerably reduced set of trials (25% of all presented trials) and participants (Experiments 3 – 6; 73/116 participants) was available for this analysis.

Figure 8: Late CPP corresponds to statistical decision confidence. **A**, Average statistical decision confidence based on simulations from behavioral models of each participant. Confidence increases with evidence strength (i.e., |f2 – f1'|) for correct trials, and decreases (initially) for incorrect trials. For very hard trials (|f2 – f1'| = 0), confidence is at the same intermediate level for correct and incorrect trials. **B**, Average amplitude (+/- standard error of mean) of late CPP (500 – 800 ms) exhibits same pattern as predicted by simulations shown in A, for trials with and without objective evidence (i.e., f2 ≠ f1 and f2 = f1, respectively).

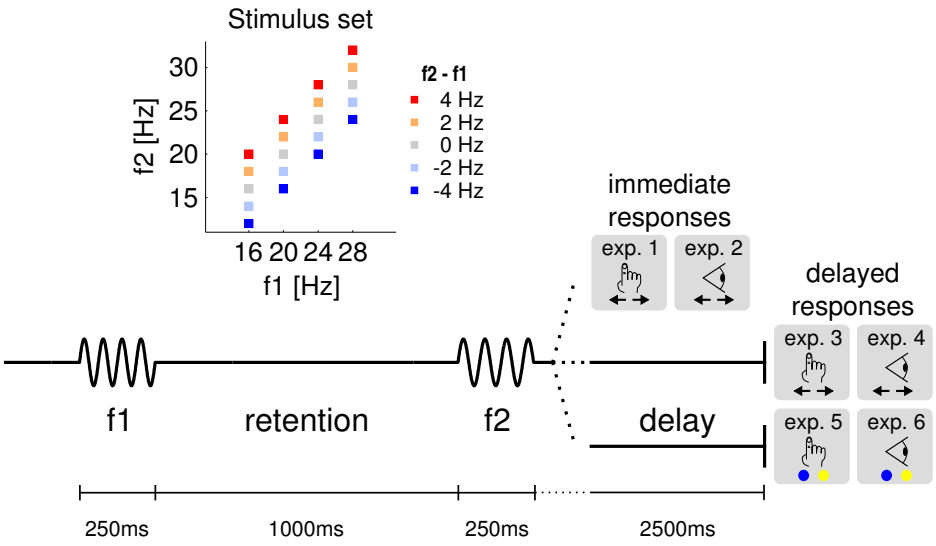
Stimulus set
f2 [Hz]
30
25
20
15
16 20 24 28
f1 [Hz]
f2 - f1
4 Hz
2 Hz
0 Hz
-2 Hz
-4 Hz
immediate responses
exp. 1
exp. 2
delayed responses
exp. 3
exp. 4
exp. 5
exp. 6
f1
retention
f2
delay
250ms
1000ms
250ms
2500ms

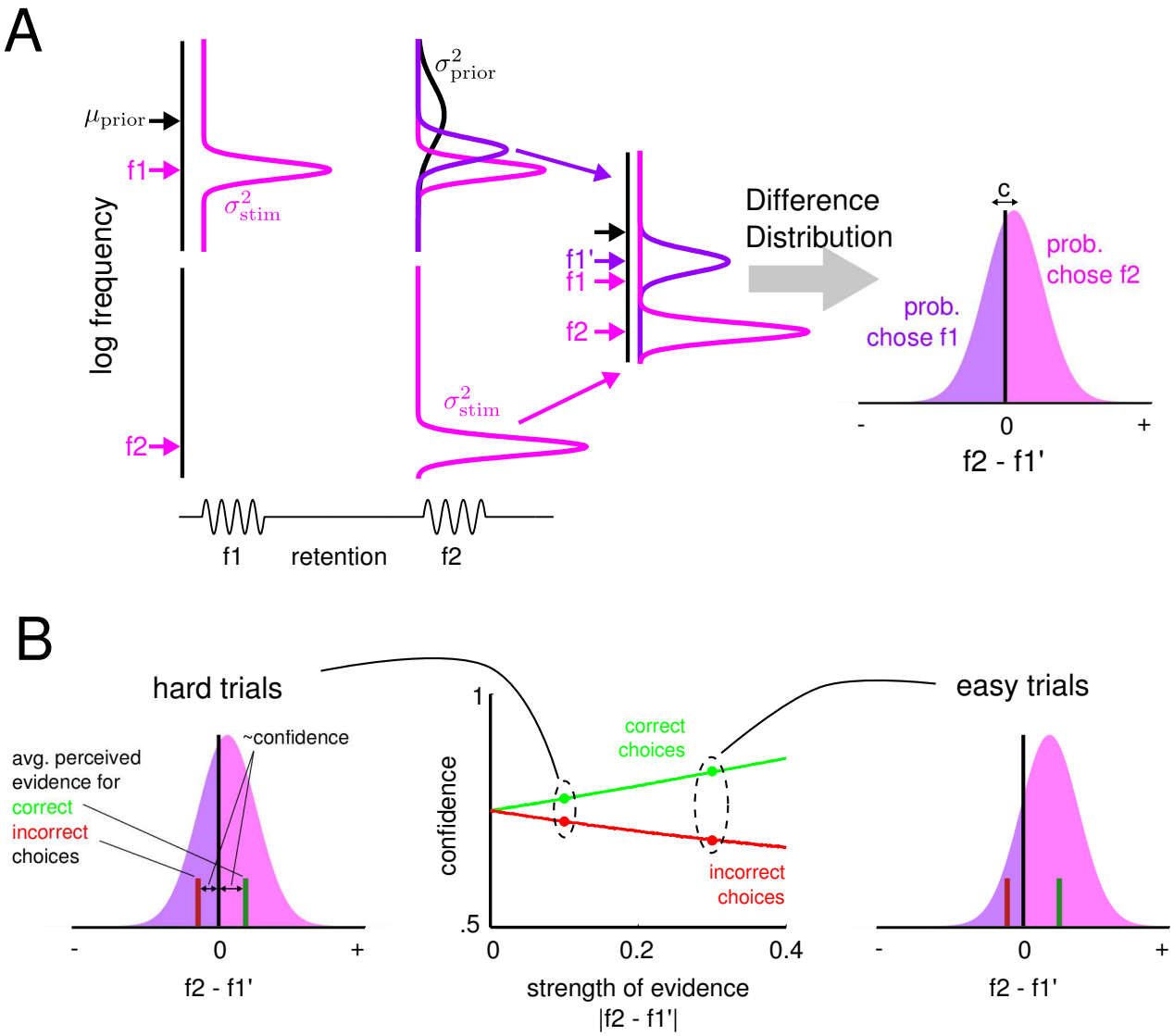
A
μ_{prior}
f1
f2
log frequency
σ^2_{stim}
σ^2_{prior}
f1'
f1
f2
σ^2_{stim}
f1
retention
f2
Difference
Distribution
c
prob.
chose f2
prob.
chose f1
-
0
+
f2 - f1'
B
hard trials
~confidence
avg. perceived
evidence for
correct
incorrect
choices
-
0
+
f2 - f1'
1
.5
confidence
correct
choices
incorrect
choices
0
0.2
0.4
strength of evidence
|f2 - f1'|
easy trials
-
0
+
f2 - f1'

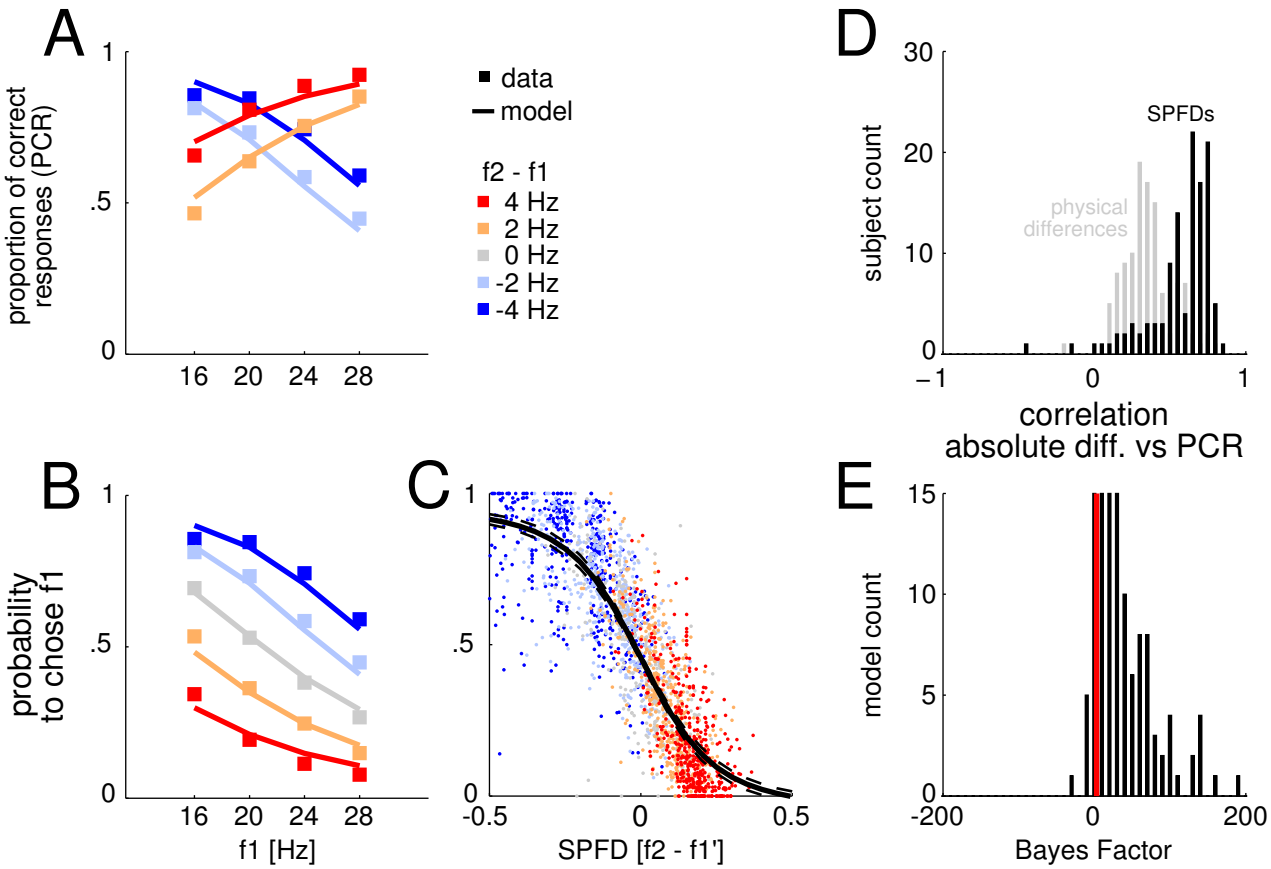
A
proportion of correct responses (PCR)
1
.5
0
16
20
24
28
data
model
f2 - f1
4 Hz
2 Hz
0 Hz
-2 Hz
-4 Hz
B
probability to chose f1
1
.5
0
16
20
24
28
f1 [Hz]
C
1
.5
0
-0.5
0
0.5
SPFD [f2 - f1']
D
subject count
30
20
10
0
−1
0
1
SPFDs
physical differences
correlation absolute diff. vs PCR
E
model count
15
10
5
0
-200
0
200
Bayes Factor

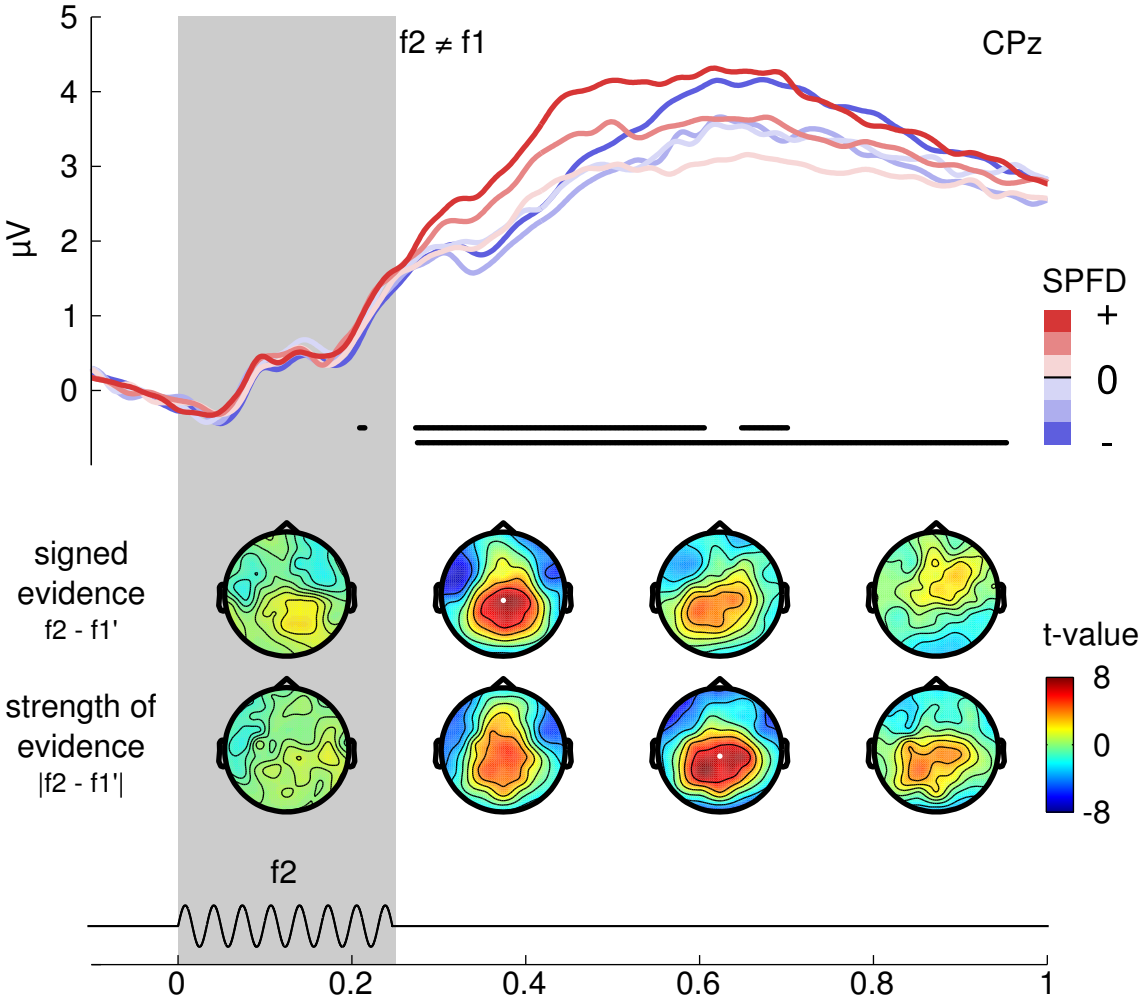
f2 ≠ f1
CPz
μV
5
4
3
2
1
0
SPFD
+
0
-
signed evidence
f2 - f1'
strength of evidence
|f2 - f1'|
t-value
8
0
-8
f2
0
0.2
0.4
0.6
0.8
1

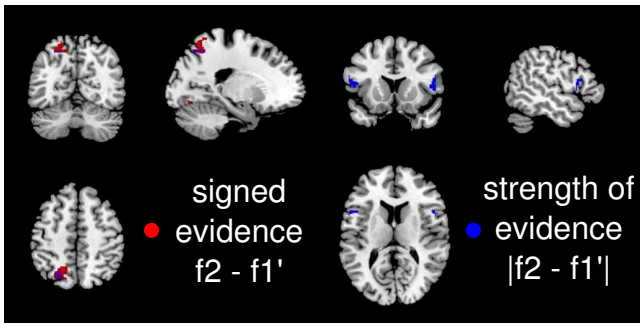
signed
evidence
f2 - f1'
strength of
evidence
|f2 - f1'|

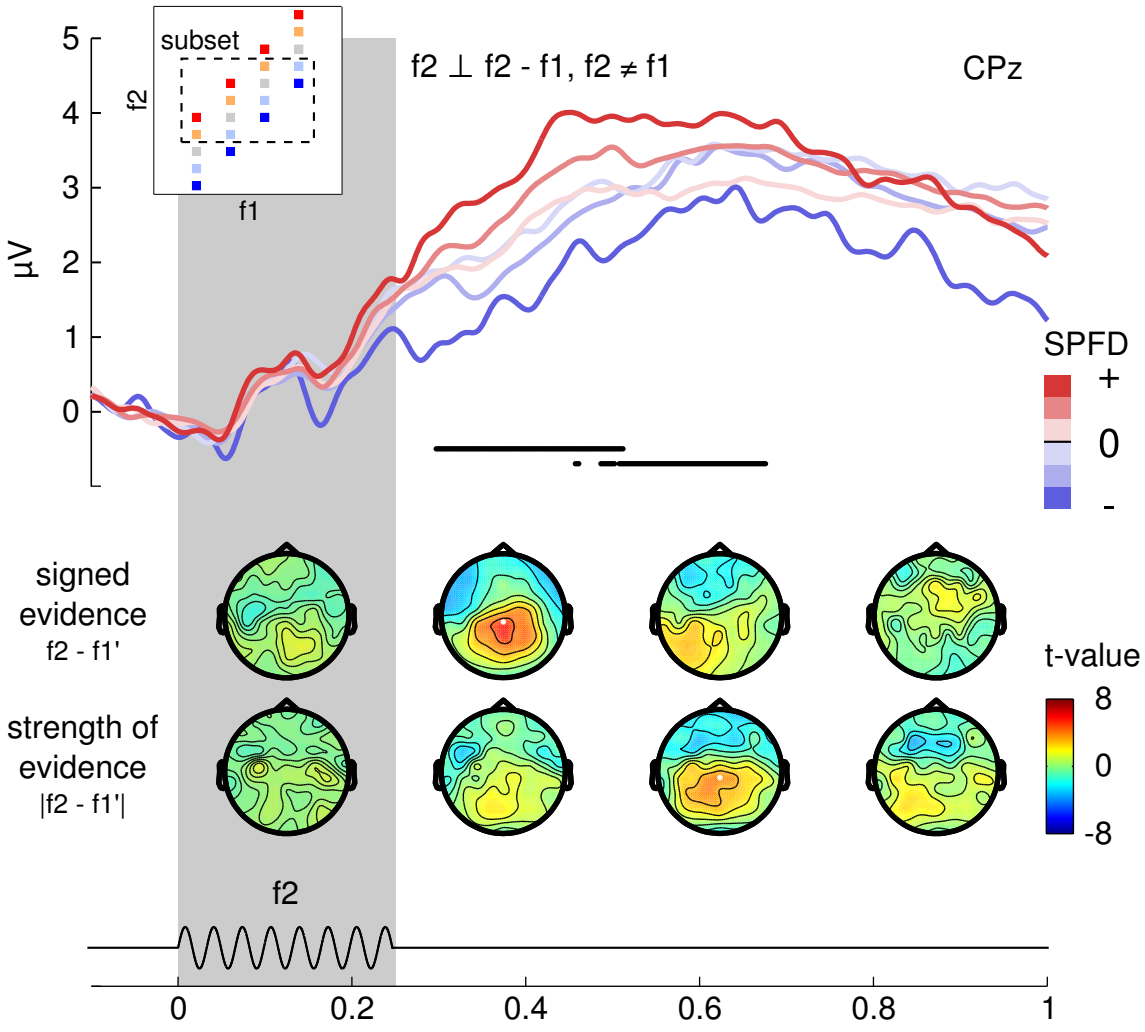
subset
f2
f1
f2 ⊥ f2 - f1, f2 ≠ f1
CPz
μV
5
4
3
2
1
0
SPFD
+
0
-
signed
evidence
f2 - f1'
strength of
evidence
|f2 - f1'|
t-value
8
0
-8
f2
0
0.2
0.4
0.6
0.8
1

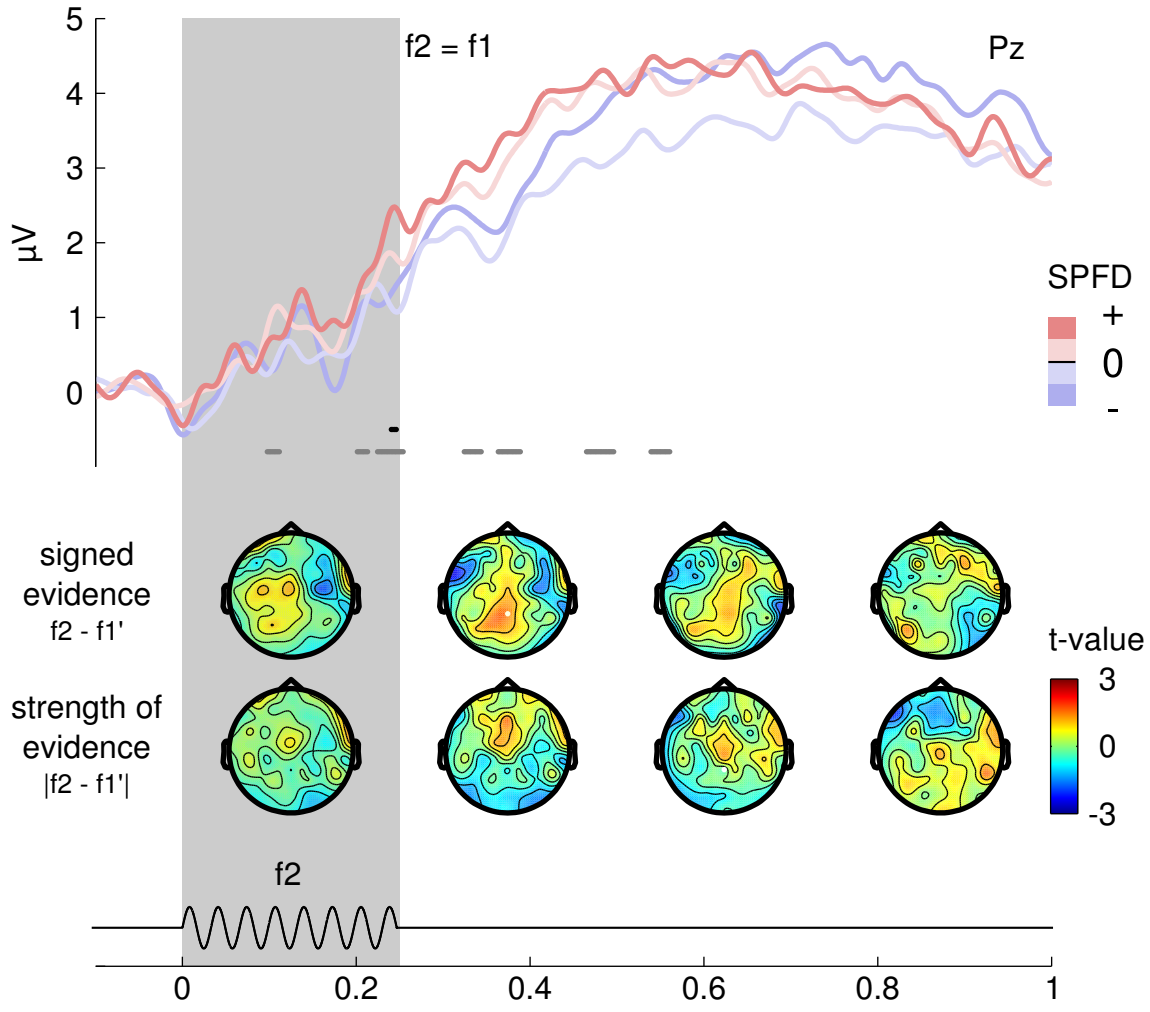
f2 = f1
Pz
µV
5
4
3
2
1
0
SPFD
+
0
-
signed evidence
f2 - f1'
strength of evidence
|f2 - f1'|
t-value
3
0
-3
f2
0
0.2
0.4
0.6
0.8
1

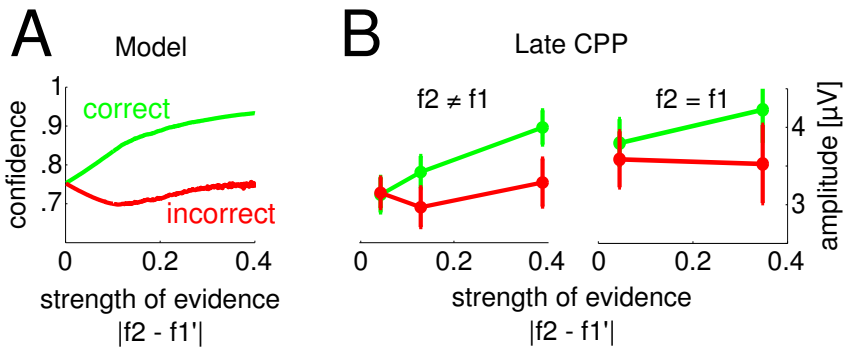
A
Model
confidence
1
.9
.8
.7
correct
incorrect
0
0.2
0.4
strength of evidence
|f2 - f1'|
B
Late CPP
f2 ≠ f1
f2 = f1
amplitude [μV]
4
3
0
0.2
0.4
strength of evidence
|f2 - f1'|

B Anlagen

Eidesstattliche Erklärung

Hiermit erkläre ich an Eides statt,

- dass ich die vorliegende Arbeit eigenständig und ohne unerlaubte Hilfe verfasst habe,
- dass Ideen und Gedanken aus Arbeiten anderer entsprechend gekennzeichnet wurden,
- dass ich mich nicht bereits anderwärtig um einen Doktorgrad beworben habe und keinen Doktorgrad in dem Promotionsfach Psychologie besitze, sowie
- dass ich die zugrundeliegende Promotionsordnung vom 08.08.2016 anerkenne.

Ort, Datum Unterschrift

Erklärung gemäß § 7 Abs. 3 Satz 4 der Promotionsordnung über den Eigenanteil an den veröffentlichten oder zur Veröffentlichung vorgesehenen eingereichten wissenschaftlichen Schriften im Rahmen meiner publikationsbasierten Arbeit

I. Name, Vorname: Herding, Jan

Institut: Arbeitsbereich Neurocomputation and Neuroimaging

Promotionsfach: Psychologie

Titel: M.Sc.

II. Nummerierte Aufstellung der eingereichten Schriften (Titel, Autoren, wo und wann veröffentlicht bzw. eingereicht):

1. **Herding, J.***, Spitzer, B.*, & Blankenburg, F. (2016). Upper beta band oscillations in human premotor cortex encode subjective choices in a vibrotactile comparison task. *Journal of cognitive neuroscience, 28(5)*: 668 – 679.
2. ***Herding, J.**, Ludwig, S., & Blankenburg, F. (2017). Response-Modality-Specific Encoding of Human Choices in Upper Beta Band Oscillations during Vibrotactile Comparisons. Frontiers in Human Neuroscience, 11.*
3. Ludwig, S.*, **Herding, J.***, & Blankenburg, F. (submitted in April 2017). Choice consequences determine choice signals: Oscillatory EEG-Signatures of Postponed Somatosensory Decisions. *Human Brain Mapping*.
4. **Herding, J.**, Ludwig, S., Spitzer, B., & Blankenburg, F. (submitted in April 2017). Centro-parietal EEG Potentials in Perceptual Decision Making: From Subjective Evidence to Confidence. *Journal of Neuroscience*.

* shared authorship

III. Darlegung des eigenen Anteils an diesen Schriften:

Die Bewertung des Eigenanteils richtet sich nach der Skala: “vollständig – überwiegend – mehrheitlich – in Teilen” und enthält nur für den jeweiligen Artikel relevante Arbeitsbereiche.

zu II. 1.: Konzeption (in Teilen), Versuchsdesign (in Teilen), Programmierung (überwiegend), Datenerhebung (vollständig), Datenauswertung (vollständig), Ergebnisdiskussion (mehrheitlich), Erstellen des Manuskriptes (überwiegend).

zu II. 2.: Konzeption (mehrheitlich), Versuchsdesign (überwiegend), Programmierung (vollständig), Datenerhebung (vollständig), Datenauswertung (vollständig), Ergebnisdiskussion (überwiegend), Erstellen des Manuskriptes (vollständig).

zu II. 3.: Konzeption (in Teilen), Versuchsdesign (in Teilen), Programmierung (überwiegend), Datenerhebung (vollständig), Datenauswertung (in Teilen), Ergebnisdiskussion (in Teilen), Erstellen des Manuskriptes (in Teilen).

zu II. 4.: Konzeption (mehrheitlich), Datenauswertung (vollständig), Ergebnisdiskussion (überwiegend), Erstellen des Manuskriptes (vollständig).

IV. Die Namen und Anschriften nebst E-Mail oder Fax der jeweiligen Mitautorinnen oder Mitautoren:

zu II. 1.: Bernhard Spitzer, Department of Experimental Psychology, University of Oxford, Oxford, UK.
E-mail: bernardodispitz@googlemail.com

Felix Blankenburg, Arbeitsbereich Neurocomputation and Neuroimaging, Fachbereich für Erziehungswissenschaft und Psychologie, Freie Universität Berlin, Habelschwerdter Allee 45, 14195 Berlin.
E-mail: felix.blankenburg@fu-berlin.de

zu II. 2.: Simon Ludwig, Arbeitsbereich Neurocomputation and Neuroimaging, Fachbereich für Erziehungswissenschaft und Psychologie, Freie Universität Berlin, Habelschwerdter Allee 45, 14195 Berlin.
E-mail: simonludwig.sl@gmail.com

Felix Blankenburg, s.o.

zu II. 3.: Simon Ludwig, s.o.

Felix Blankenburg, s.o.

zu II. 4.: Simon Ludwig, s.o.

Bernhard Spitzer, s.o.

Felix Blankenburg, s.o.

Datum, Unterschrift der Doktorandin/des Doktoranden

Ich bestätige die von Jan Herding unter III. abgegebene Erklärung:

Name: Felix Blankenburg Unterschrift: . . . . . .

Name: Bernhard Spitzer Unterschrift: . . . . . .

Name: Simon Ludwig Unterschrift: . . . . . .